Communication over MIMO Multi-User Systems:

Signaling and Fairness

by

Mohammad Ali Maddah-Ali

A thesis

presented to the University of Waterloo

in fulfillment of the

thesis requirement for the degree of

Doctor of Philosophy

in

Electrical and Computer Engineering

Waterloo, Ontario, Canada, 2007

I hereby declare that I am the sole author of this thesis. This is a true copy of the thesis, including any required final revisions, as accepted by my examiners.

I understand that my thesis may be made electronically available to the public.

Abstract

Employment of the multiple-antenna transmitters/receivers in communication systems is known as a promising solution to provide high-data-rate wireless links. In the multi-user environments, the problems of signaling and fairness for multi-antenna systems have emerged as challenging problems. This dissertation deals with these problems in several multi-antenna multi-user scenarios.

In part one, a simple signaling method for the multi-antenna broadcast channels is proposed. This method reduces the MIMO broadcast system to a set of parallel channels. The proposed scheme has several desirable features in terms of: (i) accommodating users with different number of receive antennas, (ii) exploiting multi-user diversity, and (iii) requiring low feedback rate. The simulation results and analytical evaluations indicate that the achieved sum-rate is close to the sum-capacity of the underlying broadcast channel.

In part two, for multiple-antenna systems with two transmitters and two receivers, a new non-cooperative scenario of data communication is studied in which each receiver receives data from both transmitters. For such a scenario, a signaling scheme is proposed which decomposes the system into two broadcast or two multi-access sub-channels. Using the decomposition scheme, it is shown that this signaling scenario outperforms the other known non-cooperative schemes in terms of the achievable multiplexing gain. In particular for some special cases, the achieved multiplexing gain is

the same as the multiplexing gain of the system, where the full cooperation is provided between the transmitters and/or between the receivers.

Part three investigates the problem of fairness for a class of systems for which a subset of the capacity region, which includes the sum-capacity facets, forms a polymatroid structure. The main purpose is to find a point on the sum-capacity facet which satisfies a notion of fairness among active users. This problem is addressed in the cases where the complexity of achieving interior points is not feasible, and where the complexity of achieving interior points is feasible.

In part four, K-user memoryless interference channels are considered; where each receiver sequentially decodes the data of a subset of transmitters before it decodes the data of the designated transmitter. A greedy algorithm is developed to find the users which are decoded at each receiver and the corresponding decoding order such that the minimum rate of the users is maximized. It is proven that the proposed algorithm is optimal.

The results of the parts three and four are presented for general channels which include the multiple-antenna systems as special cases.

help and patience in the process of this work.

To my parents:

Abbas Maddah-Ali

and

Tayebeh Oleyki

To my beloved wife:

Hajar Mahdavi-doost

Contents

List of Figures

List of Notations and Abbreviations

MIMO	Multiple-Input Multiple-Output
MISO	Multiple-Input Single-Output
SIMO	Single-Input Multiple-Output
SNR	Signal to Noise Ratio
SINR	Signal to Interference plus Noise Ratio
MG	Multiplexing Gain
MV	Modulation Vector
RSV	Right Singular Vector
LSV	Left Singular Vector
CDF	Cumulative Distribution Function
PDF	Probability Density Function
AWGN	Additive White Gaussian Noise
Boldface Upper-Case Letters	Matrices
Boldface Lower-Case Letters	Vectors
$(\mathbf{H})^{\dagger}$	Transpose conjugate of $\mathbf{H}$
$\det(\mathbf{H})$	Determinant of $\mathbf{H}$
$\mathrm{Tr}(\mathbf{H})$	Trace of $\mathbf{H}$
$\mathbf{H} \succeq 0$	Matrix $\mathbf{H}$ is positive semi-definite
$\mathbf{1}_n$	n-dimensional vector with all entries equal to one

$\mathbf{I}_{n \times n}$	n-dimensional identity matrix
$\mathbf{H} \perp \mathbf{G}$	Columns of $\mathbf{H}$ are orthogonal to columns of $\mathbf{G}$
$\Omega(\mathbf{H})$	The sub-space spanned by columns of $\mathbf{H}$
$\mathrm{N}(\mathbf{H})$	The null space of the matrix $\mathbf{H}$
$\mathbf{h}^{(i)}$	The ith column of the matrix $\mathbf{H}$
$[a_{p,q}]_{(p,q)}^{m \times n}$	$m \times n$ matrix with $a_{p,q}$ as entry (p,q)
$\mathcal{C}$	The set of complex numbers
$\mathcal{R}$	The set of real numbers
$z^{\{j\}}$	The jth largest of K variables $\{z_1, \ldots, z_K\}$
$F_{j:K}(.)$	CDF of the jth largest variable among K variables
$\mathcal{OC}^{M \times N}$	The set of $M \times N$ complex matrices with mutually orthogonal and normal columns.
$\mathfrak{f}, \mathfrak{g}, \mathfrak{h}$	Set functions
$\mathcal{B}(\mathfrak{f}, E)$	Polymatroid over the dimensions listed in E with the set function $\mathfrak{f}$
$\mathbf{x}(i:j)$	A vector including the entries i to j of the vector $\mathbf{x}$
$(.)^{\langle j \rangle}$	Index for the jth nested polymatroid
$|S|$	Cardinality of the set S
E	Set of integers $E = \{1, \cdots, |E|\}$
$\boldsymbol{\pi}$	A permutation of the set E

$(.)^{[j]}$	Index for the jth link in the interference channel
ρ	Multiplexing gain
K	Number of users
M	Number of transmit antennas
N	Number of receive antennas
a	Number of active users
r	Index for receivers
t	Index for transmitters
α	Counter in algorithms
P_T	Total power
$\mathbf{P}_t$	Covariance of the transmit signal by transmitter t
$E(.)$	Expectation
$\Pr(.)$	Probability
$\mathcal{L}_\infty$	Power offset
$R_{\text{Sum-Capacity}}$	Sum Capacity
R	Sum rate
ϑ_t	Data-rate of transmitter t
$\mathbf{v}, \mathbf{V}$	Modulation vector, modulation matrix
$\mathbf{u}, \mathbf{U}$	Demodulation vector, demodulation matrix
$\mathbf{s}$	Transmit vector

μ_{rt}	Number of data streams sent from transmitter t to receiver r
$\gamma(n, z)$	Incomplete Gamma function of order n
$\Gamma(z)$	Gamma function
$\lfloor z \rfloor$	Floor of z
$\lceil z \rceil$	Ceiling of z
$\mathbf{x}(S)$	$\sum_{i \in S} x_i$
$\mathbf{D}(S)$	$\sum_{i \in S} \mathbf{D}_i$
$\nabla_{\mathbf{x}}$	Gradient with respect to $\mathbf{x}$

Chapter 1

Introduction

In the recent years, the expectation for multimedia services in wireless systems and the demand for connectivity have exponentially been increasing. This, in turn, puts pressure on the valuable resource of frequency spectrum, and necessitates the development of spectrally efficient signaling schemes. On the other hand, the explosive improvement in VLSI technology provides the possibility of implementing more sophisticated algorithms in low-power high-speed electronic processors with a reasonable cost.

The most effective scheme to increase the spectral efficiency is the scheme known as *frequency reuse*. In this scheme, several links communicate at the same time and at the same frequency through a shared channel. As a result, the overall data rate in a bandwidth would increases. The main source of impairment in this scheme is the *interference* of the users over each other, which is called the *co-channel interference*. The most challenging part of the signaling design based on the frequency reuse scheme

is to mange and mitigate the destructive effects of the co-channel interference. This is essential to attain the overall throughput promised in the multi-user information theory. On the other hand, in such systems, there is an inherent competition among the users to exploit the resources of the shared medium. In the presence of this competition, proving *fairness* among the users, while achieving a high spectral efficiency, emerges as a challenging part of signaling design.

A well-known method to cope with the co-channel interference is to impose constraint on the geographic distances among the concurrent links and to control the power of the transmitters [20, 60]. While this method is widely utilized in the current cellular systems, it is not suitable for the dense networks.

Another scheme to reduce the effect of interference is to provide cooperation among the transmitters and/or among the receivers. The most famous structure, resulted from full cooperation, is the multiple-input multiple-output (MIMO) systems. In these systems, each transmitter and/or receiver is equipped with several antennas. In other words, each transmitter (receiver) is formed by the several fully-cooperated transmit (receive) units. By taking advantage of the cooperation among the transmit units, the interference of the data streams sent by the transmit units over each other can be completely canceled-out by using some pre-processing operations. Similarly, the interference of the data streams received by receive units (antennas) can be canceled out. It is shown that in point to point multiple-antenna system, the capacity of the system linearly increase with the minimum number of transmit and receive antennas [58]. In

fact, by using multiple antennas at both sides of communication links, the additional dimension of space is integrated to the available dimensions of time and frequency [57, 58]. Such an extra dimension would be helpful to mitigate the co-channel interference in the MIMO multi-user systems.

Using multiple-antenna systems changes the transmit and receive signals from the scaler quantities to the vector quantities. In the new space, a lot of results, proven for the scalar systems, are no longer valid. This includes the problems of optimal signaling and fairness.

This thesis deals with the problems of signaling and fairness in some MIMO multi-user systems. However, the results on fairness are presented in general forms which include the MIMO systems as special cases.

The organization of this thesis is as follows. The rest of this chapter is devoted to a brief summary of the materials presented in the following chapters. In chapter two, an efficient signaling scheme over MIMO broadcast channels is proposed and its performance is analyzed. In chapter three, for a multiple-antenna system with two transmitters and two receivers, a new scenario of signaling, X channel, is proposed and its performance is evaluated. In chapter four, we investigate the problem of fairness for a wide class of multiuser systems for which the whole or a major subset of the capacity region (which include the sum-capacity facet) forms a structure known as Polymtroid. This includes the MIMO broadcast channels and the multi-access channels as special cases. In chapter five, the problem of fairness for general memoryless interference chan-

nels is investigated.

Summary of the Dissertation

Chapter two presents a simple signaling method for broadcast channels with multiple transmit multiple receive antennas. This method reduces the MIMO broadcast system to a set of parallel channels. The proposed scheme has several desirable features in terms of: (i) accommodating users with different number of receive antennas, (ii) exploiting multi-user diversity, and (iii) requiring low feedback rate. To analyze the performance of the scheme, an upper-bound on the outage probability of each sub-channel is derived which is used to establish the diversity order and the asymptotic sum-rate of the scheme. It is shown that the diversity order of the jth data stream, $1 \leq j \leq M$, is equal to $N(M-j+1)(K-j+1)$, where M, N, and K indicate the number of transmit antennas, the number of receive antennas, and the number of users, respectively. Furthermore, it is proven that the throughput of this scheme scales as $M \log \log(K)$ and asymptotically $(K \longrightarrow \infty)$ tends to the sum-capacity of the MIMO broadcast channel. The simulation results indicate that the achieved sum-rate is close to the sum-capacity of the underlying broadcast channel.

Chapter three investigates a new scenario of data communication for multiple-antenna systems with two transmitters and two receivers in which each receiver receives data from both transmitters (X-Channels). In this scenario, it is assumed that each transmitter is unaware of the other transmitter's data (non-cooperative scenario). In

this chapter, two signaling schemes are proposed for X channels which are based on using some linear filters at the transmitters and the receivers. The filters are designed such that the system is decomposed into either two non-interfering multi-antenna broadcast sub-channels or two non-interfering multi-antenna multi-access sub-channels. In addition, the null spaces of the channels are exploited to achieve the highest multiplexing gain in the system. By using the decomposition schemes, the multiplexing gain (MG) of this scenario is derived, which shows improvement as compared with the other known non-cooperative schemes. In particular, it is shown that for some specific cases, the achieved MG is the same as the MG of the system if full cooperation is provided either between the transmitters or between the receivers.

Chapter four studies the problem of fairness in a wide class of multi-user systems for which a subset of capacity region, including the corner points and the sum-capacity facet, has a special structure known as polymatroid. Multiaccess channels with fixed input distributions and multiple-antenna broadcast channels are examples of such systems. Any interior point of the sum-capacity facet can be achieved by time-sharing among corner points or by an alternative method known as *rate-splitting*. The main purpose of this part is to find a point on the sum-capacity facet which satisfies a notion of fairness among active users. This problem is addressed in two cases: (i) where the complexity of achieving interior points is not feasible, and (ii) where the complexity of achieving interior points is feasible. For the first case, the corner point for which the minimum rate of the active users is maximized (max-min corner point) is desired

for signaling. A simple greedy algorithm is introduced to find the optimum max-min corner point. For the second case, the polymatroid properties are exploited to locate a rate-vector on the sum-capacity facet which is optimally fair in the sense that the minimum rate among all users is maximized (max-min rate). In the case that the rate of some users can not increase further (attain the max-min value), the algorithm recursively maximizes the minimum rate among the rest of the users.

Chapter five considers K-user memoryless interference channels, where each receiver sequentially decodes the data of a subset of transmitters before it decodes the data of the designated transmitter. Therefore, the data rate of each transmitter depends on (i) the subset of receivers which decode the data of that transmitter, (ii) the decoding order, employed at each of these receivers. In this chapter, a greedy algorithm is developed to find the users which are decoded at each receiver and the corresponding decoding order such that the minimum rate of the users is maximized. It is proven that the proposed algorithm is optimal.

Chapter 6 presents a summary of the thesis contributions and discusses several future research directions.

Chapter 2

Signaling Over MIMO Broadcast Channels

2.1 Introduction

Multiple input multiple output (MIMO) systems have received considerable attention as a promising solution to provide reliable and high data rate communication [17, 57, 58]. More recently, the work on MIMO systems has been extended to MIMO multi-user channels [63, 64, 66, 71]. In [63, 64], a duality between the broadcast channel and the multiple access channel is introduced. This duality is applied to characterize the sum-capacity of the broadcast channel as a convex optimization problem. In [71], a reformulation of the sum-capacity as a min-max optimization problem is introduced and a signaling method which achieves the sum-capacity is presented. It is shown

7

that in an optimal signaling (maximizing the sum-rate), the power is allocated to, at most, M^2 uses (active users), where M is the number of transmit antennas [72]. In practical systems, the number of users is large. In this case, finding the set of active users by solving the optimization problem is a complex operation. In addition, to perform such a computation, all the channel state information is required at the base station which necessitates a high data rate feedback link. The duality and signaling method introduced in [63, 64, 71] are based on a result, known as *dirty paper coding*, on cancelling known interference at the transmitter [7]. Dirty paper coding states that in an AWGN channel with interference, if the transmitter non-causally knows the interference, the capacity of the channel is the same as the capacity of the channel without interference. A method for approximate implementation of the dirty paper coding is presented in [12, 13].

A number of research works have focused on practical methods for signaling over MIMO broadcast channels. In [65], a simple method that supports one user at a given time is presented. This method exploits a special kind of diversity, *multiuser diversity*, which is available in the multiuser system with independent channels [34]. To exploit multiuser diversity, the transmission resources are allocated to the user(s) which result in the highest throughput for the given channel condition. Unlike [65], the signaling method presented in other related works support multiple users at a given time. In [43], a variation of channel inversion method is used, where the inverse of the channel matrix is regularized and the data is perturbed to reduce the energy of the transmitted signal.

However, in this method, the pre-coding matrix depends on the data, and therefore, the method is computationally extensive.

In addition, no method for selecting active users is suggested. In [3], a signaling method based on the QR decomposition and dirty paper coding is introduced. The QR decomposition converts the channel matrix, and consequently the interference matrix[1], to a lower triangular form. Dirty paper coding eliminates the remaining interference. By modifying the QR decomposition, a greedy method for selecting active users which exploits multiuser diversity is presented in [61]. References [3, 43, 61] present methods to support M simultaneous users, each with one receive antenna.

When there is more than one antenna at the receiver, a generalized version of the zero forcing method is utilized in [6, 56]. However, the methods of [6, 56] are highly restrictive in the sense that the number of transmit antennas must be greater than the total number of the receive antennas. In addition, similar to the conventional zero forcing, the method presented in [6, 56] degrades the signal-to-noise-ratio (SNR).

In this chapter, an efficient sub-optimum method for selecting the set of active users and signaling over such users is proposed. This method converts the interference matrix – but not necessarily the channel matrix – to a lower-triangular form. This is in contrast to the earlier method proposed in [3, 61] which uses QR decomposition to triangularis the channel matrix. In the proposed method, first, the direction in which each user has the maximum gain is determined. The base station selects the best user in terms of the

---

[1]The entry (p, q) of the interference matrix denotes the interference of user p over user q

largest maximum gain, where the corresponding direction is used as the modulation vector (MV) for that user. The algorithm proceeds in a recursive manner where in each step, the search for the best direction is performed in the null space of the previously selected MVs. Finally, the transmitted signal is formed as a linear combination over the selected MVs. It is shown that in this method, data stream j has no interference on data stream i, $i = 1, \cdots, j-1$. Dirty paper coding is used to eliminate the remaining interference. Thus, the underlying sub-channels can be treated independent of each other in terms of encoding/decoding and provision of QoS. In addition, this method offers other desirable features such as: (i) accommodating users with different number of receive antennas, (ii) exploiting multi-user diversity, and (iii) requiring low feedback rate. It is easy to see that for the special case of $N = 1$, the proposed algorithm is the same as the methods presented in [3, 61].

To analyze the performance of the scheme, an upper-bound on the outage probability of each sub-channel is derived which is used to establish the diversity order and the asymptotic sum-rate of the scheme. It is shown that the diversity order of the jth data stream, $1 \leq j \leq M$, is equal to $N(M - j + 1)(K - j + 1)$. Furthermore, it is proven that the throughput of this scheme scales as $M \log \log(K)$ and asymptotically $(K \longrightarrow \infty)$ tends to the sum-capacity of the MIMO broadcast channel. The simulation results indicate that the achieved sum-rate is close to the sum-capacity of the underlying broadcast channel.

The rest of the chapter is organized as follows: In Section 2.2, the system model

and the proposed signaling method are presented. In Section 2.3, an algorithm to select the active users and the corresponding MVs is developed. The performance analysis of the system is presented in Section 2.4. In this section, an upper-bound on the outage probability of each sub-channel is derived which is used to establish the diversity order and the asymptotic sum-rate of the scheme. In Section 2.5, the simulation results and comparisons with the sum-capacity of the MIMO broadcast are discussed. In Section 2.6, the proposed algorithm is modified to reduce the required rate of the feedback. Some concluding remarks are provided in Section 2.7.

2.2 Preliminaries

Consider a MIMO broadcast channel with M transmit antennas and K users, where the rth user is equipped with N_r receive antennas. In a flat fading environment, the baseband model of this system is given by,

$$\mathbf{y}_r = \mathbf{H}_r \mathbf{s} + \mathbf{w}_r, \quad 1 \le r \le K, \tag{2.1}$$

where $\mathbf{H}_r \in \mathcal{C}^{N_r \times M}$ denotes the channel matrix from the base station to user r, $\mathbf{s} \in \mathcal{C}^{M \times 1}$ represents the transmitted vector, and $\mathbf{y}_r \in \mathcal{C}^{N_r \times 1}$ signifies the received vector by user r. The vector $\mathbf{w}_r \in \mathcal{C}^{N_r \times 1}$ is white Gaussian noise with a zero-mean and unit-variance.

The base station supports M simultaneous data streams, distributed among at most M users (*active users*), indexed by $\pi(j)$, $j = 1, \ldots, M$. The transmitted vector $\mathbf{s}$ is

equal to:

$$\mathbf{s} = \sum_{j=1}^{M} d_j \mathbf{v}_j,\qquad(2.2)$$

where $\mathbf{v}_j \in \mathcal{C}^{M \times 1}$, $j = 1, \ldots, M$, is the modulation vector (MV) corresponding to user $\pi(j)$, $\pi(j) \in \{1, 2, \ldots, K\}$, and d_j contains the information for user $\pi(j)$. Note that with this formulation, a given user may receive multiple data streams. Vectors $\mathbf{v}_j$, $j = 1, \ldots, M$, form an orthonormal set. Dirty-paper coding is used such that for $i > j$, the interference of data stream i over data stream j is canceled.

To detect the data stream j, user $\pi(j)$ multiplies the received vector by a demodulation vector $\mathbf{u}_j^{\dagger}$. In the next section, we propose a method to select the set of active users $\{\pi(1), \pi(2), \ldots, \pi(M)\} \subset \{1, 2, \ldots, K\}$, modulation vectors $\mathbf{v}_j$, and demodulation vectors $\mathbf{u}_j$, for $j = 1, \ldots, M$.

2.3 Selecting active users, modulation, and demodulation vectors

Assuming channel state information (CSI) is available at the base station, the proposed algorithm works as follows. First, for each user, the maximum *gain* and the corresponding *direction* are determined[2]. Next, the best user in terms of the largest gain is chosen as an active user. The MV for the selected user is along the corresponding direction.

---

[2]The gain of the channel $\mathbf{H}$ along the direction (unit vector) $\mathbf{x}$ is defined as the square root of $\mathbf{x}^{\dagger}\mathbf{H}^{\dagger}\mathbf{H}\mathbf{x}$.

These steps are repeated recursively until the M MVs and the set of active users are determined. In each step, the search for the best direction is performed in the null space of the previously selected MVs. It is shown that in this manner, any given MV has no interference over the previously selected MVs. In the following, the proposed algorithm is presented in details.

Algorithm 2.1.

1. *Set $j = 1$ and $\boldsymbol{\Xi} = [0]_{M \times M}$.*

2. *Find σ_j^2, where*

$$\sigma_j^2 = \max_r \max_{\mathbf{x}} \mathbf{x}^\dagger \mathbf{H}_r^\dagger \mathbf{H}_r \mathbf{x}.$$

$$s.t. \qquad \mathbf{x}^\dagger \mathbf{x} = 1$$

$$\boldsymbol{\Xi}^\dagger \mathbf{x} = 0. \tag{2.3}$$

Set $\pi(j)$ and $\mathbf{v}_j$ equal to the optimizing parameters r and $\mathbf{x}$, respectively.

3. *Set*

$$\mathbf{u}_j = \frac{1}{\sigma_j} \mathbf{H}_{\pi(j)} \mathbf{v}_j. \tag{2.4}$$

4. *Substitute $\mathbf{v}_j$ in column j of matrix $\boldsymbol{\Xi}$.*

5. *Set $j \leftarrow j + 1$. If $j \leq M$, move to step two; otherwise, stop.*

In Step 2 of the algorithm, maximization over r selects the best user, and therefore, exploits the multiuser diversity. Maximization over $\mathbf{x}$ determines the best MV for each

user, and at the same time converts the interference matrix to a lower triangular form, implying that data stream j has no interference over data stream i, $i = 1, \ldots, j - 1$. This property has been proven in the following theorem.

Theorem 2.2. *Consider the following optimization problem:*

$$\max_{\mathbf{x}} \quad \mathbf{x}^\dagger \mathbf{H}^\dagger \mathbf{H} \mathbf{x},$$

$$s.t. \quad \mathbf{x}^\dagger \mathbf{x} = 1$$

$$\mathbf{\Xi}^\dagger \mathbf{x} = 0, \tag{2.5}$$

where $\mathbf{H}$ *and* $\mathbf{\Xi} = [\boldsymbol{\xi}^{(1)}, \boldsymbol{\xi}^{(2)}, \ldots, \boldsymbol{\xi}^{(\hat{o})}]$ *are complex matrices. Let* $\mathbf{v}$ *be the vector that maximizes (2.5) and* σ^2 *be the corresponding optimum value. Define vector* $\mathbf{u}$ *as follows:*

$$\mathbf{u} = \frac{\mathbf{H}\mathbf{v}}{\sigma}. \tag{2.6}$$

If there exists a vector $\widehat{\mathbf{v}}$ *such that* $\mathbf{\Xi}^\dagger \widehat{\mathbf{v}} = 0$ *and* $\mathbf{v}^\dagger \widehat{\mathbf{v}} = 0$, *then*

$$\mathbf{u}^\dagger \mathbf{H} \widehat{\mathbf{v}} = 0. \tag{2.7}$$

Proof. According to (2.6),

$$\mathbf{u}^\dagger \mathbf{H} \widehat{\mathbf{v}} = \left(\frac{\mathbf{H}\mathbf{v}}{\sigma} \right)^\dagger \mathbf{H} \widehat{\mathbf{v}} = \frac{1}{\sigma} \mathbf{v}^\dagger \mathbf{H}^\dagger \mathbf{H} \widehat{\mathbf{v}}. \tag{2.8}$$

To optimize the cost function in (2.5), Lagrange multipliers technique is adopted.

$$L(\mathbf{x}, \hat{\lambda}, \widehat{\theta}) = -\mathbf{x}^\dagger \mathbf{H}^\dagger \mathbf{H} \mathbf{x} + \hat{\lambda}(\mathbf{x}^\dagger \mathbf{x} - 1) + \widehat{\boldsymbol{\theta}} \, \mathbf{\Xi}^\dagger \mathbf{x}, \tag{2.9}$$

where $\hat{\lambda}$ and $\widehat{\boldsymbol{\theta}} = [\hat{\theta}_1, \hat{\theta}_2, \ldots, \hat{\theta}_{\hat{\varrho}}]$ are Lagrange multipliers. The gradient of $L(\mathbf{x}, \hat{\lambda}, \widehat{\boldsymbol{\theta}})$, corresponding to the vector $\mathbf{x}$, is

$$\nabla_{\mathbf{x}} L(\mathbf{x}, \hat{\lambda}, \widehat{\boldsymbol{\theta}}) = -2\mathbf{H}^\dagger \mathbf{H} \mathbf{x} + 2\hat{\lambda}\mathbf{x} + \sum_{l=1}^{\hat{\varrho}} \hat{\theta}_l \boldsymbol{\xi}^{(l)}. \tag{2.10}$$

Since $\mathbf{v}$ maximizes the cost function, $\mathbf{v}$ satisfies (2.10). Therefore,

$$\nabla_{\mathbf{x}} L(\mathbf{x}, \hat{\lambda}, \widehat{\boldsymbol{\theta}}) = -2\mathbf{H}^\dagger \mathbf{H} \mathbf{v} + 2\hat{\lambda}\mathbf{v} + \sum_{l=2}^{\hat{\varrho}} \hat{\theta}_l \boldsymbol{\xi}^{(l)} = 0. \tag{2.11}$$

Multiplying both sides of (2.11) by $\widehat{\mathbf{v}}^\dagger$ results in

$$\nabla_{\mathbf{x}} L(\mathbf{x}, \hat{\lambda}, \widehat{\boldsymbol{\theta}}) = -2\widehat{\mathbf{v}}^\dagger \mathbf{H}^\dagger \mathbf{H} \mathbf{v} + 2\hat{\lambda}\widehat{\mathbf{v}}^\dagger \mathbf{v} + \widehat{\mathbf{v}}^\dagger \sum_{l=2}^{\hat{\varrho}} \hat{\theta}_l \boldsymbol{\xi}^{(l)} = 0. \tag{2.12}$$

If $\widehat{\mathbf{v}}^\dagger \mathbf{v} = 0$ and $\widehat{\mathbf{v}}^\dagger \boldsymbol{\xi}^{(l)} = 0$ for $l = 1, \ldots, \hat{\varrho}$ are substituted into in (2.12),

$$\widehat{\mathbf{v}}^\dagger \mathbf{H}^\dagger \mathbf{H} \mathbf{v} = 0. \tag{2.13}$$

Finally, (5.14) and (2.13) result in

$$\mathbf{u}^\dagger \mathbf{H} \widehat{\mathbf{v}} = 0. \tag{2.14}$$

$\square$

The interference of data stream i over data stream j is equal to $\mathbf{u}_j^\dagger \mathbf{H}_{\pi(j)} \mathbf{v}_i$. Noting (2.3) which derive $\mathbf{v}_j$ and according to $\mathbf{v}_j^\dagger \mathbf{v}_i = 0$, Theorem 2.2 implies that $\mathbf{u}_j^\dagger \mathbf{H}_{\pi(j)} \mathbf{v}_i = 0$, for $i > j$. This means that data stream i has no interference over data stream j, $j = 1, \ldots, i - 1$. Note that if $i < j$, the interference of data stream i over data stream j is canceled by dirty paper coding. Therefore, the MIMO broadcast channel is effectively

reduced to a set of parallel sub-channels with gains σ_j, $j = 1, \ldots, M$. As a result, the sum-rate of the system is equal to

$$R = \sum_{j=1}^{M} \log(1 + \sigma_j^2 P_j) \quad \text{Nat/Sec/Hz,} \qquad (2.15)$$

where P_j is the power allocated to data stream j, and $\sum_{j=1}^{M} P_j \leq P_T$. Note that (2.15) is based on the channel model (2.1), where the power of the noise is normalized. To maximize (2.15), the power can be allocated using water-filling [19].

In the proposed algorithm, it is assumed the CSI is available at the transmitter which necessitates a high-data-rate feedback link. In Section 2.6, the proposed algorithm is modified to reduce the rate of the feedback at the cost of adding some hand-shaking steps to the algorithm.

2.4 Performance Analysis

In this section, the performance of the proposed algorithm is investigated. To simplify the analysis, we assume: (i) available power P_T is divided equally among the active users, (ii) at most one data stream is assigned to each user. To impose the second restriction, we can simply eliminate a user, whenever that user is allocated one data stream in Step 2 of the algorithm. It is apparent that the sum-rate of the system with these two restrictions lower-bounds the maximum sum-rate achievable by the proposed algorithm. Although these assumptions simplify the derivations, it is shown that the results dealing with the asymptotic sum-rate remain valid even if we relax

these restrictive assumptions.

To study the performance of the system, we first derive an upper-bound on the outage probability of each sub-channel. Using the derived upper-bound, we study the diversity and asymptotic sum-rate achieved by the proposed algorithm. In this study, it is assumed that all users are equipped with N receive antennas.

2.4.1   Outage Probability

The outage probability of sub-channel j is defined as $\Pr(\sigma_j^2 < z)$, $j = 1, \ldots, M$, for a given z. For σ_1^2, the derivation of the outage probability $\Pr(\sigma_1^2 < z)$ is strait-forward. In the proposed algorithm, for $j = 1$, we have $\boldsymbol{\Xi} = [0]_{M \times M}$. From (2.3), we have

$$\sigma_1^2 = \max_{1 \leq r \leq K} \max_{\mathbf{x}} \mathbf{x}^\dagger \mathbf{H}_r^\dagger \mathbf{H}_r \mathbf{x}. \tag{2.16}$$

$$s.t. \qquad \mathbf{x}^\dagger \mathbf{x} = 1$$

Referring to [25], $\max_{\mathbf{x}} \mathbf{x}^\dagger \mathbf{H}_r^\dagger \mathbf{H}_r \mathbf{x}$ subject to $\mathbf{x}^\dagger \mathbf{x} = 1$ is equal to the maximum eigenvalue of the matrix $\mathbf{H}_r^\dagger \mathbf{H}_r$. Therefore, (2.16) can be written as

$$\sigma_1^2 = \max \left\{ \lambda_{\max}(\mathbf{H}_1^\dagger \mathbf{H}_1), \ldots, \lambda_{\max}(\mathbf{H}_K^\dagger \mathbf{H}_K) \right\}, \tag{2.17}$$

where $\lambda_{\max}(\mathbf{H}_r^\dagger \mathbf{H}_r)$ denotes the maximum eigenvalue of $\mathbf{H}_r^\dagger \mathbf{H}_r$. By assuming Rayleigh fading channel, the entries of $\mathbf{H}_r$, $r = 1, \ldots, K$, have independent normal distribution with zero-mean and unit-variance. Therefore, $\mathbf{H}_r^\dagger \mathbf{H}_r$ follows a Wishart distribution [31]. The distribution of the maximum eigenvalue of a Wishart matrix is formulated in the following lemma.

Lemma 2.3. *[31, 33] Assume that the entries of $A \in \mathcal{C}^{\tilde{m} \times \tilde{n}}$ have a zero mean, unit variance Gaussian distribution; then, the cumulative distribution function (CDF) of the maximum eigenvalue of the matrix $A^\dagger A$ is equal to*

$$G_{\tilde{m},\tilde{n}}(z) = \Pr\left\{\lambda_{max}(A^\dagger A) \leq z\right\} = \frac{1}{\prod_{k=1}^n \Gamma(m-k+1)\Gamma(n-k+1)} \det(\overline{\boldsymbol{\Psi}}), \quad (2.18)$$

where $n = \min\{\tilde{m}, \tilde{n}\}$, $m = \max\{\tilde{m}, \tilde{n}\}$, and $\overline{\boldsymbol{\Psi}}$ is an $n \times n$ Hankel matrix which is a function of $z \in [0, \infty)$ defined as

$$\overline{\boldsymbol{\Psi}} = [\gamma(m-n+p+q-1,z)]_{(p,q)}^{n \times n}, \qquad p,q = 1, \ldots, n, \quad (2.19)$$

and γ is incomplete gamma function

$$\gamma(n+1,z) = n!\left(1 - e^{-z}\sum_{k=1}^n \frac{z^k}{k!}\right). \quad (2.20)$$

Since $\lambda_{\max}(\mathbf{H}_r^\dagger \mathbf{H}_r)$ for different r's, $1 \leq r \leq K$, are i.i.d random variables, using (2.17) and Lemma A.1 in Appendix A, we obtain

$$\Pr(\sigma_1^2 \leq z) = G_{N,M}^K(z). \quad (2.21)$$

Unlike $\Pr(\sigma_1^2 \leq z)$, the derivation of the outage probability for σ_j^2, $j = 2, \ldots, M$, is not simple. Alternatively, we derive an upper-bound for the outage probability of each sub-channel using the CDF of the axillary variables $\widehat{\sigma}_j^2$, $j = 2, \ldots, M$, defined as follows. Let us order the values of $\max_{\mathbf{x}} \mathbf{x}^\dagger \mathbf{H}_r^\dagger \mathbf{H}_r \mathbf{x}$, $r = 1, \ldots, K$, subject to $\mathbf{x}^\dagger \mathbf{x} = 1$ and $\widehat{\boldsymbol{\Xi}}_j^\dagger \mathbf{x} = 0$, where $\widehat{\boldsymbol{\Xi}}_j$ is a unitary matrix, $j = 2, \ldots, M$, selected randomly from $\mathcal{OC}^{M \times (j-1)}$, the set of $M \times (j-1)$ complex unitary matrices. $\widehat{\sigma}_j^2$ is selected as the jth

largest element at this ordered set, i.e.

$$\widehat{\sigma}_j^2 = j^{\text{th}} \max_{r,\ 1 \leq r \leq K} \quad \max_{\mathbf{x}} \mathbf{x}^\dagger \mathbf{H}_r^\dagger \mathbf{H}_r \mathbf{x}.$$

$$s.t. \qquad \mathbf{x}^\dagger \mathbf{x} = 1$$

$$\widehat{\boldsymbol{\Xi}}_j^\dagger \mathbf{x} = 0 \tag{2.22}$$

Lemma 2.4. *The outage probability of the sub-channel j is upper-bounded by the CDF of $\widehat{\sigma}_j^2$. In other word,*

$$\Pr(\sigma_j^2 \leq z) \leq \Pr(\widehat{\sigma}_j^2 \leq z). \tag{2.23}$$

Proof. Assume that users $\pi(1), \ldots, \pi(M)$ corresponding to the MVs $\mathbf{v}_1, \ldots, \mathbf{v}_M$ have been selected. According to the proposed algorithm, $\mathbf{v}_j$, $j = 1, \ldots, M$, is in the $(M - j + 1)$-dimensional hyperplane Ω_j which is the intersection of the null spaces of the previously selected MVs, i.e.

$$\mathbf{v}_j \in \Omega_j = \left\{ \mathbf{x} \quad | \quad \mathbf{v}_1^\dagger \mathbf{x} = 0, \ldots, \mathbf{v}_{j-1}^\dagger \mathbf{x} = 0 \right\} \tag{2.24}$$

Fix the hyperplane Ω_j, and multiply the channel matrix $\mathbf{H}_{\pi(i)}$, for $i = 1, \ldots, j-1$, with a unitary matrix $\widetilde{\boldsymbol{\Phi}}_i$ selected randomly and uniformly from $\mathcal{OC}^{M \times M}$, the set of $M \times M$ complex unitary matrices.

$$\widetilde{\mathbf{H}}_{\pi(i)} = \mathbf{H}_{\pi(i)} \widetilde{\boldsymbol{\Phi}}_i, \quad i = 1, \ldots, j-1. \tag{2.25}$$

It is apparent that $\widetilde{\mathbf{H}}_{\pi(i)}$ has the gain of σ_i^2 in the direction $\widetilde{\mathbf{v}}_i = \widetilde{\boldsymbol{\Phi}}_i^\dagger \mathbf{v}_i$.

Let us define $\bar{\sigma}_j^2$ as follows:

$$\bar{\sigma}_j^2 = j^{\text{th}} \max_{r,\, 1 \leq r \leq K} \quad \max_{\mathbf{x}} \mathbf{x}^\dagger \widetilde{\mathbf{H}}_r^\dagger \widetilde{\mathbf{H}}_r \mathbf{x}.$$

$$s.t. \qquad \mathbf{x}^\dagger \mathbf{x} = 1$$

$$\mathbf{x} \in \Omega_j \qquad\qquad (2.26)$$

where $\widetilde{\mathbf{H}}_r = \mathbf{H}_r$, for $r = 1, \ldots, K$, $r \notin \{\pi(1), \ldots, \pi(j-1)\}$.

Let us define the set $\mathcal{D}$, with cardinality of $K - j + 1$, of: $\max_{\mathbf{x}} \mathbf{x}^\dagger \mathbf{H}_r^\dagger \mathbf{H}_r \mathbf{x}$ subject to $\mathbf{x}^\dagger \mathbf{x} = 1$, $\mathbf{x} \in \Omega_j$ for $r = 1, \ldots, K$, $r \notin \{\pi(1), \ldots, \pi(j-1)\}$. Similarly, let us define the set $\overline{\mathcal{D}}$, with cardinality of K, of: $\max_{\mathbf{x}} \mathbf{x}^\dagger \widetilde{\mathbf{H}}_r^\dagger \widetilde{\mathbf{H}}_r \mathbf{x}$ subject to $\mathbf{x}^\dagger \mathbf{x} = 1$, $\mathbf{x} \in \Omega_j$ for $r = 1, \ldots, K$. Regarding (2.3) and (2.26), we have $\sigma_j^2 = \max \mathcal{D}$, and $\bar{\sigma}_j^2 = j^{th} \max \overline{\mathcal{D}}$. Since $\widetilde{\mathbf{H}}_r = \mathbf{H}_r$ for $r \notin \{\pi(1), \ldots, \pi(j-1)\}$, the set $\overline{\mathcal{D}}$ is equal to the union of $\mathcal{D}$ and $j - 1$ values of $\max_{\mathbf{x}} \mathbf{x}^\dagger \widetilde{\mathbf{H}}_r^\dagger \widetilde{\mathbf{H}}_r \mathbf{x}$ subject to $\mathbf{x}^\dagger \mathbf{x} = 1$, $\mathbf{x} \in \Omega_j$ for $r \in \{\pi(1), \ldots, \pi(j-1)\}$. It follows that $\sigma_j^2 \geq \bar{\sigma}_j^2$. Consequently, for a given real number z, $\Pr(\sigma_j^2 \leq z) \leq \Pr(\bar{\sigma}_j^2 \leq z)$.

We claim that $\bar{\sigma}_j^2$ in (2.26) has the same distribution as $\hat{\sigma}_j^2$ in (2.22). As mentioned before, Ω_j is the intersection of the null spaces of $\mathbf{v}_i$, $i = 1, \ldots, j-1$. Since the channel matrices $\mathbf{H}_{\pi(i)}$, $i = 1, \ldots, j - 1$, are randomized using the unitary random matrices $\widetilde{\boldsymbol{\Phi}}_i^\dagger$, the vector space Ω_j is a random and independent hyperplane with respect to $\widetilde{\mathbf{H}}_r$, $r = 1, \ldots, K$. Furthermore, since the channel matrices $\mathbf{H}_r$, $r = 1, \ldots, K$, are multiplied with unitary matrices ($\widetilde{\boldsymbol{\Phi}}_i^\dagger$, for $\mathbf{H}_{\pi(i)}$, $i = 1, \ldots, j-1$, and identity matrix for the rest), the entries of $\widetilde{\mathbf{H}}_r$, $r = 1, \ldots, K$, have the same distribution as the entries of $\mathbf{H}_r$ (normal

i.i.d distribution with zero mean and unit variance). Therefore, in both (2.22) and (2.26), we have K matrices with the same distribution while the inner maximization is performed in an $(M - j + 1)$-dimensional hyperplane which is random and independent of the channel matrices. Thus, each realization in problem (2.22) corresponds to a realization in problem (2.26) with the same probability. Consequently, $\bar{\sigma}_j^2$ and $\hat{\sigma}_j^2$ have the same distribution. □

The following lemma helps to derive $\Pr(\hat{\sigma}_j^2 \leq z)$.

Lemma 2.5. *Consider a vector space $\widehat{\Omega}$ defined by*

$$\widehat{\Omega} = \{\mathbf{x} \quad | \quad \mathbf{x} \in \mathcal{C}^{M \times 1}, \quad \widehat{\mathbf{\Xi}}^\dagger \mathbf{x} = 0\}, \tag{2.27}$$

where $\widehat{\mathbf{\Xi}}$ is a complex matrix. Assume that $\widehat{\Omega}$ is spanned by a set of orthogonal vectors $\{\widehat{\boldsymbol{\phi}}^{(1)}, \widehat{\boldsymbol{\phi}}^{(2)}, \ldots, \widehat{\boldsymbol{\phi}}^{(\nu)}\}$, where $\nu \leq M$. Then, given the complex matrix $\mathbf{H}$, the result of the following optimization,

$$\max_{\mathbf{x}} \quad \mathbf{x}^\dagger \mathbf{H}^\dagger \mathbf{H} \mathbf{x},$$

$$s.t. \quad \mathbf{x}^\dagger \mathbf{x} = 1$$

$$\mathbf{x} \in \widehat{\Omega}, \tag{2.28}$$

is equal to $\lambda_{\max}(\widehat{\mathbf{H}}^\dagger \widehat{\mathbf{H}})$, the maximum eigenvalue of matrix $\widehat{\mathbf{H}}^\dagger \widehat{\mathbf{H}}$, where

$$\widehat{\mathbf{H}} = \mathbf{H} \widehat{\mathbf{\Phi}} \tag{2.29}$$

and

$$\widehat{\mathbf{\Phi}} = [\widehat{\boldsymbol{\phi}}^{(1)}, \widehat{\boldsymbol{\phi}}^{(2)}, \ldots, \widehat{\boldsymbol{\phi}}^{(\nu)}]. \tag{2.30}$$

Proof. $\lambda_{\max}(\widehat{\mathbf{H}}^\dagger\widehat{\mathbf{H}})$, the maximum eigenvalue of matrix $\widehat{\mathbf{H}}^\dagger\widehat{\mathbf{H}}$ is equal to [25],

$$\lambda_{\max}(\widehat{\mathbf{H}}^\dagger\widehat{\mathbf{H}}) = \max_{\mathbf{y}} \mathbf{y}^\dagger\widehat{\mathbf{H}}^\dagger\widehat{\mathbf{H}}\mathbf{y}.$$

$$s.t. \qquad \mathbf{y}^\dagger\mathbf{y} = 1 \tag{2.31}$$

If (2.29) is substituted into (2.31), we obtain

$$\lambda_{\max}(\widehat{\mathbf{H}}^\dagger\widehat{\mathbf{H}}) = \max_{\mathbf{y}} \mathbf{y}^\dagger\widehat{\boldsymbol{\Phi}}^\dagger\mathbf{H}^\dagger\mathbf{H}\widehat{\boldsymbol{\Phi}}\mathbf{y}.$$

$$s.t. \qquad \mathbf{y}^\dagger\mathbf{y} = 1. \tag{2.32}$$

Let $\mathbf{x} = \widehat{\boldsymbol{\Phi}}\mathbf{y} = y_1\widehat{\boldsymbol{\phi}}_1 + \ldots + y_\nu\widehat{\boldsymbol{\phi}}_\nu$. Since $\{\widehat{\boldsymbol{\phi}}^{(1)}, \widehat{\boldsymbol{\phi}}^{(2)}, \ldots, \widehat{\boldsymbol{\phi}}^{(\nu)}\}$ is an orthogonal vector set, then $\mathbf{y}^\dagger\mathbf{y} = \mathbf{x}^\dagger\mathbf{x}$. Also, $\mathbf{x}$ is a linear combination of vectors $\{\widehat{\boldsymbol{\phi}}^{(1)}, \widehat{\boldsymbol{\phi}}^{(2)}, \ldots, \widehat{\boldsymbol{\phi}}^{(\nu)}\}$; therefore, $\mathbf{x} \in \widehat{\Omega}$. Consequently,

$$\lambda_{\max}(\widehat{\mathbf{H}}^\dagger\widehat{\mathbf{H}}) = \max_{\mathbf{x}} \mathbf{x}^\dagger\mathbf{H}^\dagger\mathbf{H}\mathbf{x}.$$

$$s.t. \qquad \mathbf{x}^\dagger\mathbf{x} = 1$$

$$\mathbf{x} \in \widehat{\Omega}. \tag{2.33}$$

$\square$

According to Lemma 2.5, $\widehat{\sigma}_j^2$ in (2.22) is equal to

$$\widehat{\sigma}_j^2 = j^{\text{th}} \max \left\{ \lambda_{\max}(\widehat{\mathbf{H}}_{1,j}^\dagger\widehat{\mathbf{H}}_{1,j}), \ldots, \lambda_{\max}(\widehat{\mathbf{H}}_{K,j}^\dagger\widehat{\mathbf{H}}_{K,j}) \right\}, \tag{2.34}$$

where $\lambda_{\max}(\widehat{\mathbf{H}}_{r,j}^\dagger\widehat{\mathbf{H}}_{r,j})$ is the maximum eigenvalue of $\widehat{\mathbf{H}}_{r,j}^\dagger\widehat{\mathbf{H}}_{r,j}$, $\widehat{\mathbf{H}}_{r,j} = \mathbf{H}_r\widehat{\boldsymbol{\Phi}}_j$, and $\widehat{\boldsymbol{\Phi}}_j$ is a matrix with orthogonal columns which span the complex vector space $\widehat{\Omega}_j = \{\mathbf{x}|\mathbf{x} \in$

$\mathcal{C}^{M \times 1}, \quad \widehat{\boldsymbol{\Xi}}_j^{\dagger} \mathbf{x} = 0\}$. Note that in (2.22), $\widehat{\boldsymbol{\Xi}}_j$ has $j-1$ non-zero orthogonal columns. Therefore, the dimension of the complex vector space $\widehat{\Omega}_j$ is $M - (j-1)$, resulting in $\widehat{\boldsymbol{\Phi}}_j \in \mathcal{C}^{M \times (M-j+1)}$. Since the columns of $\widehat{\boldsymbol{\Phi}}_j$ are orthonormal and the entries of $\mathbf{H}_r$ have independent unit variance Gaussian distributions (Rayleigh channel), the entries of $\widehat{\mathbf{H}}_{r,j} \in \mathcal{C}^{N \times (M-j+1)}$ have independent unit variance Gaussian distributions. Furthermore, it is easy to see that $\widehat{\mathbf{H}}_{r,j}$, $r = 1, \ldots, K$, are independent for different r. Consequently, according to the definition, $\widehat{\mathbf{H}}_{r,j}^{\dagger} \widehat{\mathbf{H}}_{r,j}$, $r = 1, \ldots, K$, have Wishart distribution. Therefore, by using Lemma 2.3, we obtain

$$\Pr\left\{ \lambda_{\max}(\widehat{\mathbf{H}}_{r,j}^{\dagger} \widehat{\mathbf{H}}_{r,j}) \le z \right\} = G_{N,M-j+1}(z). \qquad (2.35)$$

Using (2.34), (2.35), Lemma A.1 in Appendix A, and regarding the independency of $\widehat{\mathbf{H}}_{r,j}$ for different r's, we obtain

$$\Pr(\widehat{\sigma}_j^2 \le z) = \sum_{i=K-j+1}^{K} \binom{K}{i} G_{N,M-j+1}^i(z)[1 - G_{N,M-j+1}(z)]^{K-i}. \qquad (2.36)$$

By using (2.21), (2.36), and Lemma 2.4, we have

Theorem 2.6.

$$\Pr(\sigma_j^2 \le z) \le \sum_{i=K-j+1}^{K} \binom{K}{i} G_{N,M-j+1}^i(z)[1 - G_{N,M-j+1}(z)]^{K-i} \qquad (2.37)$$

with equality if $j = 1$.

Theorem 2.6 provides a lower-bound on the performance of the proposed method. In the following, we use the above result to investigate the achieved diversity and the asymptotic sum-rate.

2.4.2 Diversity Analysis

The diversity order in a wireless channel is equal to the asymptotic slope $(z \to 0)$ of the outage probability curve. This quantity determines the asymptotic slope of the curve of the symbol error rate versus signal-to-noise-ratio. In the following theorem, we use this definition to establish the diversity order of the jth data stream.

Theorem 2.7. *Sub-channel j achieves the diversity order at least equal to $(K - j + 1)(M - j + 1)N$.*

Proof. To derive the minimum diversity of the sub-channel j, we first obtain the limiting function $(z \to 0)$ of the introduced upper-bound on $\Pr(\sigma_j^2 \leq z)$. In Appendix B, it is shown that

$$\lim_{z \to 0} G_{\tilde{m},\tilde{n}}(z) = c_{\tilde{m},\tilde{n}} z^{\tilde{m}\tilde{n}} \left(1 + O(z)\right), \tag{2.38}$$

where $c_{\tilde{m},\tilde{n}}$ is defined in (B.9). Using (2.38) and (2.37), we have,

$$\lim_{z \to 0} \Pr(\sigma_j^2 < z) \leq \binom{K}{K-j+1} c_{N,M-j+1}^{K-j+1} z^{(K-j+1)N(M-j+1)} \left(1 + O(z)\right), \tag{2.39}$$

where $c_{N,M-j+1}$ is equal to $c_{\tilde{m},\tilde{n}}$ by substituting N for $\tilde{m}$ and $M - j + 1$ for $\tilde{n}$ in (B.9).

Using (2.39), we conclude that the sub-channel j, $1 \leq j \leq M$, achieves the minimum diversity order of $(K - j + 1)N(M - j + 1)$. $\qquad \square$

Theorem (2.7) states that the diversity of all the sub-channels is proportional to the number of users K and number of receive antennas N. This means that the pro-

posed method exploits both multiuser and receive diversities. In addition, the transmit

diversity of sub-channel j is equal to $M - j + 1$.

Note that if we use a codebook with a fixed rate ϑ_j for the jth sub-channel and

the channels are constant for a codeword duration, the probability of error for the

sub-channel j, Pe_j, is obtained by,

$$\text{Pe}_j = \Pr\left(\log(1 + \frac{P_T}{M}\sigma_j^2) < \vartheta_j\right) \tag{2.40}$$

$$= \Pr\left(\sigma_j^2 < \frac{\exp(\vartheta_j) - 1}{\frac{P_T}{M}}\right) \tag{2.41}$$

$$\leq \binom{K}{K - j + 1} c_{N,M-j+1}^{K-j+1} \left(\frac{\exp(\vartheta_j) - 1}{\frac{P_T}{M}}\right)^{(K-j+1)N(M-j+1)}. \tag{2.42}$$

Therefore, the slope of the curve Pe_j versus P_T is at most $(K - j + 1)N(M - j + 1)$.

2.4.3 Asymptotic Sum-Rate Analysis

By using (2.15) and Theorem 2.6, a lower-bound on the average sum-rate of the pro-

posed method can be computed. However, an examination of the asymptotic behavior

$(K \to \infty)$ of the sum-rate provides insight into the performance of the proposed al-

gorithm. For this investigation, we apply some results from theory of extreme order

statistics. Appendix A contains some theorems that will be used in our following dis-

cussion.

As mentioned in (2.17), σ_1^2 is equal to the maximum of K i.i.d random variables

with common CDF of $G_{N,M}(z)$. Similarly, $\widehat{\sigma}_j^2$, $j = 2, \ldots, M$, in (2.34) is equal to the

j^{th} largest of K i.i.d random variables with common CDF of $G_{N,M-j+1}(z)$. In general, the behavior of the jth largest of K i.i.d random variables with common CDF $F(z)$ depends on the tail of the $F(z)$ (large z). In Appendix C, it is shown that

$$G_{\tilde{m},\tilde{n}}(z) = 1 - \frac{e^{-z}z^{\tilde{m}+\tilde{n}-2}}{\Gamma(\tilde{m})\Gamma(\tilde{n})}\left(1 + O(z^{-1}e^{-z})\right), \qquad (2.43)$$

which has the form of $F(z)$ in (A.13) for large z. Using (2.43) and applying Lemma A.5 from Appendix A with $\tilde{\alpha} = M + N - 2$ and $\tilde{\beta} = \Gamma(M)\Gamma(N)$ for σ_1^2, we obtain

$$\Pr\left\{\hat{\eta}_1 - \log\log(\sqrt{K}) \leq \sigma_1^2 \leq \hat{\eta}_1 + \log\log(\sqrt{K})\right\} \geq 1 - O\left(\frac{1}{\log K}\right), \qquad (2.44)$$

where

$$\hat{\eta}_1 = \log\left(\frac{K}{\Gamma(M)\Gamma(N)}\right) - (M + N - 2)\log\log\left(\frac{K}{\Gamma(M)\Gamma(N)}\right). \qquad (2.45)$$

Similarly, using (2.43) and applying Lemma A.5 with $\tilde{\alpha} = M + N - j - 1$ and $\tilde{\beta} = \Gamma(M - j + 1)\Gamma(N)$ for $\hat{\sigma}_j^2$, $j = 2, \ldots, M$, we obtain

$$\Pr\left\{\hat{\eta}_j - \log\log(\sqrt{K}) \leq \hat{\sigma}_j^2 \leq \hat{\eta}_j + \log\log(\sqrt{K})\right\} \geq 1 - O\left(\frac{1}{\log K}\right), \qquad (2.46)$$

where

$$\hat{\eta}_j = \log\left(\frac{K}{\Gamma(M - j + 1)\Gamma(N)}\right) - (M+N-1-j)\log\log\left(\frac{K}{\Gamma(M - j + 1)\Gamma(N)}\right). \quad (2.47)$$

Lemma 2.8. *For σ_j^2, $j = 1, \ldots, M$, we have,*

$$\Pr\left\{\hat{\eta}_j - \log\log(\sqrt{K}) \leq \sigma_j^2 \leq \hat{\eta}_1 + \log\log(\sqrt{K})\right\} \geq 1 - O\left(\frac{1}{\log K}\right). \qquad (2.48)$$

Proof. For $j = 1$, (2.48) is the same as (2.44). For $j = 2, \ldots, M$, the proof is as follows. From (2.46), we have

$$\Pr\left\{\hat{\eta}_j - \log\log(\sqrt{K}) \leq \hat{\sigma}_j^2\right\} \geq 1 - O\left(\frac{1}{\log K}\right). \tag{2.49}$$

Using (2.49) and Lemma 2.4, we obtain

$$\Pr\left\{\hat{\eta}_j - \log\log(\sqrt{K}) \leq \sigma_j^2\right\} \geq 1 - O\left(\frac{1}{\log K}\right). \tag{2.50}$$

On the other hand, from (2.44), we have

$$\Pr\left\{\sigma_1^2 \leq \hat{\eta}_1 + \log\log(\sqrt{K})\right\} \geq 1 - O\left(\frac{1}{\log K}\right). \tag{2.51}$$

It is easy to see that

$$\sigma_1^2 \geq \sigma_2^2 \geq \ldots \geq \sigma_M^2. \tag{2.52}$$

Using (2.51) and (2.52), we have,

$$\Pr\left\{\sigma_j^2 \leq \hat{\eta}_1 + \log\log(\sqrt{K})\right\} \geq 1 - O\left(\frac{1}{\log K}\right). \tag{2.53}$$

Equations (2.50) and (2.53) result in (2.48). This conclusion comes from the fact that if A and B are two events with $\Pr(A) \geq 1 - \epsilon_1$ and $\Pr(B) \geq 1 - \epsilon_2$, then $\Pr(A \bigcap B) \geq 1 - \epsilon_1 - \epsilon_2$. $\square$

Using Lemma 2.8, we can prove the following theorem.

Theorem 2.9.

$$\lim_{K \to \infty} \frac{R}{M \log[\frac{P_T}{M} \log(K)]} = 1, \tag{2.54}$$

with probability one, where R is the sum-rate of the proposed method. In addition,

$$\lim_{K \to \infty} R_{Sum\text{-}Capacity} - R \longrightarrow 0, \tag{2.55}$$

with probability one, where $R_{Sum\text{-}Capacity}$ indicates the sum-capacity of the MIMO broad-cast channel.

Proof. Since $\log(.)$ is an increasing function and using (2.48), we have,

$$\Pr\left\{ \log\left(1 + \frac{P_T}{M}[\hat{\eta}_j - \log\log\sqrt{K}]\right) \right.$$
$$\leq \log(1 + \frac{P_T}{M}\sigma_j^2)$$
$$\left. \leq \log\left(1 + \frac{P_T}{M}[\hat{\eta}_1 + \log\log\sqrt{K}]\right) \right\}$$
$$\geq 1 - O\left(\frac{1}{\log K}\right). \tag{2.56}$$

Consequently,

$$\lim_{K \to \infty} \Pr\left\{ \frac{\log\left(1 + \frac{P_T}{M}[\hat{\eta}_j - \log\log\sqrt{K}]\right)}{\log[\frac{P_T}{M}\log(K)]} \right.$$
$$\leq \frac{\log(1 + \frac{P_T}{M}\sigma_j^2)}{\log[\frac{P_T}{M}\log(K)]}$$
$$\left. \leq \frac{\log_2\left(1 + \frac{P_T}{M}[\hat{\eta}_1 + \log\log\sqrt{K}]\right)}{\log[\frac{P_T}{M}\log(K)]} \right\}$$
$$\geq 1 - O\left(\frac{1}{\log K}\right). \tag{2.57}$$

Using (2.45) and (2.47), we conclude that the left hand side and the right hand side of the inequalities inside $\Pr$ in (2.57) tend to the same value of one as $K \to \infty$, therefore

$$\lim_{K \to \infty} \frac{\log(1 + \frac{P_T}{M}\sigma_j^2)}{\log(\frac{P_T}{M}\log K)} = 1, \tag{2.58}$$

with probability one.

Equation (2.58) indicates that the rate of each sub-channel attains $\log[\frac{P_T}{M}\log(K)]$, when $K \to \infty$. Using (2.15), the sum-rate of the proposed method achieves $M\log[\frac{P_T}{M}\log(K)]$.

On the other hand, according to (2.56),

$$\Pr\left\{\log\left(1 + \frac{P_T}{M}\left[\hat{\eta}_j - \log\log\sqrt{K}\right]\right) \le \log\left(1 + \frac{P_T}{M}\sigma_j^2\right)\right\} \ge 1 - O\left(\frac{1}{\log K}\right). \quad (2.59)$$

In [52], it is shown that,

$$\Pr\left\{\frac{R_{\text{Sum-Capacity}}}{M} \le \log\left(1 + \frac{P_T}{M}\left[\log(KN) + O(\log\log[K])\right]\right)\right\} \ge 1 - O\left(\frac{1}{\log^2 K}\right). \quad (2.60)$$

As mentioned before, if A and B are two events with $\Pr(A) \ge 1 - \epsilon_1$ and $\Pr(B) \ge 1 - \epsilon_2$, then $\Pr(A \bigcap B) \ge 1 - \epsilon_1 - \epsilon_2$. Therefore, the probability that the inequalities inside Pr in (2.59) and (2.60) are both valid is greater than $1 - O\left(\frac{1}{\log K}\right) - O\left(\frac{1}{\log^2 K}\right)$. Subtracting these two inequalities, we obtain

$$\Pr\left\{\log(1 + \frac{P_T}{M}\sigma_j^2) - \frac{R_{\text{Sum-Capacity}}}{M} \ge \right.$$
$$\log\left(1 + \frac{P_T}{M}\left[\hat{\eta}_j - \log\log\sqrt{K}\right]\right) - \left. \log\left(1 + \frac{P_T}{M}\left[\log(KN) + O(\log\log[K])\right]\right)\right\}$$
$$\ge 1 - O\left(\frac{1}{\log K}\right) - O\left(\frac{1}{\log^2 K}\right). \quad (2.61)$$

Using (2.47), we conclude that the right side of the inequality inside Pr in (2.61) tends to zero as $K \to \infty$. Consequently, for large K, with probability one, we have

$$0 \le \log(1 + \frac{P_T}{M}\sigma_j^2) - \frac{R_{\text{Sum-Capacity}}}{M}, \quad j = 1, \ldots, M. \quad (2.62)$$

Using (2.62), we obtain that when $K \to \infty$, $R \geq R_{\text{Sum-Capacity}}$. Since $R_{\text{Sum-Capacity}}$ provides an upper bound on the sum-rate of any algorithm , we obtain

$$\lim_{K \to \infty} R_{\text{Sum-Capacity}} - R = 0, \tag{2.63}$$

with probability one. □

Equation (2.54) indicates that the average sum-rate of the proposed method increases linearly with the number of transmit antennas. Furthermore, the increase with the number of users K is proportional to $\log \log(K)$. In addition, Theorem 2.9 states that for large K, the proposed method achieves the sum-capacity of the MIMO broadcast channel. Note that these results are derived with two assumptions of equal power distribution among active users (no water-filling) and allocation of at most one data stream to each user. Apparently, Theorem 2.9 remains valid even if these two restrictive assumptions are relaxed.

2.5 Simulation Results

In this section, the outage probability and the sum-rate of the proposed method are simulated and compared with the bounds derived by the Theorem 2.6 and with the sum-capacity. In these simulations, the perfect channel state information is assumed to be available at the base station.

Figures 2.1 and 2.2 show the outage probability of each individual sub-channel as

compared with the upper-bound CDFs introduced in Theorem 2.6.
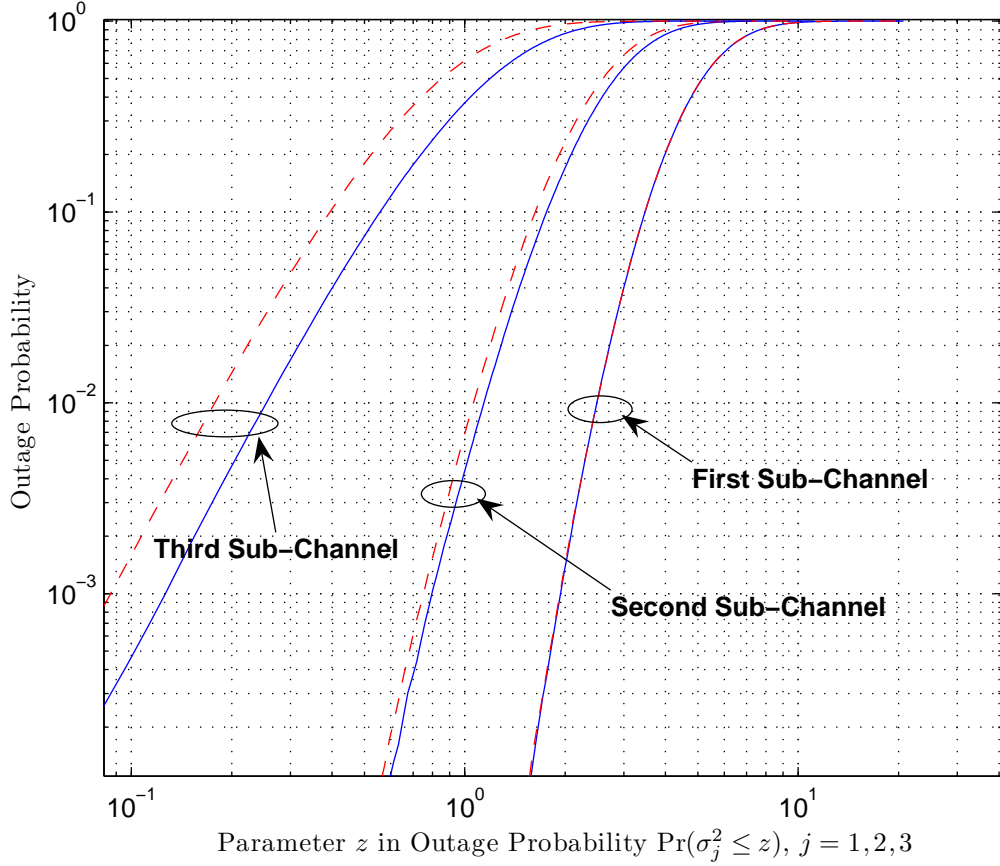
Figure 2.1: Outage Probability for the Sub-Channels (Solid Curves) and the Upper-Bound for Outage Probability (Dashed Curves) – $K = 6$, $M = 3$, $N = 1$.

Figures 2.3 and 2.4 show the sum-rate of the proposed method in comparison with the sum-capacity and the derived lower-bound on sum-rate. In the simulation of the sum-rate, the power is optimally allocated to active users by using the water-filling method, while in the simulation of the lower-bound, the power is divided equally among
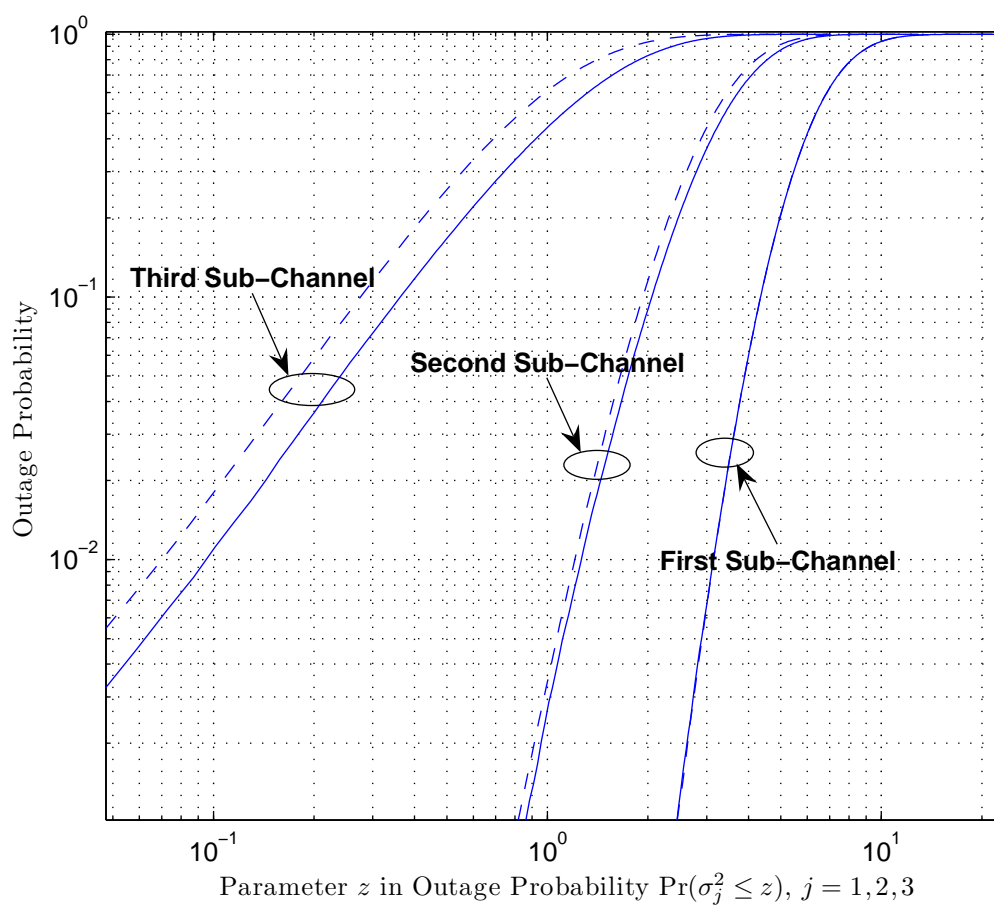
Figure 2.2: Outage Probability for the Sub-Channels (Solid Curves) and the Upper-Bound for Outage Probability (Dashed Curves) – $K = 3$, $M = 3$, $N = 2$.

the sub-channels. To compute the sum-capacity of the MIMO broadcast channel, the algorithm presented in [70] is used.

Figure 2.3 depicts the average sum-rate of the proposed method, the derived lower-bound, and the average sum-capacity versus K (number of users) for different number of receive antennas. This figure shows that the sum-rate of the proposed method is very close to the sum-capacity, even when the number of users is small. Based on this result, we conclude that the major part of the sum-capacity is achieved with only M data streams, regardless of the number of receive antennas. In addition, Fig. 2.3 shows that the derived lower-bound provides an accurate estimate of the sum-rate over a wide range of values for K.

Figure 2.4 shows the sum-rate of the proposed method in comparison with the sum-capacity as well as the derived lower-bound versus the transmit power. It can be seen that the sum-rate of the proposed scheme is very close to the sum-capacity. In addition, Fig. 2.4 shows that the derived lower-bound provides an accurate estimate of the sum-rate for the different power levels.

Figure 2.5 shows the sum-rate of the proposed method versus the values of M (number of transmit antennas). It can be seen that the average sum-rate increases linearly with the number of transmit antennas.
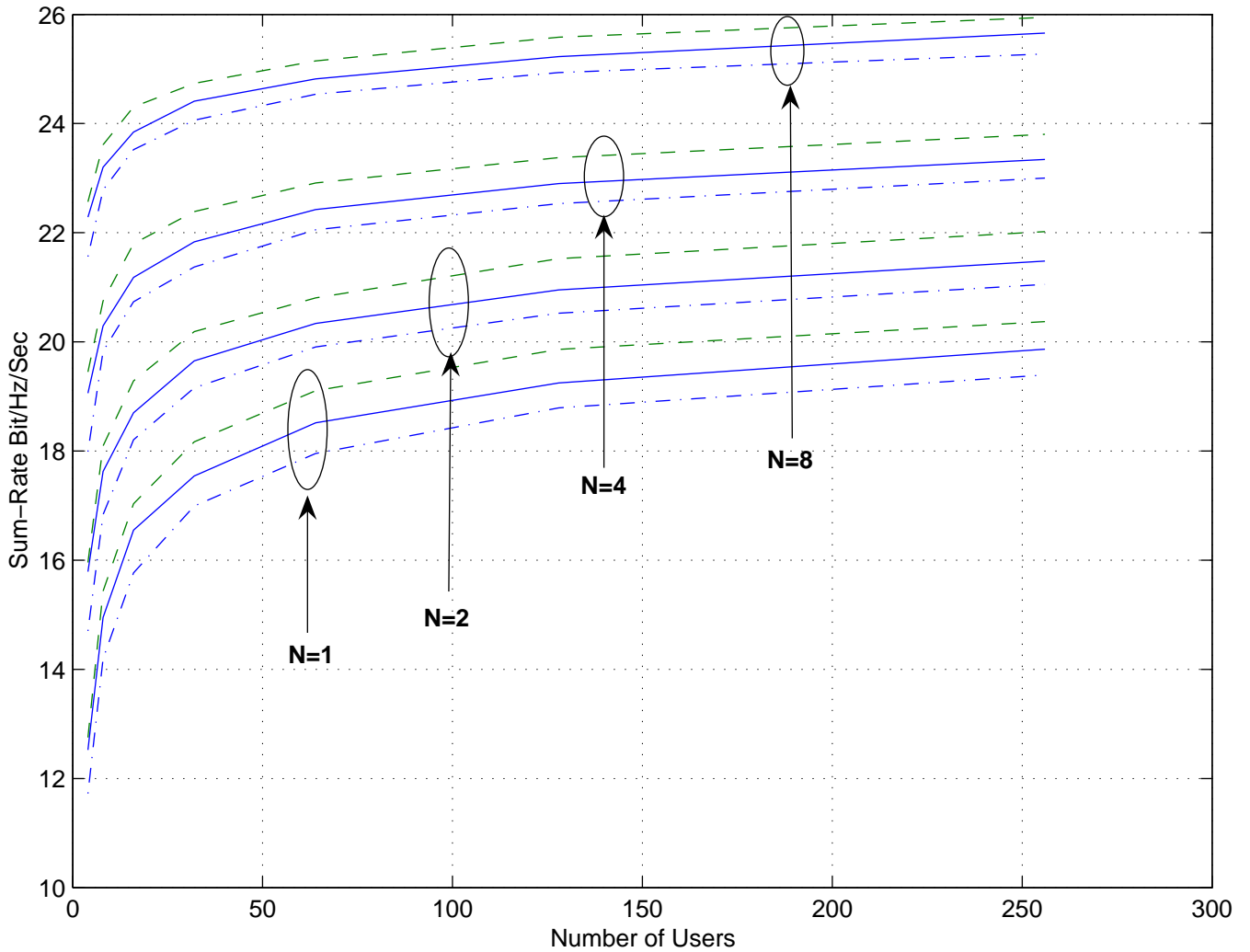
Figure 2.3: Average Sum-Rate of the Proposed Method (Solid Curves), Average Sum-Capacity (Dashed Curves), and Lower-Bound on the Sum-Rate of the Proposed Method (Dash-Dot Curves) – $M = 4$, $P_T = 15$.
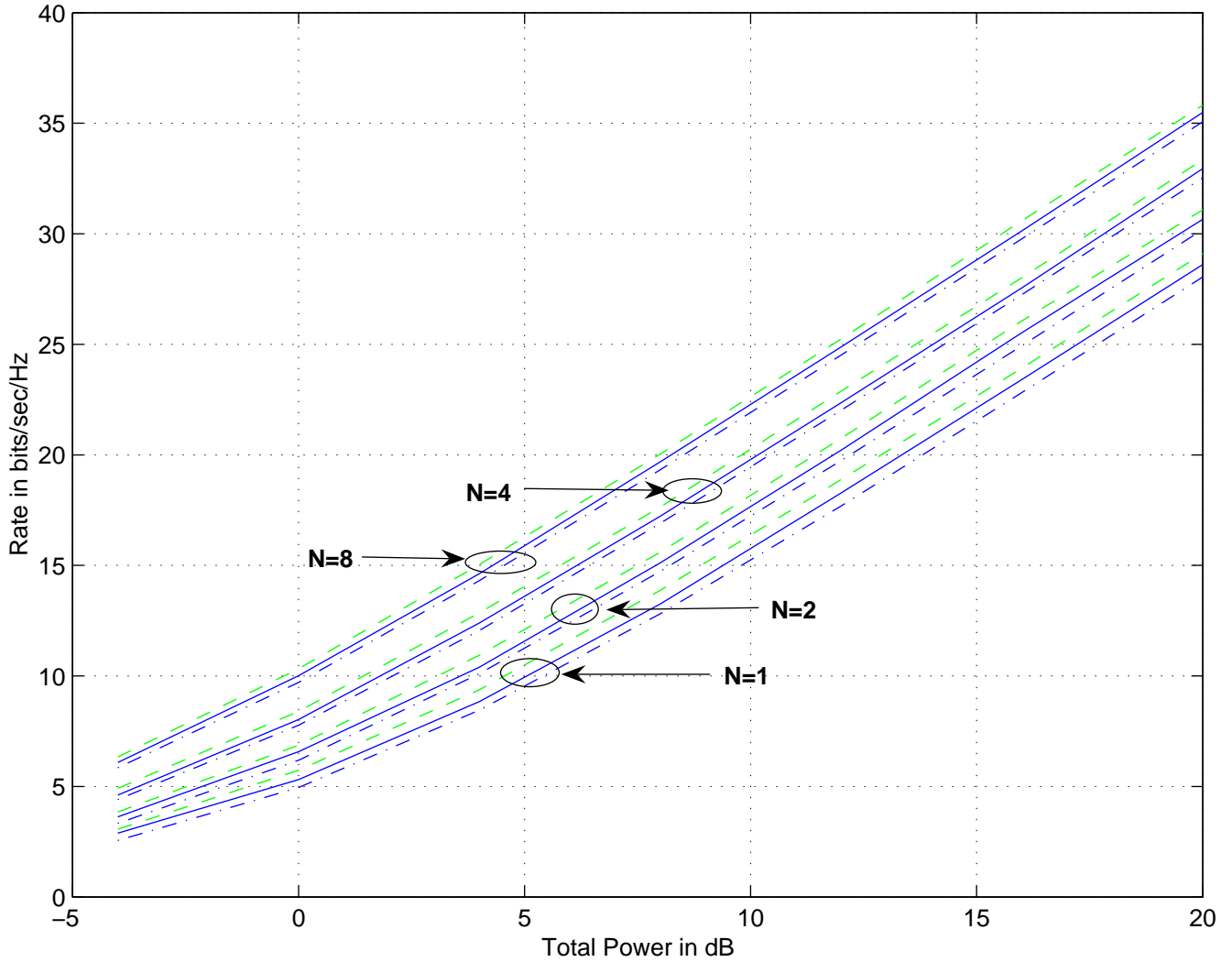
Figure 2.4: Average Sum-Rate of the Proposed Method (Solid Curves), Average Sum-Capacity (Dashed Curves), and Lower-Bound on the Sum-Rate of the Proposed Method (Dash-Dot Curves) – $M = 4$, $K = 40$.
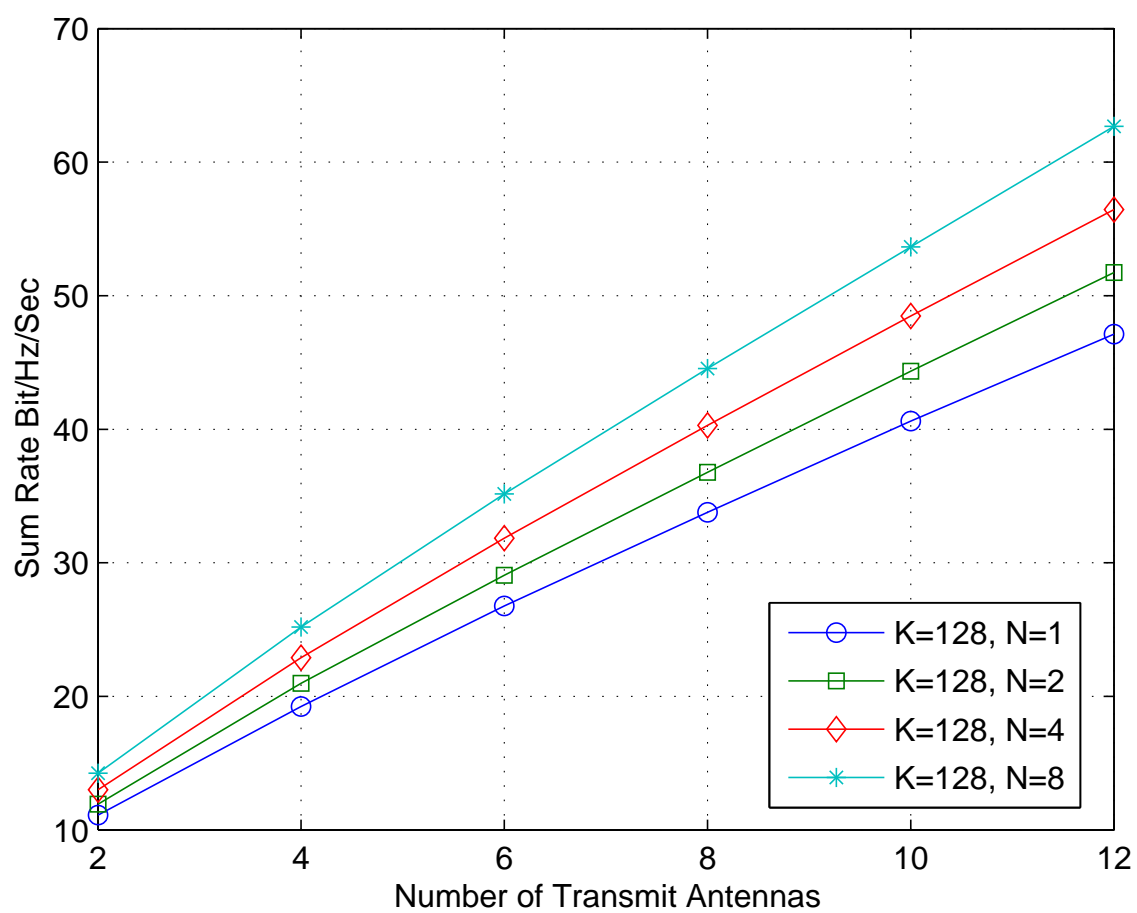
Figure 2.5: Average Sum-Rate of the Proposed Method versus the Number of Transmit Antennas

2.6 Reducing the Feedback Rate

In this section, we modify the proposed algorithm to reduce the rate of the feedback at the cost of adding some hand-shaking steps to the algorithm. As mentioned in Section 2.3, one part of the algorithm is to find the direction in which each user has maximum gain. This part of the processing can be accomplished at the receiver and then if the maximum gain of the user is larger than a given threshold, the gain and the corresponding direction are reported to the transmitter. The base station selects the best user in terms of the largest gain. By using this technique, the complete channel state information is not required at the transmitter and the rate of the feedback is significantly reduced. The details of the algorithm are presented in the following.

Algorithm 2.10.

1. *Set $j = 1$ and $\mathbf{\Xi} = [0]_{M \times M}$.*

2. *The user r, $r = 1, \ldots, K$, calculates $\tilde{\sigma}^2_{r(j)}$, defined as follows:*

$$\tilde{\sigma}^2_{r(j)} = \max_{\mathbf{x}} \mathbf{x}^\dagger \mathbf{H}_r^\dagger \mathbf{H}_r \mathbf{x}.$$

$$s.t. \quad \mathbf{x}^\dagger \mathbf{x} = 1$$

$$\mathbf{\Xi}^\dagger \mathbf{x} = 0. \tag{2.64}$$

$\tilde{\mathbf{v}}_{r(j)}$ represents the optimizing parameter $\mathbf{x}$.

3. *The user r, $r = 1, \ldots, K$, calculates*

$$\tilde{\mathbf{u}}_{r(j)} = \frac{1}{\tilde{\sigma}_{r(j)}} \mathbf{H}_r \tilde{\mathbf{v}}_{r(j)}. \qquad (2.65)$$

4. *The user r, $r = 1, \ldots, K$, sends $\tilde{\sigma}_{r(j)}^2$ and $\tilde{\mathbf{v}}_{r(j)}$ to the base station, if $\tilde{\sigma}_{r(j)}^2 \geq th(j)$. $th(j)$ is a threshold which is predetermined by the base station.*

5. *The base station selects the user with the largest $\tilde{\sigma}_{r(j)}^2$, namely $\pi(j)$. σ_j^2, $\mathbf{v}_j$, and $\mathbf{u}_j$ are the gain, the corresponding MV, and the demodulation vector of the user $\pi(j)$, respectively.*

6. *The $\pi(j)^{th}$ user sends $\mathbf{u}_j \mathbf{H}_{\pi(j)} \mathbf{v}_i$, $i = 1, \ldots, j - 1$, to the base station. This information is required for dirty paper coding.*

7. *The base station sends $\mathbf{v}_j$ to all the users. Each user substitutes $\mathbf{v}_j$ in the jth column of $\boldsymbol{\Xi}$.*

8. *Set $j \leftarrow j + 1$. If $j \leq M$ move to step two; otherwise stop.*

The performance of this method is the same as that of the first algorithm (assume that the gain of at least one user is larger than the threshold th(j)). However, the rate of the feedback required in the modified algorithm is significantly reduced as compared to that of the first algorithm.

Threshold th(j) is determined such that with high probability there exists at least one user with gain larger than th(j). Refereing to Lemma 2.8, we conclude that when

K is large, with probability one the largest gain is greater than $\hat{\eta}_j - \log\log(\sqrt{K})$. Consequently, for large k, an appropriate choice for $\text{th}(j) = \hat{\eta}_j - \log\log(\sqrt{K})$, where $\hat{\eta}_j$ is defined in (2.45).

2.7 Conclusion

In this chapter, a simple signaling method for a multi-antenna broadcast channel is proposed. This method reduces the MIMO broadcast system to a set of parallel channels. The proposed scheme has several desirable features in terms of: (i) accommodating users with different number of receive antennas, (ii) exploiting multi-user diversity, and (iii) requiring low feedback rate. The simulation results indicate that the achieved sum-rate is close to the sum-capacity of the underlying broadcast channel. To analyze the performance of the scheme, an upper-bound on the outage probability of each sub-channel is derived which is used to establish the diversity order and the asymptotic sum-rate of the scheme. It is shown that the diversity order of the jth data stream, $1 \leq j \leq M$ is equal to $N(M - j + 1)(K - j + 1)$. Furthermore, it is proven that the throughput of this scheme scales as $M \log\log(K)$ and asymptotically $(K \longrightarrow \infty)$ tends to the sum-capacity of the MIMO broadcast channel.

Chapter 3

Signaling over MIMO X Channels

3.1   Introduction

Wireless technology has been advancing at an exponential rate, due to the increasing expectations for multi-media services. This, in turn, necessitates the development of novel signaling techniques with high spectral efficiency. Using multiple antennas at both ends of wireless links is known as a unique solution to support high-data-rate communication [18, 58]. Multiple-antenna systems incorporate additional dimension of space to the transmission, resulting in a multiplicative increase in the overall through-put [58, 72]. The multiplicative increase in the rate is measured by a metric known as the *multiplexing gain (MG)*, ρ, defined as the ratio of the sum-rate of the system, R,

over the logarithm of the total power P_T in the high power regime, i.e.

$$\rho = \lim_{P_T \to \infty} \frac{R}{\log_2(P_T)}. \tag{3.1}$$

It is widely known that in a point to point multiple-antenna system, with M transmit and N receive antennas, the MG is $\min(M, N)$ [58]. In multi-antenna multi-user systems, when the full cooperation is provided at least at one side of the links (either among the transmitters or among the receivers), the system still enjoys a multiplicative increase in the throughput with the smaller value of the following two quantities: the total number of transmit antennas, and the total number of receive antennas. For example, in a multiple access channel with two transmitters, with M_1 and M_2 antennas, and one receiver with N antennas, the MG is equal to $\min(M_1 + M_2, N)$ [28]. Similarly, in a multiple-antenna broadcast channel, with one transmitter, equipped with M antennas, and two receivers, equipped with N_1 and N_2 antennas, the MG is equal to $\min(M, N_1 + N_2)$ [28]. However, for the case that cooperation is not available, the performance of the system will be deteriorated due to the interference of the links over each other. For example, in a multiple-antenna interference channel with two transmitters and two receivers, each equipped with N antennas, the MG of the system is N [28].

Extensive research efforts have been devoted to the multiple-antenna interference channels. In [62], the capacity region of the multiple-input single-output (MISO) interference channel with strong interference (see [8]) and the capacity region of the

single-input multiple-output (SIMO) interference channel with very strong interference (see [4]) are characterized. In [50], the superposition coding technique is utilized to derive an inner-bound for the capacity of the multiple-input multiple-output (MIMO) interference channels. In [69], several numerical schemes are proposed to compute sub-optimal transmit covariance matrices for the MIMO interference channels. In [28], the MG of the MIMO interference channel with general configuration for the number of transmit and receive antennas is derived. To increase the MG of such systems, the full cooperation among transmitters is proposed in [16, 54], which reduces the system to a single MIMO broadcast channel. To provide such a strong cooperation, an infinite capacity link connecting the transmitters, is presumed. In [26], the performance of single-antenna interference channels is evaluated, where the transmitters or receivers rely on the same channel, used for transmission, to provide cooperation. It is shown that the resulting MG is still one, i.e., this type of cooperation is not helpful in terms of the MG. In [28], a cooperation scheme in the shared communication channel for the MIMO interference systems is proposed and shown that such a scheme does not increase the MG.

In this chapter, we propose a new signaling scenario in multiple antenna systems with two transmitters and two receivers. In this scenario, each receiver receives data from both transmitters. It is assumed that neither the transmitters nor the receivers cooperate in signaling. In other words, each transmitter is unaware of the data of the other transmitter. Similarly, each receiver is unaware of the signal received by the

other receiver. This scenario of signaling has several applications. For example, in a wireless system where two relay nodes are utilized to extend coverage area or in a system where two base stations provide different services to the users. This system can be considered as a combination of two broadcast channels (from the transmitters' points of view) and two multi-access channels (from the receivers' points of view). By taking advantage of both perspectives, it is shown that by using some linear filters at the transmitters and the receivers, the system is decomposed to either two non-interfering multi-antenna broadcast sub-channels or two non-interfering multi-antenna multi-access sub-channels. It is proven that such a scheme outperforms other known non-cooperative schemes in terms of the achievable MG. In particular, it is shown that in the specific case that both receivers (transmitters) are equipped with N antennas, the total MG of $\rho = \lfloor \frac{4N}{3} \rfloor$ is achievable, where the two transmitters (receivers) have $\lceil \frac{\rho}{2} \rceil$ and $\lfloor \frac{\rho}{2} \rfloor$ antennas, respectively. Note that even if the full cooperation is provided either between the transmitters or between the receivers, the maximum MG is still ρ. Next, it is argued that such decomposition schemes result in some degradation (power offset) in the performance of the system. To overcome this problem, a design is proposed in which the signaling scheme is jointly designed for both sub-channels (two broadcast or two multi-access sub-channels).

The authors proposed this scenario of signaling and established the possibility of achieving higher MG initially in [39]. Later in [38], we extended the scheme proposed in [39] to more general configurations for the number of transmit and receive antennas,

and developed two signaling schemes based on: (i) linear operations at the receivers and the dirty paper coding at the transmitters, and (ii) linear operations at the transmitters and the successive decoding at the receivers. In [29], the idea of overlapping the interference terms proposed in [38] has been adopted to show that the zero-forcing scheme can achieve the multiplexing gain of the X channels for some special configurations for the number of transmit and receive antennas. Furthermore, in [29], an upper-bound on the MG of the X channels, where each transmitter and receiver is equipped with N antennas, is derived. In [10], the X channel with the partial and asymmetric cooperation among transmitters has been considered and the MG of the system has been derived.

The rest of the chapter is organized as follows. In Section 3.2, the system model is explained. In Section 3.3, the two signaling schemes which decompose the system into two broadcast or two multi-access sub-channels are explained. The performance analysis of the scheme, including computing the MG and the power offset (for some special cases) is presented in Section 3.4. In Section 3.5, the decomposition scheme is modified and a joint design for signaling scheme is proposed. Simulation results are presented in Section 3.6. Concluding remarks are presented in Section 3.7.

Notation: All boldface letters indicate vectors (lower case) or matrices (upper case). $(.)^{\dagger}$ denotes transpose conjugate operation, and $\mathcal{C}$ represents the set of complex numbers. $\mathcal{OC}^{M \times N}$ represents the set of all $M \times N$ complex matrices with mutually orthogonal and normal columns. $\mathbf{A} \perp \mathbf{B}$ means that each column of the matrix $\mathbf{A}$ is orthogonal to all columns of the matrix $\mathbf{B}$. The sub-space spanned by columns of $\mathbf{A}$ is represented

by $\Omega(\mathbf{A})$. The null space of the matrix $\mathbf{A}$ is denoted by $\mathrm{N}(\mathbf{A})$. Identity matrix is represented by $\mathbf{I}$. Adopted from MATLAB notation, $\mathbf{x}(i:j)$ denotes a vector including the entries i to j of the vector $\mathbf{x}$. The ith column of the matrix $\mathbf{A}$ is shown by $\mathbf{a}^{(i)}$.

3.2 Channel Model

We consider a MIMO system with two transmitters and two receivers. Transmitter t, $t = 1, 2$, is equipped with M_t antennas and receiver r, $r = 1, 2$, is equipped with N_r antennas. This configuration of antennas is shown by (M_1, M_2, N_1, N_2). For simplicity and without loss of generality, it is assumed that

$$M_1 \geq M_2 \text{ and } N_1 \geq N_2. \tag{3.2}$$

Assuming flat fading environment, the channel between transmitter t and receiver r is represented by the channel matrix $\mathbf{H}_{rt}$, where $\mathbf{H}_{rt} \in \mathcal{C}^{N_r \times M_t}$. The received vector $\mathbf{y}_r \in \mathcal{C}^{N_r \times 1}$ by receiver r, $r = 1, 2$, is given by,

$$\mathbf{y}_1 = \mathbf{H}_{11}\mathbf{s}_1 + \mathbf{H}_{12}\mathbf{s}_2 + \mathbf{w}_1, \tag{3.3}$$

$$\mathbf{y}_2 = \mathbf{H}_{21}\mathbf{s}_1 + \mathbf{H}_{22}\mathbf{s}_2 + \mathbf{w}_2,$$

where $\mathbf{s}_t \in \mathcal{C}^{M_t \times 1}$ represents the transmitted vector by transmitter t. The vector $\mathbf{w}_r \in \mathcal{C}^{N_r \times 1}$ is a white Gaussian noise with zero mean and identity covariance matrix. The power of $\mathbf{s}_t$ is subject to the constraint $\mathrm{Tr}(E[\mathbf{s}_t\mathbf{s}_t^\dagger]) \leq P_t$, $t = 1, 2$. P_T denotes the total transmit power, i.e. $P_T = P_1 + P_2$.

In the proposed scenario, the transmitter t sends μ_{1t} data streams to receiver 1 and μ_{2t} data streams to receiver 2.

Throughout the chapter, we have the following assumptions:

- The perfect information of the entire channel matrices, $\mathbf{H}_{rt}$, $r, t = 1, 2$, is available at both transmitters and at both receivers.

- Each transmitter is unaware of the data sent by the other transmitter, which means that there is no cooperation between transmitters. Similarly, receivers do not cooperate.

3.3   Decomposition Schemes

In what follows, we propose two signaling schemes depending on the values of (M_1, M_2, N_1, N_2). In the first scheme, by using linear transformations at the transmitters and at the receivers, the system is decomposed into two non-interfering broadcast sub-channels. Therefore, we can use any signaling scheme, developed for the MIMO broadcast channels, over the resulting sub-channels. As a dual of the first scheme, in the second scheme, linear transformations are utilized to decompose the system into two non-interfering multi-access sub-channels. It is shown that depending on the value of (M_1, M_2, N_1, N_2), one the these two schemes offer a higher MG.

In the rest of the chapter, it is assumed that

$$M_1 < N_1 + N_2, \tag{3.4}$$

$$N_1 < M_1 + M_2. \tag{3.5}$$

Otherwise, if $M_1 \geq N_1 + N_2$, the maximum multiplexing gain of $N_1 + N_2$ is achievable by a simple broadcast channel formed by the first transmitter and the two receivers. Similarly, if $N_1 \geq M_1 + M_2$, then the maximum multiplexing gain of $M_1 + M_2$ is achievable by a simple multi-access channel including the two transmitters and the first receiver. The two signaling schemes presented in this chapter cover all the possibilities for the number of transmit and receive antennas, excluding the aforementioned cases. It is conjectured that the achieved MG is optimal for all cases. The optimality is proven for some special cases of practical interest.

To attain the highest MG, we take advantage of the null-spaces of the direct or cross links.

Defintion 3.1. *We call a system as* irreducible, *if*

$$\textit{Irreducible Type I:} \quad N_1 \geq N_2 \geq M_1 \geq M_2, \tag{3.6}$$

or

$$\textit{Irreducible Type II:} \quad M_1 \geq M_2 \geq N_1 \geq N_2. \tag{3.7}$$

Otherwise the system is called reducible.

Unlike the irreducible systems, a portion of the achieved MG in a reducible X channel is attained through exploiting the null-spaces of the direct or cross links. In the reducible systems, the null-spaces of the links provide the possibility to increase the number of data streams sent from one of the transmitters to one of the receivers, without imposing any interference on the other receiver or restricting the signaling space of the other transmitter. By excluding null spaces utilized to increase the MG, the system is reduced to an equivalent system with (M_1', M_2', N_1', N_2') antennas, where $(M_1', M_2', N_1', N_2') \leq (M_1, M_2, N_1, N_2)$. As will be explained later, the null-spaces of the links in the reducible systems are exploited to the extend that the equivalent (reduced) system is not reducible anymore.

Defintion 3.2. *If the reduced X channel satisfies the condition of the type I irreducible systems, i.e.* $N_1' \geq N_2' \geq M_1' \geq M_2'$, *the original system is called* reducible to type I. *Similarly, if* $M_1' \geq M_2' \geq N_1' \geq N_2'$, *the original system is called* reducible to type II.

In what follows, it is shown that the *type I irreducible systems* and the *reducible systems to type I* can be decomposed into two non-interfering broadcast sub-channels. Moreover, it is shown that the *type II irreducible systems*, and the *reducible systems to type II* can be decomposed into two non-interfering multi-access sub-channels.

We define μ_{rt}', $r, t = 1, 2$, as the number of data streams transmitted from transmitter t to receiver r, *excluding* the number of extra data streams attained through exploiting the null-spaces of the links. In other words, μ_{rt}' represents the number of

data streams in the equivalent (reduced) channel.

3.3.1 Scheme I – Decomposition of the System into Two Broadcast Sub-Channels

As depicted in Fig. 3.1, in this scheme, the transmit filter $\mathbf{Q}_t \in \mathcal{OC}^{M_t \times (\mu_{1t} + \mu_{2t})}$ is employed at transmitter t, $t = 1, 2$. Therefore, the transmitted vectors $\mathbf{s}_t$, $t = 1, 2$, are equal to

$$\mathbf{s}_t = \mathbf{Q}_t \tilde{\mathbf{s}}_t, \tag{3.8}$$

where $\tilde{\mathbf{s}}_t \in \mathcal{C}^{(\mu_{1t} + \mu_{2t}) \times 1}$ contains μ_{1t} data streams for receiver one and μ_{2t} data streams for receiver two. The transmit filters $\mathbf{Q}_t$, $t = 1, 2$, have two functionalities: (i) Confining the transmit signal from transmitter t to a $(\mu_{1t} + \mu_{2t})$-dimensional sub-space which provides the possibility of decomposing the system into two broadcast sub-channels by using linear filters at the receivers, (ii) Exploiting the null spaces of the channel matrices to achieve the highest multiplexing gain.

At each receiver, two parallel receive filters are employed. The received vector $\mathbf{y}_1$ is passed through the filter $\mathbf{\Psi}_{11}^{\dagger}$, which is used to null out the signal coming from the second transmitter. The μ_{11} data streams, sent by transmitter one intended to receiver one, can be decoded from $\mathbf{y}_{11}$, the output of $\mathbf{\Psi}_{11}^{\dagger}$. Similarly, to decode μ_{12} data streams, sent by transmitter two to receiver one, the received vector $\mathbf{y}_1$ is passed through the receive filter $\mathbf{\Psi}_{12}^{\dagger}$, which is used to null out the signal coming from transmitter one.

Receiver two has a similar structure with parallel receive filters $\boldsymbol{\Psi}_{21}^{\dagger}$ and $\boldsymbol{\Psi}_{22}^{\dagger}$. Later, it is shown that if μ_{rt}, $r, t = 1, 2$, satisfy a set of inequalities, then it is possible to deign $\mathbf{Q}_t$ and $\boldsymbol{\Psi}_{rt}$ to meet the desired features explained earlier. It means that the system is decomposed into two non-interfering MIMO broadcast sub-channels (see Fig. 3.2).

Next, we explain how to select the design parameters including the number of data streams μ_{rt}, $r, t = 1, 2$ and the transmit/receive filters. The primary objective is to prevent the saturation of the rate of each stream in the high SNR regime. In other words, the MG of the system is $\mu_{11} + \mu_{12} + \mu_{21} + \mu_{22}$.

The integer variables ζ_{rt}, $r, t = 1, 2$, defined as follows, will be useful in our subsequent discussions:

- ζ_{11} denotes the dimension of $\Omega(\mathbf{H}_{12}\mathbf{Q}_2)$.

- ζ_{21} denotes the dimension of $\Omega(\mathbf{H}_{22}\mathbf{Q}_2)$.

- ζ_{12} denotes the dimension of $\Omega(\mathbf{H}_{11}\mathbf{Q}_1)$.

- ζ_{22} denotes the dimension of $\Omega(\mathbf{H}_{21}\mathbf{Q}_1)$.

In the sequel, we categorize the design scheme into the four general cases depending on (M_1, M_2, N_1, N_2), where in all cases, the system is either irreducible type I or reducible to type I. To facilitate the derivations, we use the auxiliary variables M_t', N_r', and μ_{rt}', for $r, t = 1, 2$. As will be explain later, for each case, M_t' and N_r' are computed directly as a function of M_t and N_r for $r, t = 1, 2$. Then, μ_{rt}', $r, t = 1, 2$, are selected

such that the following constraints are satisfied,

$$\mu'_{11}: \quad \mu'_{11} + \mu'_{12} + \mu'_{22} \le N'_1, \tag{3.9}$$

$$\mu'_{12}: \quad \mu'_{12} + \mu'_{11} + \mu'_{21} \le N'_1, \tag{3.10}$$

$$\mu'_{22}: \quad \mu'_{22} + \mu'_{21} + \mu'_{11} \le N'_2, \tag{3.11}$$

$$\mu'_{21}: \quad \mu'_{21} + \mu'_{22} + \mu'_{12} \le N'_2, \tag{3.12}$$

$$\mu'_{11} + \mu'_{21} \le M'_1, \tag{3.13}$$

$$\mu'_{22} + \mu'_{12} \le M'_2. \tag{3.14}$$

Each of the first four inequalities corresponds to one of the parameters μ'_{rt}, $r, t = 1, 2$, in the sense that if μ'_{rt}, $r, t = 1, 2$, is zero, the corresponding inequality is removed from the set of constraints. After choosing μ'_{rt}, $r, t = 1, 2$, for each case, μ_{rt}, $r, t = 1, 2$, are computed as function of μ'_{rt}, $r, t = 1, 2$, as will be explained later.

Note that we have many options to choose μ'_{rt}, $r, t = 1, 2$. It is shown that as long as the integers μ'_{rt}, $r, t = 1, 2$, satisfy (3.9) to (3.14), the system achieves the MG of $\mu_{11} + \mu_{12} + \mu_{21} + \mu_{22}$. However, it turns out that to achieve the highest MG, μ'_{rt}, $r, t = 1, 2$, should be selected such that $\mu'_{11} + \mu'_{12} + \mu'_{21} + \mu'_{22}$ is maximum.

In what follows, for each of the four cases, we explain:

1. How to compute the auxiliary variables M'_t and N'_r as a function of M_t and N_r, $r, t = 1, 2$,

2. After choosing μ'_{rt}, $r, t = 1, 2$, satisfying (3.9) to (3.14), how to compute μ_{rt},

$r, t = 1, 2,$

3. How to choose the transmit filters $\mathbf{Q}_t$, $t = 1, 2$,

4. How to compute ζ_{rt}, $r, t = 1, 2$.

Having completed these steps, the procedure of computing the receive filters $\mathbf{\Psi}_{rt}^\dagger$, $r, t = 1, 2$, is similar for all cases. Later, we will show that this scheme decomposes the system into two non-interfering broadcast sub-channels.

Scheme I − Case I: $N_1 \geq N_2 \geq M_1 \geq M_2$

In this case, the system is irreducible. Therefore, the equivalent system is the same as the original system i.e. $N_r' = N_r$, $r = 1, 2$, and $M_t' = M_t$, $t = 1, 2$.

Using the above parameters, we choose μ_{rt}', $r, t = 1, 2$, subject to (3.9)-(3.14) constraints. Since we do not exploit the null-space of any of the links to transmit data streams, μ_{rt} is the same as μ_{rt}', i.e. $\mu_{rt} = \mu_{rt}'$, $r, t = 1, 2$. In this case, $\mathbf{Q}_1$ and $\mathbf{Q}_2$ are randomly chosen from $\mathcal{OC}^{M_1 \times (\mu_{11} + \mu_{21})}$ and $\mathcal{OC}^{M_2 \times (\mu_{12} + \mu_{22})}$, respectively.

Regarding the definition of ζ_{rt}, $r, t = 1, 2$, it is easy to see that,

$$\zeta_{11} = \mu_{12} + \mu_{22}, \quad \zeta_{12} = \mu_{11} + \mu_{21}, \quad \zeta_{21} = \mu_{12} + \mu_{22}, \quad \zeta_{22} = \mu_{11} + \mu_{21}. \tag{3.15}$$

Scheme I − Case II: $N_1 \geq M_1 > N_2 \geq M_2$

In this case, at transmitter one, $(M_1 - N_2)$-dimensional sub-space $\mathrm{N}(\mathbf{H}_{21})$ is exploited to transmit $M_1 - N_2$ data streams from transmitter one to receiver one without imposing any interference at receiver two. In other words, while the component of $\mathbf{s}_1$ in $\mathrm{N}(\mathbf{H}_{21})$

does not impose any interference at receiver two, it provides the possibility to increase the number of data streams sent from transmitter one to receiver one by $M_1 - N_2$. Let us exclude the $(M_1 - N_2)$-dimensional subspace $N(\mathbf{H}_{21})$ from the available space at transmitter one. In addition, let us exclude the $(M_1 - N_2)$-dimensional subspace $\Omega(\mathbf{H}_{11}N(\mathbf{H}_{21}))$ from the available space at receiver one. Then, the system is reduced to an X channel with equivalent antennas $(M'_1, M'_2, N'_1, N'_2) = \left(M_1 - \{M_1 - N_2\}, M_2, N_1 - \{M_1 - N_2\}, N_2 \right)$ or,

$$N'_1 = N_1 + N_2 - M_1, \quad N'_2 = N_2, \quad M'_1 = N_2, \quad M'_2 = M_2. \tag{3.16}$$

Clearly, $N'_1 \geq N'_2 \geq M'_1 \geq M'_2$, therefore the original system is reducible to type I.

Let us select μ'_{rt}, $r, t = 1, 2$, subject to (3.9)-(3.14) constraints. μ'_{rt}, $r, t = 1, 2$, give us the number of data streams in the reduced X channel, excluding the $M_1 - N_2$ data streams, sent from transmitter one to receiver one relying on $N(\mathbf{H}_{21})$. Clearly, the numbers of data streams in the original system are computed as,

$$\mu_{11} = \mu'_{11} + M_1 - N_2, \quad \mu_{12} = \mu'_{12}, \quad \mu_{21} = \mu'_{21}, \quad \mu_{22} = \mu'_{22}. \tag{3.17}$$

$\mathbf{Q}_1$ is chosen as,

$$\mathbf{Q}_1 \in \mathcal{OC}^{M_1 \times (\mu_{11}+\mu_{21})}, \quad \mathbf{Q}_1 = [\mathbf{\Sigma}_1, \mathbf{\Sigma}_2], \tag{3.18}$$

where,

$$\mathbf{\Sigma}_1 \in \mathcal{OC}^{M_1 \times (N_1-M_2)}, \quad \mathbf{\Sigma}_1 \in N(\mathbf{H}_{21}), \tag{3.19}$$

$$\mathbf{\Sigma}_2 = \mathcal{OC}^{M_1 \times (\mu'_{11}+\mu_{21})}, \quad \mathbf{\Sigma}_2 \perp \mathbf{\Sigma}_1. \tag{3.20}$$

Such a structure for $\boldsymbol{\Sigma}_1$ guarantees the full usage of $N(\mathbf{H}_{21})$ for signaling.

$\mathbf{Q}_2$ is randomly chosen from $\mathcal{OC}^{M_2 \times (\mu_{12} + \mu_{22})}$.

It is easy to see that,

$$\zeta_{11} = \mu_{12} + \mu_{22}, \quad \zeta_{12} = \mu_{11} + \mu_{21}, \quad \zeta_{21} = \mu_{12} + \mu_{22}, \quad \zeta_{22} = \mu'_{11} + \mu_{21}. \tag{3.21}$$

Scheme I – Case III: $N_1 \geq M_1 \geq M_2 > N_2$ and $N_1 + N_2 \geq M_1 + M_2$

In this case,

(i) at transmitter one, $(M_1 - N_2)$-dimensional sub-space $N(\mathbf{H}_{21})$ is utilized to increase the number data streams sent from transmitter one to receiver one by $M_1 - N_2$ without imposing interference at receiver two,

(ii) at transmitter two, $(M_2 - N_2)$-dimensional sub-space $N(\mathbf{H}_{22})$ is utilized to increase the number data streams sent from transmitter two to receiver one by $M_2 - N_2$ without imposing interference at receiver two.

We exclude

(i) $(M_1 - N_2)$-dimensional sub-space $N(\mathbf{H}_{21})$ from the signaling space at transmitter one,

(ii) $(M_2 - N_2)$-dimensional sub-space $N(\mathbf{H}_{22})$ from the signaling space at transmitter two,

(iii) $(M_2 - N_1) + (M_2 - N_2)$-dimensional sub-space $\Omega\left(\mathbf{H}_{11}N(\mathbf{H}_{21})\right) \cup \Omega\left(\mathbf{H}_{12}N(\mathbf{H}_{22})\right)$ from the signaling space at receiver one.

Then, the reduced system is an equivalent X channel with (M_1', M_2', N_1', N_2'), where,

$$N_1' = N_1 + 2N_2 - M_1 - M_2, \quad N_2' = N_2, \quad M_1' = N_2, \quad M_2' = N_2, \quad (3.22)$$

where $N_1' \geq N_2' \geq M_1' \geq M_2'$. Therefore, the original system is reducible to type I. The number of data streams in the equivalent channel, μ_{rt}', $r, t = 1, 2$, are selected subject to (3.9)-(3.14) constraints. Then, we have,

$$\mu_{11} = \mu_{11}' + M_1 - N_2, \quad \mu_{12} = \mu_{12}' + M_2 - N_2, \quad \mu_{21} = \mu_{21}', \quad \mu_{22} = \mu_{22}'. \quad (3.23)$$

$\mathbf{Q}_1$ is chosen as,

$$\mathbf{Q}_1 \in \mathcal{OC}^{M_1 \times (\mu_{11} + \mu_{21})}, \quad \mathbf{Q}_1 = [\mathbf{\Sigma}_1, \mathbf{\Sigma}_2], \quad (3.24)$$

where,

$$\mathbf{\Sigma}_1 \in \mathcal{OC}^{M_1 \times (M_1 - N_2)}, \quad \mathbf{\Sigma}_1 \in \mathrm{N}(\mathbf{H}_{21}), \quad (3.25)$$

$$\mathbf{\Sigma}_2 = \mathcal{OC}^{M_1 \times (\mu_{11}' + \mu_{21})}, \quad \mathbf{\Sigma}_2 \perp \mathbf{\Sigma}_1. \quad (3.26)$$

$\mathbf{Q}_2$ is chosen as,

$$\mathbf{Q}_2 \in \mathcal{OC}^{M_2 \times (\mu_{12} + \mu_{22})}, \quad \mathbf{Q}_2 = [\mathbf{\Sigma}_3, \mathbf{\Sigma}_4], \quad (3.27)$$

where,

$$\mathbf{\Sigma}_3 \in \mathcal{OC}^{M_2 \times (M_2 - N_2)}, \quad \mathbf{\Sigma}_3 \in \mathrm{N}(\mathbf{H}_{22}), \quad (3.28)$$

$$\mathbf{\Sigma}_4 = \mathcal{OC}^{M_2 \times (\mu_{12}' + \mu_{22})}, \quad \mathbf{\Sigma}_4 \perp \mathbf{\Sigma}_3. \quad (3.29)$$

It is easy to see that,

$$\zeta_{11} = \mu_{12} + \mu_{22}, \quad \zeta_{12} = \mu_{11} + \mu_{21}, \quad \zeta_{21} = \mu'_{12} + \mu_{22}, \quad \zeta_{22} = \mu'_{11} + \mu_{21}. \quad (3.30)$$

Scheme I – Case IV: $M_1 > N_1 \geq N_2 \geq M_2$ and $N_1 + N_2 \geq M_1 + M_2$

In this case, at transmitter one, (i) $(M_1 - N_2)$-dimensional sub-space $N(\mathbf{H}_{21})$ is utilized to increase the number data streams sent from transmitter one to receiver one by $M_1 - N_2$ without imposing interference at receiver two, (ii) $(M_1 - N_1)$-dimensional sub-space $N(\mathbf{H}_{11})$ is exploited to increase the number data streams from transmitter one to receiver two by $M_1 - N_1$, without imposing interference at receiver two. By excluding the utilized subspaces at transmitter one, receiver one, and receiver two, the equivalent system is an X channel with (M'_1, M'_2, N'_1, N'_2) where,

$$N'_1 = N_1 + N_2 - M_1, \quad N'_2 = N_1 + N_2 - M_1, \quad M'_1 = N_1 + N_2 - M_1, \quad M'_2 = M_2. (3.31)$$

It is easy to see that $N'_1 \geq N'_2 \geq M'_1 \geq M'_2$. Therefore, the original system is reducible to type I.

μ'_{rt}, $r, t = 1, 2$, are selected subject to (3.9)-(3.14) constraints. Then,

$$\mu_{11} = \mu'_{11} + M_1 - N_2, \quad \mu_{12} = \mu'_{12}, \quad \mu_{21} = \mu'_{21} + M_1 - N_1, \quad \mu_{22} = \mu'_{22}. \quad (3.32)$$

In addition, $\mathbf{Q}_1$ is chosen as

$$\mathbf{Q}_1 \in \mathcal{OC}^{M_1 \times (\mu_{11} + \mu_{21})}, \quad \mathbf{Q}_1 = [\mathbf{\Sigma}_1, \mathbf{\Sigma}_2], \quad (3.33)$$

where,

$$\mathbf{\Sigma}_1 \in \mathcal{OC}^{M_1 \times (M_1 - N_2 + M_1 - N_2)}, \quad \mathbf{\Sigma}_1 \in \mathrm{N}(\mathbf{H}_{21}) \cup \mathrm{N}(\mathbf{H}_{11}), \tag{3.34}$$

$$\mathbf{\Sigma}_2 = \mathcal{OC}^{M_1 \times (\mu'_{11} + \mu'_{21})}, \quad \mathbf{\Sigma}_2 \perp \mathbf{\Sigma}_1. \tag{3.35}$$

$\mathbf{Q}_2$ is randomly chosen from $\mathcal{OC}^{M_2 \times (\mu_{12} + \mu_{22})}$.

It is easy to see that,

$$\zeta_{11} = \mu_{12} + \mu_{22}, \quad \zeta_{12} = \mu_{11} + \mu'_{21}, \quad \zeta_{21} = \mu_{12} + \mu_{22}, \quad \zeta_{22} = \mu'_{11} + \mu_{21}. \tag{3.36}$$

The next steps of the algorithm are the same for all of the aforementioned cases. We define

$$\widetilde{\mathbf{H}}_{rt} = \mathbf{H}_{rt}\mathbf{Q}_t, \ r,t = 1,2. \tag{3.37}$$

$\mathbf{\Psi}_{rt} \in \mathcal{OC}^{N_t \times (N_t - \zeta_{rt})}, \ r,t = 1,2$, are chosen such that

$$\mathbf{\Psi}_{11} \perp \widetilde{\mathbf{H}}_{12}, \tag{3.38}$$

$$\mathbf{\Psi}_{12} \perp \widetilde{\mathbf{H}}_{11}, \tag{3.39}$$

$$\mathbf{\Psi}_{21} \perp \widetilde{\mathbf{H}}_{22}, \tag{3.40}$$

$$\mathbf{\Psi}_{22} \perp \widetilde{\mathbf{H}}_{21}. \tag{3.41}$$

According to the definition of ζ_{rt}, one can always choose such matrices. Clearly, any signal sent by transmitter one does not pass through the filters $\mathbf{\Psi}_{12}^\dagger$ and $\mathbf{\Psi}_{22}^\dagger$. Similarly, any signal sent by transmitter two does not pass through the filters $\mathbf{\Psi}_{21}^\dagger$ and $\mathbf{\Psi}_{11}^\dagger$.

We define

$$\overline{\mathbf{H}}_{rt} = \mathbf{\Psi}_{rt}^\dagger \widetilde{\mathbf{H}}_{rt}, \quad r,t = 1,2, \tag{3.42}$$

$$\mathbf{w}_{rt} = \mathbf{\Psi}_{rt}^{\dagger}\mathbf{w}_r, \quad r,t = 1,2, \tag{3.43}$$

and

$$\mathbf{y}_{rt} = \mathbf{\Psi}_{rt}^{\dagger}\mathbf{y}_r, \quad r,t = 1,2. \tag{3.44}$$

Therefore, the system is decomposed into two non-interfering broadcast channels. The MIMO broadcast channel viewed from transmitter 1 is modeled by (see Fig. 3.2)

$$\begin{cases} \mathbf{y}_{11} = \overline{\mathbf{H}}_{11}\tilde{\mathbf{s}}_1 + \mathbf{w}_{11}, \\[2mm] \mathbf{y}_{21} = \overline{\mathbf{H}}_{21}\tilde{\mathbf{s}}_1 + \mathbf{w}_{21}, \end{cases} \tag{3.45}$$

and the MIMO broadcast channel viewed from transmitter two is modeled by (see Fig. 3.2)

$$\begin{cases} \mathbf{y}_{12} = \overline{\mathbf{H}}_{12}\tilde{\mathbf{s}}_2 + \mathbf{w}_{12}, \\[2mm] \mathbf{y}_{22} = \overline{\mathbf{H}}_{22}\tilde{\mathbf{s}}_2 + \mathbf{w}_{22}. \end{cases} \tag{3.46}$$

3.3.2   Scheme 2 – Decomposition of the System into Two Multi-access Sub-Channels

This scheme is indeed the dual of the scheme one, detailed in Sub-section 3.3.1. As depicted in Fig. 3.3, in this scheme, the parallel transmit filters $\mathbf{\Psi}_{11}$ and $\mathbf{\Psi}_{21}$ are employed at transmitter one, and the parallel transmit filters $\mathbf{\Psi}_{12}$ and $\mathbf{\Psi}_{22}$ are employed
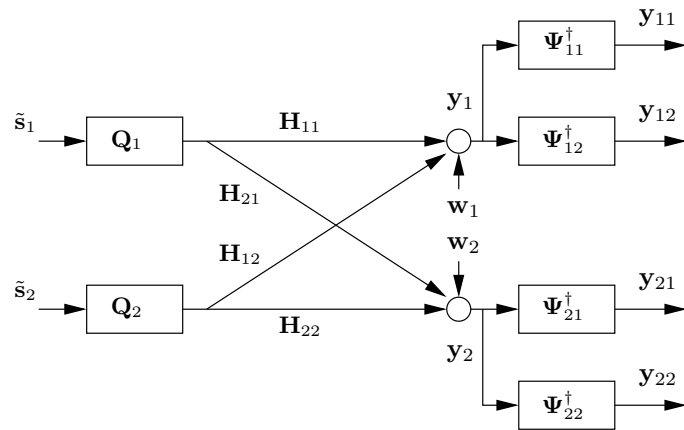
Figure 3.1: Scheme One: Decomposition of the System into Two Broadcast Sub-Channels
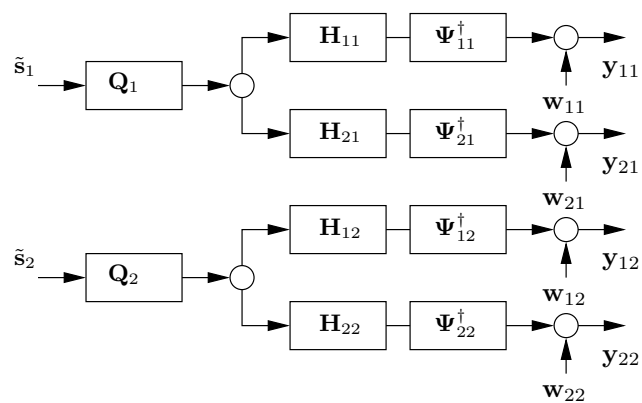
Figure 3.2: Scheme One: The Resulting Non-Interfering MIMO Broadcast Sub-Channels

at transmitter two. Therefore, the transmitted vectors are equal to

$$\mathbf{s}_1 = \boldsymbol{\Psi}_{\mathbf{11}}\mathbf{s}_{11} + \boldsymbol{\Psi}_{\mathbf{21}}\mathbf{s}_{21}, \tag{3.47}$$

$$\mathbf{s}_2 = \boldsymbol{\Psi}_{\mathbf{12}}\mathbf{s}_{12} + \boldsymbol{\Psi}_{\mathbf{22}}\mathbf{s}_{22}, \tag{3.48}$$

where $\mathbf{s}_{rt} \in \mathcal{C}^{\mu_{rt} \times 1}$ contains μ_{rt} data streams from transmitter t intended to receiver r. The transmit filter $\boldsymbol{\Psi}_{\mathbf{11}}$ nulls out the interference of the μ_{11} data streams, sent from transmitter one to receiver one, at receiver two. Similarly, the transmit filter $\boldsymbol{\Psi}_{\mathbf{21}}$ nulls out the interference of the μ_{21} data streams sent from transmitter one to receiver two at receiver one. In a similar fashion, at transmitter two, the two parallel transmit filters $\boldsymbol{\Psi}_{\mathbf{22}}$ and $\boldsymbol{\Psi}_{\mathbf{12}}$ are employed.

At receiver r terminal, the received vector is passed through the receive filter $\mathbf{Q}_r^\dagger$, where $\mathbf{Q}_r \in \mathcal{OC}^{N_r \times (\mu_{r1} + \mu_{r2})}$,

$$\tilde{\mathbf{y}}_r = \mathbf{Q}_r^\dagger \mathbf{y}_r, \quad r = 1, 2. \tag{3.49}$$

The functionalities of the receive filters $\mathbf{Q}_t$, $t = 1, 2$, are (i) to map the received signal in a $(\mu_{r1} + \mu_{r2})$-dimensional sub-space, which allows us to null out the interference terms by using transmit filters $\boldsymbol{\Psi}_{\mathbf{rt}}$, $r, t = 1, 2$, and (ii) to exploit the null spaces of the channel matrices to attain the highest MG.

Similar to the previous section, it is shown that if the numbers of data streams μ_{rt}, $r, t = 1, 2$, satisfy a set of inequalities, then it is possible to deign $\mathbf{Q}_t$ and $\boldsymbol{\Psi}_{rt}$ to meet the desired features explained earlier. Consequently, the system is decomposed into two non-interfering MIMO multi-access sub-channels (see Fig. 3.4).

Next, we explain how to select the design parameters including the numbers of data streams μ_{rt}, $r, t = 1, 2$ and the transmit/receive filters. Again, the primary objective is to prevent the saturation of the rate of each stream in the high SNR regime. In other words, the MG of the system is $\mu_{11} + \mu_{12} + \mu_{21} + \mu_{22}$.

Similar to the previous sub-section, we define the parameters ζ_{rt} , $r, t = 1, 2$, as follows.

- ζ_{11} denotes the dimension of $\Omega(\mathbf{H}_{21}^\dagger \mathbf{Q}_2)$.

- ζ_{21} denotes the dimension of $\Omega(\mathbf{H}_{11}^\dagger \mathbf{Q}_1)$.

- ζ_{12} denotes the dimension of $\Omega(\mathbf{H}_{22}^\dagger \mathbf{Q}_2)$.

- ζ_{22} denotes the dimension of $\Omega(\mathbf{H}_{12}^\dagger \mathbf{Q}_1)$.

To facilitate the derivations, we use the auxiliary variables M_t', N_r', and μ_{rt}', for $r, t = 1, 2$. For each case, the variables M_t' and N_r' are computed directly as a function of M_t and N_r for $r, t = 1, 2$. Then, the auxiliary integer variables μ_{rt}', $r, t = 1, 2$, are

selected such that the following constraints are satisfied,

$$\mu'_{11}: \qquad \mu'_{11} + \mu'_{21} + \mu'_{22} \leq M'_1, \qquad (3.50)$$

$$\mu'_{21}: \qquad \mu'_{11} + \mu'_{21} + \mu'_{12} \leq M'_1, \qquad (3.51)$$

$$\mu'_{22}: \qquad \mu'_{22} + \mu'_{12} + \mu'_{11} \leq M'_2, \qquad (3.52)$$

$$\mu'_{12}: \qquad \mu'_{22} + \mu'_{12} + \mu'_{21} \leq M'_2, \qquad (3.53)$$

$$\mu'_{11} + \mu'_{12} \leq N'_1, \qquad (3.54)$$

$$\mu'_{22} + \mu'_{21} \leq N'_2. \qquad (3.55)$$

Each of the first four inequalities corresponds to one of the parameters μ'_{rt}, $r,t = 1,2$, in the sense that if μ'_{rt}, $r,t = 1,2$, is zero, the corresponding inequality is removed from the set of constraints. After choosing μ'_{rt}, $r,t = 1,2$, for each case, μ_{rt}, $r,t = 1,2$, are computed as function of μ'_{rt}, $r,t = 1,2$.

Similar to scheme one, to achieve the highest MG, we choose μ'_{rt}, $r,t = 1,2$ subject to (3.50) to (3.55) such that $\mu'_{11} + \mu'_{12} + \mu'_{21} + \mu'_{22}$ is maximum.

In what follows, for each of the four cases, we explain:

(i) How to compute the auxiliary variables M'_t and N'_r as a function of M_t and N_r, $r,t = 1,2$,

(ii) After choosing the auxiliary variables μ'_{rt}, $r,t = 1,2$, satisfying (3.50) to (3.55), how to compute μ_{rt}, $r,t = 1,2$,

(iii) How to choose the receive filters $\mathbf{Q}_t$, $t = 1,2$,

(iv) How to compute ζ_{rt}, $r, t = 1, 2$.

Having completed these steps, the procedure of computing the filters $\boldsymbol{\Psi}_{rt}^{\dagger}$, $r, t = 1, 2$, is similar for all cases. Later, we will show that this scheme decomposes the system into two non-interfering multi-access channels.

Scheme II – Case I: $M_1 \geq M_2 \geq N_1 \geq N_2$

In this case, the system is irreducible type II. Therefore, the equivalent system is the same as the original system, i.e., $N_r' = N_r$, $r = 1, 2$ and $M_t' = M_t$, $t = 1, 2$. Using the above parameters, we choose μ_{rt}', $r, t = 1, 2$, subject to (3.50) – (3.55). Similar to Scheme I – Case I, we have $\mu_{rt} = \mu_{rt}'$, $r, t = 1, 2$. $\mathbf{Q}_1$ and $\mathbf{Q}_2$ are randomly chosen from $\mathcal{OC}^{N_1 \times (\mu_{11} + \mu_{12})}$ and $\mathcal{OC}^{N_2 \times (\mu_{21} + \mu_{22})}$, respectively.

According to the definition of ζ_{rt}, $r, t = 1, 2$, it is easy to see that

$$\zeta_{11} = \mu_{21} + \mu_{22}, \quad \zeta_{12} = \mu_{21} + \mu_{22}, \quad \zeta_{21} = \mu_{12} + \mu_{11}, \quad \zeta_{22} = \mu_{11} + \mu_{12}. \tag{3.56}$$

Scheme II – Case II: $M_1 \geq N_1 > M_2 \geq N_2$

In this case, at the receiver one, the signal coming from transmitter two does not have any component in the $(N_1 - M_2)$–dimensional subspace $\mathrm{N}(\mathbf{H}_{12}^{\dagger})$. This sub-space can be exploited to increase the number of data streams sent from transmitter one to receiver one by $N_1 - M_2$ without restricting the available signaling space at the transmitter two and at the receiver two. Consequently, the system is reduced to a system with $(M_1', M_2', N_1', N_2') = \left(M_1 - \{N_1 - M_2\}, M_2, N_1 - \{N_1 - M_2\}, N_2 \right)$ antennas, or

$$M_1' = M_1 + M_2 - N_1, \quad M_2' = M_2, \quad N_1' = M_2, \quad N_2' = N_2. \tag{3.57}$$

It is easy to see that $M_1' \geq M_2' \geq N_1' \geq N_2'$, i.e. the original system is reducible to type II. We choose μ_{rt}', $r, t = 1, 2$, subject to (3.50) – (3.55). Then, we have

$$\mu_{11} = \mu_{11}' + N_1 - M_2, \quad \mu_{12} = \mu_{12}', \quad \mu_{21} = \mu_{21}', \quad \mu_{22} = \mu_{22}'. \tag{3.58}$$

$\mathbf{Q}_1$ is chosen as,

$$\mathbf{Q}_1 \in \mathcal{OC}^{N_1 \times (\mu_{11} + \mu_{21})}, \quad \mathbf{Q}_1 = [\boldsymbol{\Sigma}_1, \boldsymbol{\Sigma}_2], \tag{3.59}$$

where,

$$\boldsymbol{\Sigma}_1 \in \mathcal{OC}^{N_1 \times (N_1 - M_2)}, \quad \boldsymbol{\Sigma}_1 \in \mathrm{N}(\mathbf{H}_{12}^\dagger), \tag{3.60}$$

$$\boldsymbol{\Sigma}_2 = \mathcal{OC}^{N_1 \times (\mu_{11}' + \mu_{12})}, \quad \boldsymbol{\Sigma}_2 \perp \boldsymbol{\Sigma}_1. \tag{3.61}$$

$\mathbf{Q}_2$ is randomly selected from $\mathcal{OC}^{N_2 \times (\mu_{21} + \mu_{22})}$.

It is easy to see that,

$$\zeta_{11} = \mu_{21} + \mu_{22}, \quad \zeta_{12} = \mu_{21} + \mu_{22}, \quad \zeta_{21} = \mu_{12} + \mu_{11}, \quad \zeta_{22} = \mu_{11}' + \mu_{12}. \tag{3.62}$$

<u>Scheme II – Case III: $M_1 \geq N_1 \geq N_2 > M_2$ and $M_1 + M_2 \geq N_1 + N_2$</u>

In this case, at receiver one, the signal coming from transmitter two has no component in the $(N_1 - M_2)-$ dimensional sub-space $\mathrm{N}(\mathbf{H}_{12}^\dagger)$. This sub-space can be exploited to increase the number of data streams sent from transmitter one to receiver one by $N_1 - M_2$ without restricting the available signaling space at transmitter two and at receiver two. In addition, at receiver two, the signal coming from transmitter two has no component in the $(N_2 - M_2)-$ dimensional sub-space $\mathrm{N}(\mathbf{H}_{22}^\dagger)$. This sub-space can be

exploited to increase the number of data streams sent from transmitter one to receiver two by $N_2 - M_2$, without restricting the available signaling space at transmitter two and at receiver one. Therefore, the reduced system has (M_1', M_2', N_1', N_2') antennas, where

$$M_1' = M_1 + 2M_2 - N_1 - N_2, \quad M_2' = M_2, \quad N_1' = M_2, \quad N_2' = M_2. \tag{3.63}$$

$M_1' \geq M_2' \geq N_1' \geq N_2'$. Therefore, the original system is reducible to type II.

After choosing μ_{rt}', $r, t = 1, 2$, subject to (3.50) – (3.55), we have

$$\mu_{11} = \mu_{11}' + N_1 - M_2, \quad \mu_{12} = \mu_{12}', \quad \mu_{21} = \mu_{21}' + N_2 - M_2, \quad \mu_{22} = \mu_{22}'. \tag{3.64}$$

$\mathbf{Q}_1$ is chosen as,

$$\mathbf{Q}_1 \in \mathcal{OC}^{N_1 \times (\mu_{11} + \mu_{21})}, \quad \mathbf{Q}_1 = [\mathbf{\Sigma}_1, \mathbf{\Sigma}_2], \tag{3.65}$$

where,

$$\mathbf{\Sigma}_1 \in \mathcal{OC}^{N_1 \times (N_1 - M_2)} \quad \mathbf{\Sigma}_1 \in \mathrm{N}(\mathbf{H}_{21}^\dagger), \tag{3.66}$$

$$\mathbf{\Sigma}_2 = \mathcal{OC}^{N_1 \times (\mu_{11}' + \mu_{12})} \quad \mathbf{\Sigma}_2 \perp \mathbf{\Sigma}_1. \tag{3.67}$$

$\mathbf{Q}_2$ is chosen as,

$$\mathbf{Q}_2 \in \mathcal{OC}^{N_2 \times (\mu_{21} + \mu_{22})}, \quad \mathbf{Q}_2 = [\mathbf{\Sigma}_3, \mathbf{\Sigma}_4], \tag{3.68}$$

where,

$$\mathbf{\Sigma}_3 \in \mathcal{OC}^{N_2 \times (N_2 - M_2)}, \quad \mathbf{\Sigma}_3 \in \mathrm{N}(\mathbf{H}_{22}^\dagger), \tag{3.69}$$

$$\mathbf{\Sigma}_4 = \mathcal{OC}^{N_2 \times (\mu_{21}' + \mu_{22})}, \quad \mathbf{\Sigma}_4 \perp \mathbf{\Sigma}_3. \tag{3.70}$$

Therefore, we have,

$$\zeta_{11} = \mu_{21} + \mu_{22}, \quad \zeta_{12} = \mu'_{21} + \mu_{22}, \quad \zeta_{21} = \mu_{12} + \mu_{11}, \quad \zeta_{22} = \mu'_{11} + \mu_{12}. \tag{3.71}$$

Scheme II – Case IV: $N_1 > M_1 \geq M_2 \geq N_2$ and $M_1 + M_2 \geq N_1 + N_2$

In this case, (i) $(N_1 - M_2)-$ dimensional sub-space $\mathrm{N}(\mathbf{H}_{12}^{\dagger})$ is utilized to increase the number of data streams sent from transmitter one to receiver one by $(N_1 - M_2)$, (ii) $(N_1 - M_1)-$ dimensional sub-space $\mathrm{N}(\mathbf{H}_{11}^{\dagger})$ is utilized to increase the number of data streams sent from transmitter two to receiver one by $(N_1 - M_1)$. Therefore, we have,

$$M'_1 = M_1 + M_2 - N_1, \quad M'_2 = M_1 + M_2 - N_1, \quad N'_1 = M_1 + M_2 - N_1, \quad N'_2 = N_2,$$
$$\mu_{11} = \mu'_{11} + N_1 - M_2, \quad \mu_{12} = \mu'_{12} + N_1 - M_1, \quad \mu_{21} = \mu'_{21}, \qquad \mu_{22} = \mu'_{22}, \tag{3.72}$$

where $M'_1 \geq M'_2 \geq N'_1 \geq N'_2$ i.e., the original system is reducible to type II. $\mathbf{Q}_1$ is chosen as,

$$\mathbf{Q}_1 \in \mathcal{OC}^{N_1 \times (\mu_{11} + \mu_{21})}, \quad \mathbf{Q}_1 = [\mathbf{\Sigma}_1, \mathbf{\Sigma}_2], \tag{3.73}$$

where,

$$\mathbf{\Sigma}_1 \in \mathcal{OC}^{N_1 \times (N_1 - M_2 + N_1 - M_2)}, \quad \mathbf{\Sigma}_1 \in \mathrm{N}(\mathbf{H}_{12}^{\dagger}) \cup \mathrm{N}(\mathbf{H}_{11}^{\dagger}), \tag{3.74}$$

$$\mathbf{\Sigma}_2 = \mathcal{OC}^{N_1 \times (\mu'_{11} + \mu'_{12})}, \quad \mathbf{\Sigma}_2 \perp \mathbf{\Sigma}_1. \tag{3.75}$$

$\mathbf{Q}_2$ is randomly selected from $\mathcal{OC}^{N_2 \times (\mu_{21} + \mu_{22})}$. In this case, we have,

$$\zeta_{11} = \mu_{21} + \mu_{22}, \quad \zeta_{12} = \mu_{21} + \mu_{22}, \quad \zeta_{21} = \mu'_{12} + \mu_{11}, \quad \zeta_{22} = \mu'_{11} + \mu_{12}. \tag{3.76}$$

The next steps of the algorithm are the same for all above cases. We define

$$\widetilde{\mathbf{H}}_{rt} = \mathbf{Q}_r^\dagger \mathbf{H}_{rt}, \ r, t = 1, 2. \tag{3.77}$$

$\boldsymbol{\Psi}_{rt} \in \mathcal{OC}^{M_r \times (M_r - \zeta_{rt})}$, $r, t = 1, 2$, are chosen such that,

$$\boldsymbol{\Psi}_{11} \perp \widetilde{\mathbf{H}}_{21}^\dagger, \tag{3.78}$$

$$\boldsymbol{\Psi}_{21} \perp \widetilde{\mathbf{H}}_{11}^\dagger, \tag{3.79}$$

$$\boldsymbol{\Psi}_{12} \perp \widetilde{\mathbf{H}}_{22}^\dagger, \tag{3.80}$$

$$\boldsymbol{\Psi}_{22} \perp \widetilde{\mathbf{H}}_{12}^\dagger. \tag{3.81}$$

According to the definition of ζ_{rt}, we can always choose such matrices. Clearly, any signal passed through the filters $\boldsymbol{\Psi}_{11}^\dagger$ and $\boldsymbol{\Psi}_{12}^\dagger$ has no interference at the output of the filter $\mathbf{Q}_2$. Similarly, any signal passed through the filters $\boldsymbol{\Psi}_{21}^\dagger$ and $\boldsymbol{\Psi}_{22}^\dagger$ has no interference at the output of the filter $\mathbf{Q}_2$. We define

$$\overline{\mathbf{H}}_{rt} = \widetilde{\mathbf{H}}_{rt} \boldsymbol{\Psi}_{rt}, \quad r, t = 1, 2, \tag{3.82}$$

and

$$\tilde{\mathbf{w}}_r = \mathbf{Q}_r^\dagger \mathbf{w}_r, \quad r, t = 1, 2. \tag{3.83}$$

This system is decomposed into two non-interfering multiple-access channels: (i) the multi-access channel viewed by receiver one with channels $\overline{\mathbf{H}}_{11}$ and $\overline{\mathbf{H}}_{12}$, modeled by (see Fig. 3.4),

$$\tilde{\mathbf{y}}_1 = \overline{\mathbf{H}}_{11} \mathbf{s}_{11} + \overline{\mathbf{H}}_{12} \mathbf{s}_{12} + \tilde{\mathbf{w}}_1, \tag{3.84}$$

and, (ii) the multi-access channel viewed by receiver two with channels $\overline{\mathbf{H}}_{21}$ and $\overline{\mathbf{H}}_{22}$, modeled by (see Fig. 3.4),

$$\tilde{\mathbf{y}}_2 = \overline{\mathbf{H}}_{21}\mathbf{s}_{21} + \overline{\mathbf{H}}_{22}\mathbf{s}_{12} + \tilde{\mathbf{w}}_2. \tag{3.85}$$
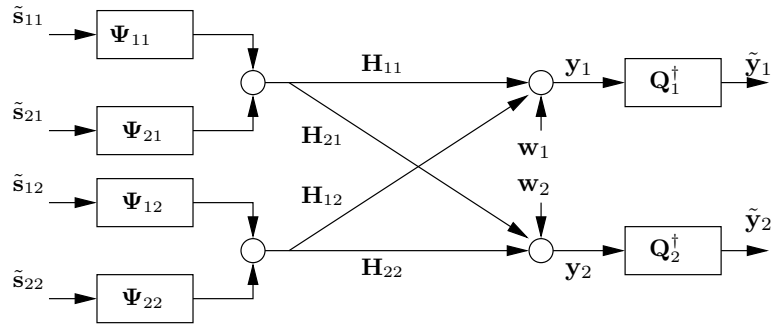
Figure 3.3: Scheme Two: Decomposition of the System into Two Multi-Access Sub-Channels
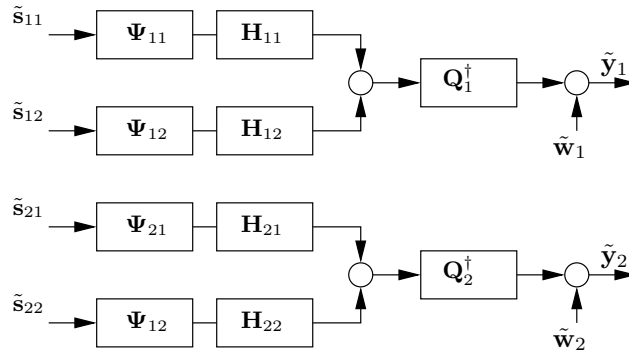
Figure 3.4: Scheme Two: The Resulting Non-Interfering MIMO Multi-Access Sub-Channels

3.4 Performance Evaluation

The decomposition schemes, presented in Section 3.3, simplify the procedure of the performance evaluation for the X channels in the high SNR regime. In what follows, the MG of the X channel is studied. In addition, for some special cases, a metric known as *power offset* is evaluated.

3.4.1 Multiplexing Gain

Theorem 3.3. *The MIMO X channel with (M_1, M_2, N_1, N_2) antennas, decomposed into two non-interfering broadcast or multi-access sub-channels, achieves the multiplexing gain of $\mu_{11} + \mu_{21} + \mu_{12} + \mu_{22}$, if μ_{rt}, $r, t = 1, 2$, are selected according to the schemes presented in Section 3.3.*

Proof. As explained in Sub-section 3.3.1, the X channel is decomposed into two non-interfering broadcast sub-channels (3.45) and (3.46). The first broadcast sub-channel is formed with the channel matrices $\overline{\mathbf{H}}_{11} \in \mathcal{C}^{(\mu_{11}+\mu_{21})\times(N_1-\zeta_{11})}$, and $\overline{\mathbf{H}}_{21} \in \mathcal{C}^{(\mu_{11}+\mu_{21})\times(N_2-\zeta_{21})}$. The inequalities (3.9) and (3.12) guarantee that $N_1 - \zeta_{11} \geq \mu_{11}$ and $N_2 - \zeta_{21} \geq \mu_{21}$. Therefore, as long as the matrix $[\overline{\mathbf{H}}_{11}^{\dagger}, \overline{\mathbf{H}}_{21}^{\dagger}]$ is full rank, the broadcast sub-channel achieves the MG of $\mu_{11} + \mu_{21}$ by sending μ_{11} data streams to receiver one and μ_{21} data streams to receiver two. It is easy to see that the $[\overline{\mathbf{H}}_{11}^{\dagger}, \overline{\mathbf{H}}_{21}^{\dagger}]$ is full rank with probability one. Similarly, the second broadcast sub-channel is formed with the channel matrices $\overline{\mathbf{H}}_{12} \in \mathcal{C}^{(\mu_{12}+\mu_{22})\times(N_1-\zeta_{12})}$, and $\overline{\mathbf{H}}_{22} \in \mathcal{C}^{(\mu_{12}+\mu_{22})\times(N_2-\zeta_{22})}$. Constraints (3.11) and (3.12)

respectively guarantee that $N_1 - \zeta_{21} \geq \mu_{21}$ and $N_2 - \zeta_{22} \geq \mu_{22}$. Therefore, as long as the matrix $[\overline{\mathbf{H}}_{12}^\dagger, \overline{\mathbf{H}}_{22}^\dagger]$ is full rank, the second broadcast sub-channel achieves the MG of $\mu_{12} + \mu_{22}$ by sending μ_{12} data streams to receiver one and μ_{22} data streams to receiver two.

A similar arguments are valid for the scheme presented in Sub-section 3.3.2.   □

Next, the MG of some special cases is computed in a closed-form.

Corollary 3.4. *For the special case of $N_1 = N_2 = N$ in the scheme of Sub-section 3.3.1, the MG of $\rho = \lfloor \frac{4N}{3} \rfloor$ is achievable where the total number of transmit antennas is equal to ρ, which are divided between transmitters as $M_1 = \lceil \frac{\rho}{2} \rceil$ and $M_2 = \lfloor \frac{\rho}{2} \rfloor$.*

Proof. By direct verification in the Scheme I – Case I.   □

Corollary 3.5. *In the special case of $M_1 = M_2 = M$ in the scheme presented in Sub-section 3.3.2, the MG of $\rho = \lfloor \frac{4M}{3} \rfloor$ is achievable where the total number of receive antennas is equal to ρ, which are divided between receivers as $N_1 = \lceil \frac{\rho}{2} \rceil$ and $N_2 = \lfloor \frac{\rho}{2} \rfloor$.*

Proof. By direct verification in the Scheme II – Case I.   □

Regarding Theorem 3.3, the MG of the X channel outperforms the MG of the interference channel with the same number of antennas. For example, the MGs of a X channels with $(3, 3, 3, 3)$, $(4, 3, 4, 3)$, $(9, 5, 8, 7)$ antennas are 4, 5, and 11 respectively, while the MGs of the interference channels with the same number of antennas are respectively 3, 4, and 9 [28]. For all the cases listed in Corollaries 3.4 and 3.5, the MG

of the X channel is the same as the MG of the system with full cooperation between transmitters or between receivers. For example, the multiplexing gains of the X channels with $(2, 2, 3, 3)$, $(3, 3, 2, 2)$, $(3, 2, 4, 4)$, and $(3, 3, 5, 5)$ antennas are respectively 4, 4, 5, and 6.

The improvement in MG of the X channels as compared to the interference channels can be attributed to two phenomena as explained next.

- For simplicity, we consider an X channel with $(2, 2, 3, 3)$ antennas, and assume that transmitter t sends one data stream d_{rt} to receiver r, $r = 1, 2$. Therefore, there are four data streams in the shared wireless medium. At receiver one, we are interested to decode d_{11} and d_{12}, while d_{22} and d_{21} are treated as interference. The signaling scheme is designed such that at the receiver one terminal, the interference terms d_{21} and d_{22} are received in the directions for which the distractive components are along each other. Therefore, at receiver one with three antennas, one direction is occupied with the destructive component of both interference terms d_{21} and d_{22}, while we have two interference-free dimensions to receive d_{11} and d_{12}. The design scheme provides similar condition at the receiver two terminal, while d_{22} and d_{21} are desired data streams and d_{22} and d_{21} are interference terms. Such overlaps of interference terms in each receiver save the available spatial dimensions to exploit the highest MG.

- It is well-known that the MG for a point-to-pint MIMO channel, a MIMO broad-

cast channel, and a MIMO multi-access channel is the same, as long as in all three systems we have the same total number of transmit antennas and the same total number of receive antennas. The immediate conclusion is that to attain the maximum MG, the cooperation at one side of the communication link is enough.

Now, consider an interference channel with $M_1 = M_2 = 2$ and $N_1 = N_2 = 3$, and assume that two data streams d_1 and d_2 are sent from transmitter one to receiver one and two data streams d_3 and d_4 are sent from transmitter two to receiver two. In this scenario, the data streams d_1 and d_2 have the possibility of cooperation at two points: (i) at transmitter one, and (ii) at receiver one. Similarly, the data streams d_3 and d_4 have the possibility of cooperation at two points: (i) at transmitter two, and (ii) at receiver two. Regarding the aforemention discussion, the system does not gain MG from the provided cooperation for d_1 and d_2 at both transmitter one and receiver one. Similar argument is valid for d_3 and d_4. However, the performance of the system is deteriorated because there is no possibility of cooperation between (d_1, d_2) and (d_3, d_4).

Let us consider an X channels with $(2, 2, 3, 3)$ antennas. In the X channels, the cooperation between d_{11} and d_{21} is provided at transmitter one, and the cooperation between d_{12} and d_{22} is provided at transmitter two. Similarly, the cooperation between d_{11} and d_{12} is provided at receiver one, and the cooperation between d_{21} and d_{22} is provided at receiver two.

3.4.2 Power Offset

In Corollaries 3.4 and 3.5, some special cases are listed for which the MG of the X channel is the same as the MG of a point-to-point MIMO system resulting from full cooperation between transmitters and/or between receivers. However, it does not mean that the system does not gain any improvement through cooperation. The gain of the cooperation is reflected in a metric known as the *power offset*. The power offset is defined as the negative of the zero-order term in the expansion of the sum-rate with respect to the total power, normalized with multiplexing gain, i.e.,

$$R = \rho(\log_2(P_T) - \mathcal{L}_\infty) + o(1), \tag{3.86}$$

where P_T denotes the total power, and $\mathcal{L}_\infty$ denotes the power offset in 3dB unit. In this definition, it is assumed that the noise is normalized as in system model (3.3). The power offset was first introduced in [49] to evaluate the performance of the different CDMA schemes. Later, the power offset for MIMO channels in [36] and some special cases of MIMO broadcast channels in [30] were computed. In what follows, the result of [30] is adopted to compute the power offset of some special cases of MIMO X channels.

Theorem 3.6. *In an X channel with* $(M_1, M_2, N_1, N_2) = (2\bar{k}, 2\bar{k}, 3\bar{k}, 3\bar{k})$ *antennas* ($\bar{k}$ *is a positive integer number), where the entries of channel matrices have Rayleigh distribution, if the decomposition scheme is employed, the power offset is equal to,*

$$\mathcal{L}_\infty(M_1, M_2, N_1, N_2) = \mathcal{L}_\infty(2\bar{k}, 2\bar{k}) - \frac{1}{2}\Big(\log_2(\alpha) + \log_2(1 - \alpha)\Big), \tag{3.87}$$

in 3dB units, where $P_1 = \alpha P_T$, $P_2 = (1 - \alpha)P_T$, $0 \leq \alpha \leq 1$,

$$\mathcal{L}_\infty(M, N) = \log_2 M + \frac{1}{\ln(2)} \left(\bar{\gamma} + 1 - \sum_{i=1}^{\tilde{M}-\tilde{N}} \frac{1}{i} - \frac{\tilde{M}}{\tilde{N}} \sum_{i=\tilde{M}-\tilde{N}+1}^{\tilde{M}} \frac{1}{i} \right), \tag{3.88}$$

$\bar{\gamma} = 0.5772$, $\tilde{M} = \max\{M, N\}$, *and* $\tilde{N} = \min\{M, N\}$. *Furthermore, the power offset of the X channel with* $(2\bar{k}, 2\bar{k}, 3\bar{k}, 3\bar{k})$ *antennas with respect to a MIMO Rayleigh Channel with* $4\bar{k}$ *transmit antennas and* $6\bar{k}$ *receive antennas is equal to,*

$$\frac{3}{2\ln(2)} \sum_{i=2\bar{k}+1}^{6\bar{k}} \frac{1}{i} - 1 - \frac{1}{2}\left(\log_2(\alpha) + \log_2(1 - \alpha) \right) \tag{3.89}$$

in 3dB unit.

Proof. In this case, the transmit filter $\mathbf{Q}_1$, is randomly chosen from $\mathcal{OC}^{2\bar{k} \times 2\bar{k}}$, independent of $\mathbf{H}_{11}$ and $\mathbf{H}_{21}$. In addition, the receive filters $\boldsymbol{\Psi}_{11} \in \mathcal{OC}^{2\bar{k} \times 2\bar{k}}$ and $\boldsymbol{\Psi}_{21} \in \mathcal{OC}^{2\bar{k} \times 2\bar{k}}$ are independent of $\mathbf{H}_{11}$, and $\mathbf{H}_{21}$, respectively. Therefore, the matrices $\overline{\mathbf{H}}_{11}$, and $\overline{\mathbf{H}}_{21}$, defined in (3.42), have Rayleigh distribution. Similar arguments are valid for $\overline{\mathbf{H}}_{12}$, and $\overline{\mathbf{H}}_{22}$. Therefore, the system is decomposed to two broadcast sub-channels, each with the Rayleigh distribution. Therefore, the sum-rate of the MIMO broadcast sub-channel, viewed from transmitter t, is approximated by [30]

$$2\bar{k}[\log_2(P_t) - \mathcal{L}_\infty(2\bar{k}, 2\bar{k})] + o(1). \tag{3.90}$$

By summation of the approximated formulas for the two MIMO broadcast sub-channels, (3.87) is obtained.

In [36], it is proven that the power offset for a MIMO Rayleigh channel with M

transmit and N receive antennas is obtained by (3.88). By substituting $M = 4\bar{k}$ and $N = 6\bar{k}$ in (3.88), and subtracting (3.88) from (3.87), (3.89) is derived. $\qquad\qquad\square$

3.5 Joint Design

The decomposition schemes proposed in Section 3.3 simplify the signaling design and the performance evaluation for the X channels. However, such decomposition schemes deteriorate the performance of the system because: (i) $\boldsymbol{\Psi}_{rt}$, $r, t = 1, 2$, are chosen such that the interference terms are forced to be zero, while the statistical properties of the interference should be exploited to design these filters, (ii) $\mathbf{Q}_t$, $t = 1, 2$ are chosen randomly, while the gain of the channel matrices in the different directions should be considered in choosing $\mathbf{Q}_t$, $t = 1, 2$. For example, consider an X channel with $(2, 2, 3, 3)$ antennas. In Sub-section 3.3.1, the receive filters $\boldsymbol{\Psi}_{rt}$, $r, t = 1, 2$, are chosen such that the interference of each broadcast sub-channel over the other one is forced to be zero. In low SNR regimes, the performance of the system is improved by choosing whitening filters for $\boldsymbol{\Psi}_{rt}$, $r, t = 1, 2$, instead of zero-forcing filters. In high SNR, the whitening filters converge to zero-forcing filters, and the resulting improvement diminishes. Note that in the X channel with $(2, 2, 3, 3)$, the transmit filters $\mathbf{Q}_t$, $t = 1, 2$, are such that the entire two-dimensional spaces available at transmitter one and two are used for signaling. Therefore, we can not improve the signaling scheme by modifying $\mathbf{Q}_t$, $t = 1, 2$.

In a system with $(3, 3, 3, 3)$ antennas, the same arguments for $\boldsymbol{\Psi}_{rt}$, $r, t = 1, 2$ are

valid. In this case, the transmit filters $\mathbf{Q}_t$, $t = 1, 2$, are chosen randomly, therefore the signaling space at each transmitter is confined to a randomly-selected two-dimensional sub-space of a three-dimensional space. One can take advantage of the degrees of freedom available for choosing $\mathbf{Q}_t$ to find the signaling sub-spaces at transmitter one and two for which the channels offer the highest gains.

Optimizing the filters $\mathbf{Q}_t$ and $\mathbf{\Psi}_{rt}$, $r, t = 1, 2$, depends on the signaling scheme employed for the MIMO broadcast or multi-access sub-channels. On the other hand, designing the signaling schemes for the sub-channels depends on the selected filters. Therefore, we have to jointly develop the design parameters. In what follows, we elaborate a joint design scheme based on a generalized version of Zero-Forcing Dirty Paper Coding (ZF-DPC) scheme, presented in [37], for the resulting broadcast sub-channels in Scheme I. In this scheme, the number of data streams μ_{rt}, $r, t = 1, 2$, and also integer parameters μ'_{rt}, $r, t = 1, 2$ are selected as explained in Sub-section 3.3.1. In addition, we use filters $\mathbf{Q}_t$ and $\mathbf{\Psi}^{\dagger}_{rt}$, r, t, in a similar fashion as shown in Fig. 3.1 , but with a different design.

According to the generalized ZF-DPC, explained in [37] for MIMO broadcast channels, the vectors $\tilde{\mathbf{s}}_t$, $t = 1, 2$, are equal to linear superpositions of some modulation vectors where the data is embedded in the coefficients. The modulation matrix $\mathbf{V}_t \in \mathcal{OC}^{(\mu_{1t} + \mu_{2t}) \times (\mu_{1t} + \mu_{2t})}$ is defined as

$$\mathbf{V}_t = [\mathbf{v}_t^{(1)}, \mathbf{v}_t^{(2)}, \ldots, \mathbf{v}_t^{(\mu_{1t} + \mu_{2t})}], \tag{3.91}$$

where $\mathbf{v}_t^{(i)}$, $i = 1, \ldots, \mu_{1t} + \mu_{2t}$, denote the modulation vectors, employed by transmitter t, to send μ_{1t} data streams to receiver one and μ_{2t} data streams to receiver two. The vectors $\tilde{\mathbf{s}}_1$ and $\tilde{\mathbf{s}}_2$ are equal to

$$\tilde{\mathbf{s}}_1 = \mathbf{V}_1 \mathbf{d}_1, \tag{3.92}$$

$$\tilde{\mathbf{s}}_2 = \mathbf{V}_2 \mathbf{d}_2, \tag{3.93}$$

where the vector $\mathbf{d}_t \in \mathcal{C}^{(\mu_{1t} + \mu_{2t}) \times 1}$ represents the $\mu_{1t} + \mu_{2t}$ streams of independent data. The covariance of the vector $\mathbf{d}_t$ is denoted by the diagonal matrix $\mathbf{P}_t$, i.e. $E[\mathbf{d}_t \mathbf{d}_t^\dagger] = \mathbf{P}_t$, $t = 1, 2$. At transmitter t, the data streams which modulate the vectors $\mathbf{v}_t^{(i)}$, $i = 1, \ldots, \mu'_{1t}$ and $i = \mu'_{1t} + \mu'_{21} + 1, \ldots, \mu_{1t} + \mu'_{2t}$, are intended for the receiver one, and the data streams which modulate the vectors $\mathbf{v}_t^{(i)}$, $i = \mu'_{1t} + 1, \ldots, \mu'_{1t} + \mu'_{2t}$ and $i = \mu_{1t} + \mu'_{2t} + 1, \ldots, \mu_{1t} + \mu_{2t}$, are intended for receiver two. We define $\mathbf{d}_{1t}$ and $\mathbf{d}_{2t}$ as

$$\mathbf{d}_{1t} = \begin{bmatrix} \mathbf{d}_t(1 : \mu'_{11}) \\ \mathbf{d}_t(\mu'_{11} + \mu'_{21} + 1 : \mu_{11} + \mu'_{21}) \end{bmatrix}, \tag{3.94}$$

and

$$\mathbf{d}_{2t} = \begin{bmatrix} \mathbf{d}_t(\mu'_{11} + 1 : \mu'_{11} + \mu'_{21}) \\ \mathbf{d}_t(\mu_{11} + \mu'_{21} + 1 : \mu_{11} + \mu_{21}) \end{bmatrix}, \tag{3.95}$$

which represent the data streams, sent by transmitter t to receiver one and two, respectively. The modulation and demodulation vectors are designed such that the data stream i has no interference over the data stream j for $j < i$. Choosing the codeword for the data stream j, the interference of the data stream j over data stream i is

non-causally known, and therefore can be effectively canceled out based on the dirty-paper-coding (DPC) theorem [7]. However, if the data streams i and j are sent to the same receiver, none of them has interference over the other, and DPC is not needed.

At receiver one, to decode $\mathbf{d}_{11}$, the signal coming from transmitter two, i.e. $\widetilde{\mathbf{H}}_{12}\mathbf{V}_{12}\mathbf{d}_2$, is treated as interference, therefore the covariance of the interference plus noise, $\mathbf{R}_{11}$, is equal to,

$$\mathbf{R}_{11} = \widetilde{\mathbf{H}}_{12}\mathbf{V}_2\mathbf{P}_2\mathbf{V}_2^\dagger\widetilde{\mathbf{H}}_{12} + \mathbf{I}, \tag{3.96}$$

where $\widetilde{\mathbf{H}}_{12}$ is defined in (3.77). The received vector $\mathbf{y}_1$ is passed through the whitening filter $\mathbf{\Psi}_{11}^\dagger = \mathbf{R}_{11}^{-\frac{1}{2}}$. The output of $\mathbf{\Psi}_{11}^\dagger$ is passed through the filter $\mathbf{U}_{11}^\dagger$ which maximizes the effective SNR. The design of $\mathbf{U}_{rt}^\dagger$, $r, t = 1, 2$, is explained later. Similarly, to decode $\mathbf{d}_{21}$ at receiver two, the signal from transmitter two, i.e. $\widetilde{\mathbf{H}}_{22}\mathbf{V}_2\mathbf{d}_2$ is treated as interference. The received vector $\mathbf{y}_2$ is passed through the whitening filter $\mathbf{\Psi}_{21}^\dagger = \mathbf{R}_{21}^{-\frac{1}{2}}$, where

$$\mathbf{R}_{21} = \widetilde{\mathbf{H}}_{22}\mathbf{V}_2\mathbf{P}_2\mathbf{V}_2^\dagger\widetilde{\mathbf{H}}_{22} + \mathbf{I}. \tag{3.97}$$

The output of $\mathbf{\Psi}_{21}^\dagger$ is passed through the filter $\mathbf{U}_{21}^\dagger$ which maximizes the effective SNR.

Let us assume that the modulation matrix $\mathbf{V}_2$, the covariance matrix $\mathbf{P}_2$, and the transmit filter $\mathbf{Q}_2$ are known, therefore one can compute $\mathbf{\Psi}_{11}^\dagger$ and $\mathbf{\Psi}_{21}^\dagger$. In the sequel, we explain how to choose $\mathbf{Q}_1$, $\mathbf{V}_1$, $\mathbf{P}_1$, $\mathbf{U}_{11}$, and $\mathbf{U}_{21}$.

The following algorithm is proposed to compute the columns of the matrix $\mathbf{Q}_1 \in \mathcal{OC}^{M_1 \times (\mu_{11}+\mu_{21})}$. The proposed algorithm is greedy in the sense that in each step, the di-

rection along which the corresponding link has the highest gain is added to the columns of the matrix $\mathbf{Q}_1$. In the algorithm, the following four sets of vectors are sequentially included in the columns of $\mathbf{Q}_1$: (i) the μ'_{11} mutually orthogonal directions for which the equivalent channel matrix $\mathbf{\Psi}^{\dagger}_{11}\mathbf{H}_{11}$ has the highest gains, (ii) the μ'_{21} mutually orthogonal directions for which the equivalent channel matrix $\mathbf{\Psi}^{\dagger}_{21}\mathbf{H}_{21}$ has the highest gains, (iii) if $\mu_{11} - \mu'_{11} \neq 0$, a set of directions such that $\mathrm{N}(\mathbf{H}_{21}) \in \Omega(\mathbf{Q}_1)$, (iv) if $\mu_{21} - \mu'_{21} \neq 0$, a set of directions such that $\mathrm{N}(\mathbf{H}_{11}) \in \Omega(\mathbf{Q}_1)$. Each set of vectors are chosen orthogonal to the previously selected columns. In what follows, we detail the algorithm in four stages.

Stage I

- Choose $\mathbf{q}_1^{(i)}$, $i = 1, \ldots, \mu'_{11}$, as μ'_{11} right singular vectors (RSV) corresponding to the μ'_{11} largest singular values of the matrix $\mathbf{\Psi}^{\dagger}_{11}\mathbf{H}_{11}$.

Stage II

- Choose $\mathbf{\Phi}_1 = [\phi_1, \ldots, \phi_{\mu_{11}+\mu_{21}-\mu'_{11}}]$ such that $[\mathbf{\Phi}_1, \mathbf{q}_1^{(1)}, \ldots, \mathbf{q}_1^{(\mu'_{11})}]$ forms a unitary matrix.

- Choose $\mathbf{q}_1'^{(i)}$, $i = 1, \ldots, \mu'_{21}$, as the μ'_{21} RSVs corresponding to the μ'_{21} largest singular values of the matrix $\mathbf{\Psi}^{\dagger}_{21}\mathbf{H}_{21}\mathbf{\Phi}_1$.

- Let $\mathbf{q}_1^{(\mu'_{11}+i)} = \mathbf{\Phi}_1\mathbf{q}_1'^{(i)}$, $i = 1, \ldots, \mu'_{21}$.

Stage III

- If $\mu_{11} - \mu'_{11} \neq 0$, then choose $\mathbf{q}_1^{(i)}$, $i = \mu'_{11} + \mu'_{21} + 1, \ldots, \mu_{11} + \mu'_{21}$, such that

$$\Omega([\mathbf{q}_1^{(1)}, \ldots, \mathbf{q}_1^{(\mu_{11}+\mu'_{21})}]) = \Omega([\mathbf{q}_1^{(1)}, \ldots, \mathbf{q}_1^{(\mu'_{11}+\mu'_{21})}, \mathrm{N}(\mathbf{H}_{21})]).$$

Stage IV

- If $\mu_{21} - \mu'_{21} \neq 0$, then choose $\mathbf{q}_1^{(i)}$, $i = \mu_{11} + \mu'_{21} + 1, \ldots, \mu_{11} + \mu_{21}$, such that

$$\Omega([\mathbf{q}_1^{(1)}, \ldots, \mathbf{q}_1^{(\mu_{11}+\mu_{21})}]) = \Omega([\mathbf{q}_1^{(1)}, \ldots, \mathbf{q}_1^{(\mu_{11}+\mu'_{21})}, \mathrm{N}(\mathbf{H}_{11})]).$$

After computing $\mathbf{Q}_1$, the broadcast sub-channel with $\overline{\mathbf{H}}_{11}$ and $\overline{\mathbf{H}}_{21}$, defined in Sub-section 3.3.1 as $\overline{\mathbf{H}}_{r1} = \mathbf{\Psi}_{r1}^\dagger \mathbf{H}_{r1} \mathbf{Q}_1$, $r = 1, 2$, is formed. Here, we explain how to choose the modulation and demodulation vectors for this broadcast sub-channel, based on the scheme presented in [37]. In the scheme presented in [37], the modulation vectors for different users can be selected iteratively in a specific order. Here, the modulation vectors are selected in the following order: (i) μ'_{11} modulation vectors for receiver one, (ii) μ'_{21} modulation vectors for receiver two, (iii) $\mu_{11} - \mu'_{11}$ modulation vectors for receiver one, (iv) $\mu_{21} - \mu'_{21}$ modulation vectors for receiver two. Here is the detail of the proposed scheme to find the modulation and the demodulation vectors.

Step one - Choosing μ'_{11} modulation vectors for receiver one

1) Respectively choose $\mathbf{v}_1^{(i)}$ and $\mathbf{u}_{11}^{(i)}$, $i = 1, \ldots, \mu'_{11}$, as RSV and left singular vector (LSV), corresponding to the ith largest singular value, $\sigma_{11}^{(i)}$, of the matrix $\overline{\mathbf{H}}_{11}$. Therefore, we have [25]

$$\sigma_{11}^{(i)} = \parallel \overline{\mathbf{H}}_{11} \mathbf{v}_1^{(i)} \parallel, \ i = 1, \ldots, \mu'_{11}, \tag{3.98}$$

$$\mathbf{u}_{11}^{(i)} = \frac{\overline{\mathbf{H}}_{11}\mathbf{v}_{11}^{(i)}}{\sigma_{11}^{(i)}}, \;\; i = 1, \ldots, \mu'_{11}. \tag{3.99}$$

With the above choice of the matrix $\mathbf{Q}_1$, it is easy to see that $\mathbf{v}_1^{(i)}$ is equal to the column i of the identity matrix $\mathbf{I}_{(\mu_{11}+\mu_{21})\times(\mu_{11}+\mu_{21})}$, for $i = 1, \ldots, \mu'_{11}$.

Step two - Choosing μ'_{21} modulation vectors for receiver two

2) Define $\boldsymbol{\varphi}_1^{(1)}, \ldots, \boldsymbol{\varphi}_1^{(\mu_{11}+\mu_{21}-\mu'_{11})}$ such that $[\mathbf{v}_1^{(1)}, \ldots, \mathbf{v}_1^{(\mu'_{11})}, \boldsymbol{\varphi}_1^{(1)}, \ldots, \boldsymbol{\varphi}_1^{(\mu_{11}+\mu_{21}-\mu'_{11})}]$ forms a unitary matrix. Then, define $\widehat{\overline{\mathbf{H}}}_{21}$ as

$$\widehat{\overline{\mathbf{H}}}_{21} = \overline{\mathbf{H}}_{21}[\boldsymbol{\varphi}_1^{(1)}, \ldots, \boldsymbol{\varphi}_1^{(\mu_{11}+\mu_{21}-\mu'_{11})}]. \tag{3.100}$$

3) Respectively choose $\overline{\mathbf{v}}_{21}^{(i)}$ and $\mathbf{u}_{21}^{(i)}$ as the RSV and LSV, corresponding to the ith largest singular value $\sigma_{21}^{(i)}$ of the matrix $\widehat{\overline{\mathbf{H}}}_{21}$. Therefore, we have,

$$\sigma_{21}^{(i)} = \| \widehat{\overline{\mathbf{H}}}_{21}\overline{\mathbf{v}}_{21}^{(i)} \|, \;\; i = 1, \ldots, \mu'_{21}, \tag{3.101}$$

$$\mathbf{u}_{21}^{(i)} = \frac{\widehat{\overline{\mathbf{H}}}_{21}\overline{\mathbf{v}}_{21}^{(i)}}{\sigma_{21}^{(i)}}, \;\; i = 1, \ldots, \mu'_{21}. \tag{3.102}$$

Then, let

$$\mathbf{v}_1^{(\mu'_{11}+i)} = [\boldsymbol{\varphi}_1^{(1)}, \ldots, \boldsymbol{\varphi}_1^{(\mu_{11}+\mu_{21}-\mu'_{11})}]\overline{\mathbf{v}}_{21}^{(i)}, \;\; i = 1, \ldots, \mu'_{21}. \tag{3.103}$$

It is easy to see that with the aforementioned choice of $\mathbf{Q}_1$, $\mathbf{v}_1^{(\mu'_{11}+i)}$ is equal to the column $\mu'_{11} + i$ of the matrix $\mathbf{I}_{(\mu_{11}+\mu_{21})\times(\mu_{11}+\mu_{21})}$, for $i = 1, \ldots, \mu'_{21}$.

Step three - Choosing $\mu_{11} - \mu'_{11}$ modulation vectors for receiver one

4) Define $\boldsymbol{\varphi}_2^{(1)}, \ldots, \boldsymbol{\varphi}_2^{(\mu_{11}+\mu_{21}-\mu'_{11}-\mu'_{21})}$ such that $[\mathbf{v}_1^{(1)}, \ldots, \mathbf{v}_1^{(\mu'_{11}+\mu'_{21})}, \boldsymbol{\varphi}_2^{(1)}, \ldots, \boldsymbol{\varphi}_2^{(\mu_{11}+\mu_{21}-\mu'_{11}-\mu'_{21})}]$

forms a unitary matrix. Then, define $\widehat{\overline{\mathbf{H}}}_{11}$ as

$$\widehat{\overline{\mathbf{H}}}_{11} = \overline{\mathbf{H}}_{11}[\boldsymbol{\varphi}_2^{(1)}, \ldots, \boldsymbol{\varphi}_2^{(\mu_{11}+\mu_{21}-\mu'_{11}-\mu'_{21})}]. \tag{3.104}$$

5) Respectively choose $\overline{\mathbf{v}}_{11}^{(i)}$ and $\mathbf{u}_{11}^{(i+\mu'_{11})}$ as the RSV and LSV, corresponding to the ith

largest singular value of the matrix $\widehat{\overline{\mathbf{H}}}_{11}$, denoted by $\sigma_{11}^{(i+\mu'_{11})}$, for $i = 1, \ldots, \mu_{11} -$

μ'_{11}. Therefore, we have,

$$\sigma_{11}^{(i+\mu'_{11})} = \| \widehat{\overline{\mathbf{H}}}_{11} \overline{\mathbf{v}}_{11}^{(i)} \|, \ \ i = 1, \ldots, \mu_{11} - \mu'_{11}, \tag{3.105}$$

$$\mathbf{u}_{11}^{(i+\mu'_{11})} = \frac{\widehat{\overline{\mathbf{H}}}_{11} \overline{\mathbf{v}}_{11}^{(i)}}{\sigma_{11}^{(i+\mu'_{11})}}, \ \ i = 1, \ldots, \mu_{11} - \mu'_{11}. \tag{3.106}$$

Then,

$$\mathbf{v}_1^{(\mu'_{11}+\mu'_{21}+i)} = [\boldsymbol{\varphi}_2^{(1)}, \ldots, \boldsymbol{\varphi}_2^{(\mu_{11}+\mu_{21}-\mu'_{11}-\mu'_{21})}]\overline{\mathbf{v}}_{11}^{(i)}, \ \ i = 1, \ldots, \mu_{11} - \mu'_{11}. \tag{3.107}$$

Step four - Choosing $\mu_{21} - \mu'_{21}$ modulation vectors for receiver two

6) Define $\boldsymbol{\varphi}_3^{(1)}, \ldots, \boldsymbol{\varphi}_3^{(\mu_{21}-\mu'_{21})}$ such that $[\mathbf{v}_1^{(1)}, \ldots, \mathbf{v}_1^{(\mu_{11}+\mu'_{21})}, \boldsymbol{\varphi}_3^{(1)}, \ldots, \boldsymbol{\varphi}_3^{(\mu_{21}-\mu'_{21})}]$ forms

a unitary matrix. Then, define $\widehat{\overline{\overline{\mathbf{H}}}}_{21}$ as

$$\widehat{\overline{\overline{\mathbf{H}}}}_{21} = \overline{\mathbf{H}}_{21}[\boldsymbol{\varphi}_3^{(1)}, \ldots, \boldsymbol{\varphi}_3^{(\mu_{21}-\mu'_{21})}]. \tag{3.108}$$

7) Respectively choose $\overline{\overline{\mathbf{v}}}_{21}^{(i)}$ and $\mathbf{u}_{21}^{(i+\mu'_{21})}$ as RSV and LSV, corresponding to the ith

largest singular value of the matrix $\widehat{\overline{\overline{\mathbf{H}}}}_{11}$, denoted by $\sigma_{21}^{(i+\mu'_{21})}$, for $i = 1, \ldots, \mu_{21} -$

μ'_{21}. Therefore, we have,

$$\sigma_{21}^{(i+\mu'_{21})} = \| \widehat{\overline{\overline{\mathbf{H}}}}_{21} \overline{\overline{\mathbf{v}}}_{21}^{(i)} \|, \ \ i = 1, \ldots, \mu_{21} - \mu'_{21}, \tag{3.109}$$

$$\mathbf{u}_{21}^{(i+\mu'_{21})} = \frac{\widehat{\widehat{\mathbf{H}}}_{21}\overline{\overline{\mathbf{v}}}_{21}^{(i)}}{\sigma_{21}^{(i+\mu'_{21})}}, \ i = 1,\ldots,\mu_{21} - \mu'_{21}. \tag{3.110}$$

Then, let

$$\mathbf{v}_{1}^{(\mu_{11}+\mu'_{21}+i)} = [\boldsymbol{\varphi}_{3}^{(1)},\ldots,\boldsymbol{\varphi}_{3}^{(\mu_{21}-\mu'_{21})}]\overline{\overline{\mathbf{v}}}_{21}^{(i)}, \ i = 1,\ldots,\mu_{11} - \mu'_{11}, \tag{3.111}$$

As shown in [37], by using this scheme, the broadcast channel, viewed from transmitter one is reduced to a set of parallel channels with gains $\sigma_{11}^{(i)}$, $i = 1,\ldots,\mu_{11}$ and $\sigma_{21}^{(j)}$, $j = 1,\ldots,\mu_{21}$. For power allocation, the power P_1 can be equally divided among the data streams or the water-filling algorithm can be used for optimal power allocation [19].

Similar procedure is applied for transmitter two to compute $\mathbf{Q}_2$, $\mathbf{V}_2$, $\mathbf{U}_{12}$, $\mathbf{U}_{22}$, $\mathbf{P}_2$, where

$$\mathbf{R}_{22} = \mathbf{H}_{21}\mathbf{V}_1\mathbf{P}_1\mathbf{V}_1^{\dagger}\mathbf{H}_{21}^{\dagger} + \mathbf{I}, \tag{3.112}$$

$$\boldsymbol{\Psi}_{22}^{\dagger} = \mathbf{R}_{22}^{-\frac{1}{2}}, \tag{3.113}$$

$$\mathbf{R}_{12} = \mathbf{H}_{11}\mathbf{V}_1\mathbf{P}_1\mathbf{V}_1^{\dagger}\mathbf{H}_{11}^{\dagger} + \mathbf{I}, \tag{3.114}$$

$$\boldsymbol{\Psi}_{12}^{\dagger} = \mathbf{R}_{12}^{-\frac{1}{2}}. \tag{3.115}$$

Note that to compute $\mathbf{Q}_1$, $\mathbf{V}_1$, and $\mathbf{P}_1$, we need to know $\mathbf{Q}_2$, $\mathbf{V}_2$, and $\mathbf{P}_2$ ($\boldsymbol{\Psi}_{11}$, and $\boldsymbol{\Psi}_{21}$ are functions of $\mathbf{Q}_2$, $\mathbf{V}_2$, and $\mathbf{P}_2$), and vice versa. To derive the modulation vectors, we can randomly initialize the matrices, and iteratively follow the scheme, until

the resulting matrices converge. Simulation results show that the algorithm converges very fast.

The dual of the proposed scheme here can be employed to improve Scheme II, presented in section 3.3.2.

3.6   Simulation Results

In the simulation part, we assume that the entries of the channel matrices have complex normal distribution with zero mean and unit variance.

Figure. 3.5 shows the sum-rate versus power for a X channel with $(2, 2, 3, 3)$ antennas, where the decomposition scheme presented in Section 3.3 is employed. Therefore, the achievable sum-rate is indeed equal the twice of the sum-capacity of a MIMO broadcast channel with 2 transmit antennas, and two user each with one antennas. The sum-capacity of the MIMO broadcast channel is fully characterized in [63, 64, 71]. To compute the sum-capacity, the effective algorithm presented in [70] is utilized. As a comparison, the capacity of a point-to-point MIMO channel with 4 transmit and 6 receive antennas is depicted. It is easy to see that both curves have the same slope (multiplexing gain). In addition, as expected by (3.89), the sum-rate of the X channel has 6.2 dB power loss in comparison with that of the MIMO channel.

Figure 3.6 shows the sum-rate versus power for an X channel with $(2, 2, 3, 3)$ and $(3, 3, 3, 3)$ antennas, where ZD-DPC scheme is used. As it is shown in Fig. 3.6, for the

case of $(2, 2, 3, 3)$ antennas, the joint design scheme has better performance than the decomposition scheme in low SNR regimes. The improvement is mainly due to utilizing whitening filters instead of zero-forcing filters. It is easy to see that in the high SNR, the whitening filters converge to zero-forcing filters. Note that in this case, optimizing $\mathbf{Q}_t$, $t = 1, 2$ offers no improvement. The reason is that the entire two-dimensional space available at each transmitter is utilized and there is no room for improvement. As depicted in Fig. 3.6, for the case of $(3, 3, 3, 3)$-antenna X channel, the joint design scheme has better performance as compared with the decomposition scheme in both high and low SNR regimes. The improvement relies on the fact that in this case at each transmitter, a two-dimensional sub-space of the three-dimensional space is needed for signaling. By using the scheme presented in Section 3.5, a sub-space for which the channel gains are optimal is chosen.

3.7 Conclusion

In a multiple-antenna system with two transmitters and two receivers, a new non-cooperative scenario of data communication is studied in which each receiver receives data from both transmitters. It is shown that by using some linear filters at the transmitters and at the receivers, the system is decomposed into two broadcast or two multi-access sub-channels. Using the decomposition scheme, it is shown that this signaling method outperforms other known non-cooperative schemes in terms
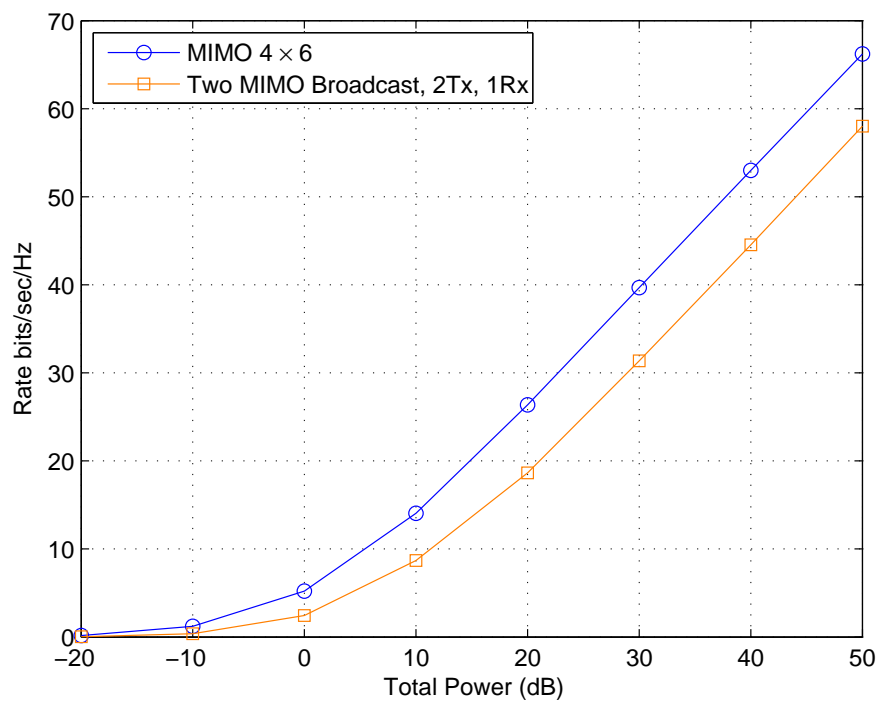
Figure 3.5: The Sum-capacity of Point-to-Point MIMO Channel with 4 Transmit and 6 Receive Antennas, and the Sum-Rate of the X Channel with (2,2,3,3) Antennas Achieved based on Decommission Scheme I
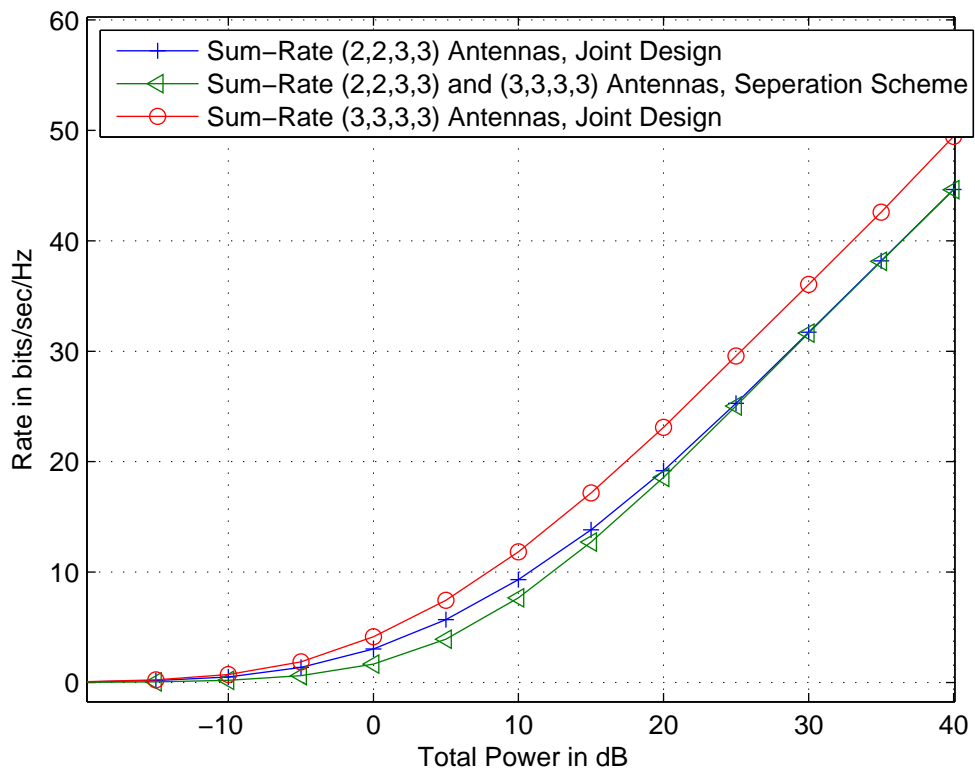
Figure 3.6: The Sum-Rate of the X Channels using ZF-DPC Scheme over the Decomposed Channels and the Sum-Rate of the X Channels achieved by Jointly Designed ZF-DPC Scheme

of the achieved multiplexing gain. In particular, it is shown that for a system with $(\lceil \frac{1}{2} \lfloor \frac{4N}{3} \rfloor \rceil, \lfloor \frac{1}{2} \lfloor \frac{4N}{3} \rfloor \rfloor, N, N)$ and $(N, N, \lceil \frac{1}{2} \lfloor \frac{4N}{3} \rfloor \rceil, \lfloor \frac{1}{2} \lfloor \frac{4N}{3} \rfloor \rfloor)$ antennas, the multiplexing gain of $\lfloor \frac{4N}{3} \rfloor$ is achievable, which is the MG of the system where full-cooperation between the transmitters or between the receivers is provided.

Chapter 4

Fairness in Multiuser Systems with Polymatroid Capacity Region

4.1 Introduction

In the multi-user scenarios, multiple transmitters/receivers share a common communication medium, and therefore, there is an inherent competition in accessing the channel. Information theoretic results for such systems imply that in order to achieve a high spectral efficiency, the users with stronger channel should have a higher portion of the resources. The drawback to this is the loss of the fairness among the users. Providing fairness, while achieving high-spectral efficiency, is thus a challenging problem.

A lot of research has addressed this problem and suggested different criteria to design a fair system. One of the first criteria is known as *max-min* measure. In this method,

the main effort is to maximize the minimum rate of the users, by giving the highest priority to the user with the worst channel. In other words, this method penalizes the users with better channel and sacrifices overall efficiency.

By relaxing the strict condition on fairness, the spectral efficiency can be increased. By compromising between fairness and throughput, proportional fairness is proposed in [32]. Based on this criterion, the rates of users with a stronger channel can be increased with the cost of decreasing the rates of users with a weaker channel. Any change in the rates is acceptable if the total proportional increase in the rates of some users is larger than the total proportional decrease in the rates of the rest. In fact, by relaxing the strict condition on fairness, the spectral efficiency increases. In [23], a criterion based on Nash Bargaining solution in the context of Game Theory is proposed. This method generalizes the proportional fairness and increases the efficiency of the system.

All of the aforementioned methods deal with a general multi-user system. However, for a wide class of multi-user systems, the capacity region has a special structure that we can exploit to provide fairness. Particularly in some multiuser systems, the boundary of the capacity region includes a facet on which the sum-rate is maximum (sum-capacity facet). In such systems, one can benefit from the available degrees of freedom, and determine the fairest rate-vector on the sum-capacity facet.

As a special case, we consider a class of multi-user systems, in which the whole or a subset of the capacity region which includes the corner points and the sum-capacity

facet forms a structure known as polymatroid. For this class of multi-user systems, the sum-capacity facet has $a!$ corner points, where a is the number of users with non-zero power (active users). The sum-capacity facet is the convex hull of these corner points. This means that the interior points of the sum-capacity facet can be attained by time-sharing among such corner points. As an example of such systems, it is shown that the capacity region of multiaccess channels (MAC) with fixed and independent input distributions forms a polymatroid [59]. In MAC, the sum-capacity is achieved by successive decoding. Applying different orders for the users in successive decoding results in different rate-vectors, all with the sum-rate equal to the sum-capacity. The resulting rate-vectors correspond to the corner points of the sum-capacity facet. Any point in the convex hull of these corner points is on the boundary. In [73], it is proven that the Marton inner bound (see [42]) for capacity region of the broadcast channel under fixed joint probability of the auxiliary and input variables, with some conditions, has a polymatroid structure[1]. As another example, we will show that a subset of the capacity region for multiple-input multiple-output (MIMO) broadcast channel which includes the corner points forms a polymatroid.

In [59], the optimal dynamic power allocation strategy for time-varying single-

---

[1]Throughout the chapter, we deal with the systems where the underlying capacity region or a its subset which included sum-capacity facet forms a polymatroid. Apparently, the proposed method can be applied over any achievable region which has the similar geometrical structure. In this case, the sum-capacity facet is replaced with maximum-sum-rate facet.

antenna multiple-access channel is established. To this end, the polymatroid properties of the capacity region for time-invariant multiple-access channel with fixed input distributions have been exploited. In [53], the polymatroid properties have been used to find a fair power allocation strategy. This problem is formulated by representing a point on the face of the contra-polymatroid (see [24, 59]) as a convex combination of its extreme points.

This article aims at finding a point on the sum-capacity facet which satisfies a notion of fairness among active users by exploiting the properties of polymatroids. In order to provide fairness, the minimum rate among all users is maximized (max-min rate). In the case that the rate of some users can not increase further (attain the max-min value), the algorithm recursively maximizes the minimum rate among the rest of the users. Since this rate-vector is in the face of the polymatroid, it can be achieved by time sharing among the corner points. It is shown that the problem of deriving the time-sharing coefficients to attain this point can be decomposed to some lower-dimensional subproblems. An alternative approach to attain an interior point for multiple access channels is *rate splitting* [21, 45]. This method is based on splitting all input sources except one into two parts and treating each spilt input as two virtual inputs (or two virtual users). By splitting the sources appropriately and successive decoding of virtual users in a suitable order, any point on the sum-capacity facet can be attained [21, 45]. Similar to the time-sharing procedure, we show that the problem of rate-splitting can be decomposed to some lower-dimensional subproblems.

There are cases that the complexity of achieving interior points is not feasible. This motivates us to compute the corner point for which the minimum rate of the active users is maximized (max-min corner point). A simple greedy algorithm is introduced to find the max-min corner point.

The rest of the chapter is organized as follows. In Section 4.2, the structure of the polymatroid is presented. In addition, the relationship between the capacity region of some channels and the polymatroid structure is described. Section 4.3 discusses the case in which the optimal fair corner point is computed. In Section 4.4, the optimal fair rate-vector on the sum-capacity facet is computed by exploiting polymatroid structures. In addition, it is shown that the problem of deriving the time-sharing coefficients and rate-splitting can be solved by decomposing the problem into some lower-dimensional subproblems.

4.2 Preliminaries

4.2.1 Polymatroid Structure

Defintion 4.1. *[68, Ch. 18]: Let $E = \{1, 2, \ldots, a\}$ and $\mathfrak{f} : 2^E \longrightarrow \mathcal{R}_+$ be a set function. The polyhedron*

$$\mathcal{B}(\mathfrak{f}, E) = \{(x_1, \ldots, x_a) : \mathbf{x}(S) \leq \mathfrak{f}(S), \forall S \subset E, \forall x_i \geq 0\} \tag{4.1}$$

is a polymatroid, if the set function $\mathfrak{f}$ satisfies

$$(normalized) \qquad \mathfrak{f}(\emptyset) = 0 \qquad\qquad (4.2)$$

$$(increasing) \qquad \mathfrak{f}(S) \leq \mathfrak{f}(T) \ if \ S \subset T \qquad\qquad (4.3)$$

$$(submodular) \quad \mathfrak{f}(S) + \mathfrak{f}(T) \geq \mathfrak{f}(S \cap T) + \mathfrak{f}(S \cup T) \qquad\qquad (4.4)$$

Any function $\mathfrak{f}$ that satisfies the above properties is termed as rank function. *Note that (4.1) imposes $2^{|E|}$ constraints on any given vector $(x_1, \ldots, x_a) \in \mathcal{B}(\mathfrak{f}, E)$.*

Corresponding to each permutation $\boldsymbol{\pi}$ of the set E, the polymatroid $\mathcal{B}(\mathfrak{f}, E)$ has a corner point $\boldsymbol{v}(\boldsymbol{\pi}) \in \mathcal{R}_+^a$ which is equal to:

$$v_{\pi(i)}(\boldsymbol{\pi}) = \begin{cases} \mathfrak{f}(\{\pi(i)\}) & i = 1 \\ \\ \mathfrak{f}(\{\pi(1), \ldots, \pi(i)\}) \\ \quad - \mathfrak{f}(\{\pi(1), \ldots, \pi(i-1)\}) & i = 2, \ldots, a \end{cases} \qquad (4.5)$$

Consequently, the polymatroid $\mathcal{B}(\mathfrak{f}, E)$ has $a!$ corner points corresponding to different permutations of the set E. All the corner points are on the facet $\mathbf{x}(E) = \mathfrak{f}(E)$. In addition, any point in the polymatroid on the facet $\mathbf{x}(E) = \mathfrak{f}(E)$ is in the convex hull of these corner points. The hyperplane $\mathbf{x}(E) = \mathfrak{f}(E)$ is called as dominant face, or simply face of the polymatroid. In this chapter, we use the term *sum-capacity facet* to denote the face of the polymatroid.

4.2.2 Capacity Region and Polymatroid Structure

For a wide class of multi-user systems, the whole or a subset of the capacity region forms a polymatroid structure. As the first example, consider a multiaccess system with a users, where the distribution of inputs are independent and equal to $p(x_1), \ldots, p(x_M)$. Then, the capacity region of such a system is characterized by [2, 35]

$$\left\{ \boldsymbol{\vartheta} \in \mathcal{R}_+^a | \boldsymbol{\vartheta}(S) \leq I\left(y; \{x_i, i \in S\} | \{x_i, i \in S^c\}\right) \quad \forall S \subset E \right\}, \tag{4.6}$$

where y is the received signal, $\boldsymbol{\vartheta}$ represents rate vector, I denotes the mutual information, and S^c is equal to $E - S$. It has been shown that the above polyhedron forms a polymatroid [59].

As the second example, we consider the capacity region of a multiple-antenna broadcast system. In the sequel, we show that a subset of the capacity region which includes the corner points and sum-capacity facet forms a polymatroid.

Consider a MIMO Broadcast Channel (MIMO-BC) with M transmit antennas and K users, where the rth user is equipped with N_r receive antennas. In a flat fading environment, the baseband model of this system is given by

$$\mathbf{y}_r = \mathbf{H}_r \mathbf{s} + \mathbf{w}_r, \quad 1 \leq r \leq K, \tag{4.7}$$

where $\mathbf{H}_r \in \mathcal{C}^{N_r \times M}$ denotes the channel matrix from the base station to user r, $\mathbf{s} \in \mathcal{C}^{M \times 1}$ represents the transmitted vector, and $\mathbf{y}_r \in \mathcal{C}^{N_r \times 1}$ signifies the received vector by user r. The vector $\mathbf{w}_r \in \mathcal{C}^{N_r \times 1}$ is a white Gaussian noise with zero-mean and identity-matrix covariance. Consider an order of the users $(\pi(1), \pi(2), \ldots, \pi(K))$. By assuming

that user $\pi(i)$ knows the codewords selected for the users $\pi(j)$, $j = 1, \ldots, i - 1$, the interference of the users $\pi(j)$, $j = 1, \ldots, i-1$, over user $\pi(i)$ can be effectively canceled based on dirty-paper-coding theorem [7]. Therefore, the rate of user $\pi(i), i = 1, \ldots, K$, is equal to

$$\vartheta_{\pi(i)} = \log \frac{\det \left(\mathbf{I}_{N_r,N_r} + \mathbf{H}_{\pi(i)} \left(\sum_{j \geq i} \mathbf{P}_{\pi(j)}^{\text{dual}} \right) \mathbf{H}_{\pi(i)}^{\dagger} \right)}{\det \left(\mathbf{I}_{N_r,N_r} + \mathbf{H}_{\pi(i)} \left(\sum_{j > i} \mathbf{P}_{\pi(j)}^{\text{dual}} \right) \mathbf{H}_{\pi(i)}^{\dagger} \right)}, \tag{4.8}$$

where $\mathbf{P}_{\pi(j)}^{\text{dual}}$ is the covariance of the signal vector to user $\pi(j)$. The capacity region is characterized as the convex hull of the union of such rate-vectors over all permutations $(\pi(1), \pi(2), \ldots, \pi(K))$ and over all positive semi-definite covariance matrices $\mathbf{P}_i^{\text{dual}}$, $i = 1, \ldots, K$ such that $\text{Tr} \left(\sum_{r=1}^{K} \mathbf{P}_r^{\text{dual}} \right) \leq P_T$, where P_T denotes the total transmit power [67]. In [3, 63, 64], a duality between the MIMO-BC and the MIMO-MAC is established. In the dual MIMO-MAC, the channel between user r and the base station is $\mathbf{H}_r^{\dagger}$ and the covariance of the power allocated to user r is $\mathbf{P}_r$. The relationship between $\mathbf{P}_r$ and $\mathbf{P}_r^{\text{dual}}$, $r = 1, \ldots, K$, has been derived [63]. The duality is used to characterize the sum-capacity of the MIMO-BC as follows

$$\begin{aligned} R_{\text{Sum-Capacity}} \quad &= \quad \max_{\mathbf{P}_1, \ldots, \mathbf{P}_K} \log \det \left(\mathbf{I}_{M,M} + \sum_{r=1}^{K} \mathbf{H}_r^{\dagger} \mathbf{P}_r \mathbf{H}_r \right). \\ s.t. \quad &\sum_{r=1}^{K} \text{Tr}(\mathbf{P}_r) \leq P_T, \\ &\mathbf{P}_r \succeq 0 \end{aligned} \tag{4.9}$$

The above optimization problem determines the power allocated to each user in the dual MIMO-MAC, and consequently, the power of each user in the MIMO-BC. Note that

only a subset of users is active and the power allocated to the rest is zero. Equation (4.9) determines the so-called sum-capacity facet. If the cardinality of the set of active users is a, i.e. $E = \{1, \cdots, a\}$, the sum-capacity facet has $a!$ corner points corresponding to different permutations of the active users. Note that the rates of the non-active users remain zero regardless of the permutation. The corner point corresponding to a permutation can be computed using (4.8). Assuming the active users are indexed by $i = 1, \ldots, a$, we define

$$\mathbf{D}_i = \mathbf{H}_i^\dagger \mathbf{P}_i^* \mathbf{H}_i, i = 1, \ldots, a, \tag{4.10}$$

where $\mathbf{P}_i^*$, $i = 1, \ldots, a$, correspond to optimizing matrices in (4.9). It is shown that the corner point in (4.8) can be reformulated as [63]

$$\vartheta_{\pi(i)} = \log \frac{\det \left(\mathbf{I}_{M,M} + \sum_{j \leq i} \mathbf{D}_{\pi(j)} \right)}{\det \left(\mathbf{I}_{M,M} + \sum_{j < i} \mathbf{D}_{\pi(j)} \right)}, \quad i = 1, \ldots, a, \tag{4.11}$$

which is the corner point of the dual MAC.

Regarding the polymatroid structure of the multiaccess channels and considering the duality of the MIMO-MAC and MIMO-BC, we can observe the polymatroid structure of a subset of MIMO-BC capacity region which includes the sum-capacity facet. However, to provide a better insight about the problem, we introduce a special polymatroid and establish its relationship with the capacity region of the MIMO-BC. For a set of positive semi-definite matrices $\mathbf{D}_i$, we define the set function $\mathfrak{g}$ as,

$$\mathfrak{g}(S) = \log \det \left(\mathbf{I} + \mathbf{D}(S) \right) \quad \text{for} \quad S \subset E. \tag{4.12}$$

Lemma 4.2. *Given* $\mathfrak{g}(S)$ *defined in (4.12), the polyhedron* $\mathcal{B}(\mathfrak{g}, E)$ *defined as follows is a polymatroid.*

$$\mathcal{B}(\mathfrak{g}, E) = \{(x_1, \ldots, x_a) \in \mathcal{R}_+^a : \mathbf{x}(S) \leq \mathfrak{g}(S), \ \forall S \subset E\}. \tag{4.13}$$

Proof. Clearly, $\mathfrak{g}(\emptyset) = 0$. Assume $\mathbf{B} \succeq 0$ and $\mathbf{C} \succeq 0$ are two Hermitian matrices. If $\mathbf{B} - \mathbf{C} \succeq 0$, then $\det(\mathbf{B}) \geq \det(\mathbf{C})$ [67, Proposition I.2]. Furthermore, if $\mathbf{\Delta} \succeq 0$, then [67, Proposition I.3]

$$\frac{\det(\mathbf{\Delta} + \mathbf{B} + \mathbf{C})}{\det(\mathbf{\Delta} + \mathbf{B})} \leq \frac{\det(\mathbf{B} + \mathbf{C})}{\det(\mathbf{B})}. \tag{4.14}$$

Using above properties, it is straight-forward to prove (4.3) and (4.4) for the set function $\mathfrak{g}(.)$. $\qquad\square$

In the set function $\mathfrak{g}(S)$, define $\mathbf{D}_i$ as defined in (4.10). It is easy to verify that the polymatroid $\mathcal{B}(\mathfrak{g}, E)$ is a subset of the capacity region of the MIMO-BC. The hyperplane $\mathbf{x}(E) = \mathfrak{g}(E)$ and its corner points (4.11) are the same as the sum-capacity facet and its corner points. Due to this property, we focus on the polymatroid $\mathcal{B}(\mathfrak{g}, E)$ (see Fig. 4.1).

4.3 The Fairest Corner Point

As mentioned, in some cases, the complexity of computing and implementing an appropriate time-sharing or rate-splitting algorithm is not feasible. This motivates us to compute the corner point for which the minimum rate of the active users is maximized
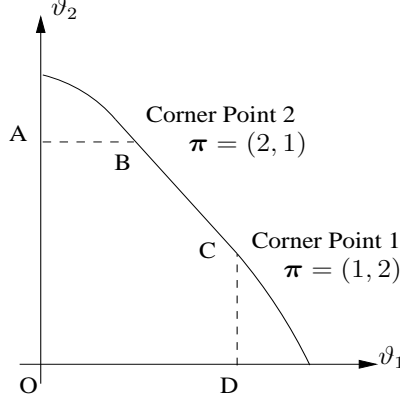
Figure 4.1: Capacity Region of the MIMO-BC and Its Corner Points. The Region OABCD Is a Polymatroid. The Line BC Is the Sum-Capacity Facet.

(max-min corner point). In the following, we present a simple greedy algorithm to find the max-min corner point of a general polymatroid $\mathcal{B}(\mathfrak{f}, E)$.

Algorithm 4.3.

  1. *Set $\alpha = a$, $S = \varnothing$.*

  2. *Set $\pi^*(\alpha)$ as*

$$\pi^*(\alpha) = \arg \min_{z \in E, z \notin \mathcal{S}} \mathfrak{f}\left(E - S - \{z\}\right). \tag{4.15}$$

  3. *If $\alpha > 1$, then $S \longleftarrow S \cup \{\pi^*(\alpha)\}$, $\alpha \longleftarrow \alpha - 1$, and go to Step 2; otherwise stop.*

The following theorem proves the optimality of the above algorithm.

Theorem 4.4. *Let the vector $\boldsymbol{v}(\boldsymbol{\pi}^*)$ be the corner point of the polymatroid $\mathcal{B}(\mathfrak{f}, E)$ corresponding to the permutation $\boldsymbol{\pi}^* = (\pi^*(1), \ldots, \pi^*(a))$. For any other permutation*

$$\boldsymbol{\pi} = (\pi(1), \ldots, \pi(a)),$$

$$\min_i v_{\pi^*(i)}(\boldsymbol{\pi}^*) \geq \min_i v_{\pi(i)}(\boldsymbol{\pi}). \tag{4.16}$$

Proof. Assume that in the permutation $\boldsymbol{\pi}^*$, the user $\hat{t}$ which is located in position l in the permutation $\boldsymbol{\pi}^*$ (i.e. $\hat{t} = \pi^*(l)$) has the minimum rate

$$v_{\pi^*(l)}(\boldsymbol{\pi}^*) = \min_i v_{\pi^*(i)}(\boldsymbol{\pi}^*). \tag{4.17}$$

Let us define two sets:

- The set of users located before $\pi^*(l)$ in $\boldsymbol{\pi}^*$: $\underline{\Phi} = \{\pi^*(1), \ldots, \pi^*(l-1)\}$.

- The set of users located after $\pi^*(l)$ in $\boldsymbol{\pi}^*$: $\underline{\Psi} = \{\pi^*(l+1), \ldots, \pi^*(a)\}$.

Using (4.5), we have

$$v_{\hat{t}}(\boldsymbol{\pi}^*) = \mathfrak{f}(\underline{\Phi} \cup \{\hat{t}\}) - \mathfrak{f}(\underline{\Phi}). \tag{4.18}$$

In the following, we consider different scenarios which generate new permutations and prove that in all cases, (4.16) is valid.

Case 1. *Permutation in $\underline{\Phi}$ and $\underline{\Psi}$:* By considering (4.18), it is apparent that any permutation of the users in $\underline{\Phi}$ and $\underline{\Psi}$ does not change the rate of the user $\pi^*(l)$ (see Fig. 4.2).

Case 2. *Moving a set of users from $\underline{\Psi}$ to the set $\underline{\Phi}$:* Assume a set $\underline{\Upsilon}$ of users, $\underline{\Upsilon} \subset \underline{\Psi}$, is moved from $\underline{\Psi}$ to the set $\underline{\Phi}$ to generate a new permutation $\boldsymbol{\pi}$ (see Fig. 4.3). The rate of the user $\hat{t}$ in the new permutation is equal to:

$$v_{\hat{t}}(\boldsymbol{\pi}) = \mathfrak{f}(\underline{\Phi} \cup \underline{\Upsilon} \cup \{\hat{t}\}) - \mathfrak{f}(\underline{\Phi} \cup \underline{\Upsilon}). \tag{4.19}$$
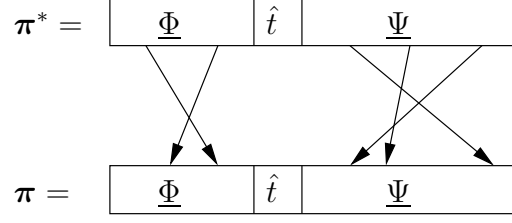
Figure 4.2: Case 1. Permutation in $\underline{\Phi}$ and $\underline{\Psi}$.

From (4.4), we can show that

$$\mathfrak{f}(\underline{\Phi} \cup \{\hat{t}\}) + \mathfrak{f}(\underline{\Phi} \cup \underline{\Upsilon}) \geq \mathfrak{f}(\underline{\Phi} \cup \underline{\Upsilon} \cup \{\hat{t}\}) + \mathfrak{f}(\underline{\Phi}). \tag{4.20}$$

Using (4.18), (4.19), and (4.20), we conclude that $v_{\hat{t}}(\boldsymbol{\pi}) \leq v_{\hat{t}}(\boldsymbol{\pi}^*)$, and therefore, $\min_i v_{\pi(i)}(\boldsymbol{\pi}) \leq \min_i v_{\pi^*(i)}(\boldsymbol{\pi}^*)$.
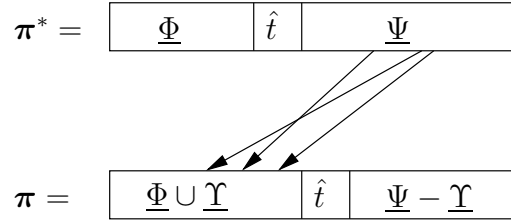
Figure 4.3: Case 2. Moving a set of users from $\underline{\Psi}$ to the set $\underline{\Phi}$.

Case 3. *Moving one or more users from the set $\underline{\Phi}$ to the set $\underline{\Psi}$ (with or without moving some users from the set $\underline{\Psi}$ to the set $\underline{\Phi}$):* Assume that one or more users move from $\underline{\Phi}$ to $\underline{\Psi}$ (with or without moving some users from the set $\underline{\Psi}$ to the set $\underline{\Phi}$) to generate the new permutation $\boldsymbol{\pi}$. As depicted in Fig. 4.4, assume that the user ν is positioned last in the permutation $\boldsymbol{\pi}$ among the users moved from $\underline{\Phi}$ to $\underline{\Psi}$ (user $\pi(1)$ is positioned first and user $\pi(a)$ is positioned last in the permutation $\boldsymbol{\pi}$).
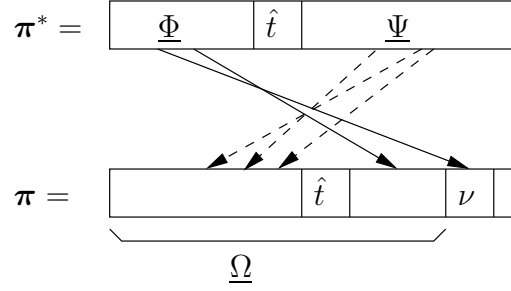
Figure 4.4: Case 3. Moving one or more users from the set $\underline{\Phi}$ to the set $\underline{\Psi}$ (with or without moving some users from the set $\underline{\Psi}$ to the set $\underline{\Phi}$).

Let $\underline{\Omega}$ be the set of users located before the user ν in the permutation $\boldsymbol{\pi}$. Using (4.5), we have,

$$\upsilon_\nu(\boldsymbol{\pi}) = \mathfrak{f}(\underline{\Omega} \cup \{\nu\}) - \mathfrak{f}(\underline{\Omega}). \tag{4.21}$$

It is clear that,

$$\{\hat{t}\} \cup \underline{\Phi} - \{\nu\} \subset \underline{\Omega}. \tag{4.22}$$

Using (4.4) with $S = \underline{\Phi} \cup \{\hat{t}\}$ and $T = \underline{\Omega}$, and regarding (4.22), we have,

$$\mathfrak{f}(\underline{\Omega} \cup \{\nu\}) - \mathfrak{f}(\underline{\Omega}) \le \mathfrak{f}(\underline{\Phi} \cup \{\hat{t}\}) - \mathfrak{f}(\underline{\Phi} \cup \{\hat{t}\} - \{\nu\}). \tag{4.23}$$

On the other hand, the user ν is in the set $\underline{\Phi}$ in permutation $\boldsymbol{\pi}^*$. It means that in Step 2 of the algorithm, this user has been compared with other users in the set $\underline{\Phi} \cup \{\hat{t}\}$ to be located in the position l, but the user $\hat{t}$ has been chosen for the position, i.e. $\mathfrak{f}\left(\underline{\Phi} \cup \{\hat{t}\} - \{\hat{t}\}\right) \le \mathfrak{f}\left(\underline{\Phi} \cup \{\hat{t}\} - \{\nu\}\right)$, therefore,

$$\mathfrak{f}\left(\underline{\Phi}\right) \le \mathfrak{f}\left(\underline{\Phi} \cup \{\hat{t}\} - \{\nu\}\right). \tag{4.24}$$

Using (4.18), (4.21), (4.23), and (4.24), we conclude that $\upsilon_{\nu}(\boldsymbol{\pi}) \leq \upsilon_{\hat{t}}(\boldsymbol{\pi}^{*})$, and therefore, we have $\min_{i} \upsilon_{\pi(i)}(\boldsymbol{\pi}) \leq \min_{i} \upsilon_{\pi^{*}(i)}(\boldsymbol{\pi}^{*})$. Note that the permutation of users located before (or after) the user ν in the permutation $\boldsymbol{\pi}$ does not increase $\upsilon_{\nu}(\boldsymbol{\pi})$. $\square$

Remark: For multiple access channels, the above algorithm suggests that to attain the fairest corner point with successive decoding, at each step, one should decode the strongest user (the user with the highest rate, while the signals of the remaining users are considered as interference). Note that in MAC, the corner point corresponding to the specific permutation $\boldsymbol{\pi}$ is obtained by the successive decoding in the reverse order of the permutation.

It is worth mentioning that by using a similar algorithm, one can find the corner point for which the maximum rate is minimum. The algorithm is as follows:

Algorithm 4.5.

1. *Set* $\alpha = 1$, $S = \varnothing$.

2. *Set* $\pi^{*}(\alpha)$ *as*

$$\pi^{*}(\alpha) = \arg \max_{z \in E, z \notin \mathcal{S}} \mathfrak{f}\left(S + \{z\}\right). \tag{4.25}$$

3. *If* $\alpha < a$, *then* $S \longleftarrow S \cup \{\pi^{*}(\alpha)\}$, $\alpha \longleftarrow \alpha + 1$, *and go to Step 2; otherwise stop.*

The optimality of the above algorithm can be proven by a similar method as used to prove Theorem 4.4.

4.4   Optimal Rate-Vector on the Sum-Capacity Facet

4.4.1   Max-Min Operation over a Polymatroid

In the following, the polymatroid properties are exploited to locate an optimal fair point on the sum-capacity facet. For an optimal fair point, the minimum rate among all the users should be maximized (max-min rate). For a sum-capacity of $R_{\text{Sum-Capacity}}$, a fair rate allocation would ideally achieve an equal rate of $\dfrac{R_{\text{Sum-Capacity}}}{a}$ for the a active users. Although this rate-vector is feasible for some special cases (see Fig. 4.5), it is not attainable in the general case (see Fig. 4.6). The maximum possible value for the minimum entry of a vector $\mathbf{x}$, where $\mathbf{x} \in \mathcal{B}(\mathfrak{f}, E)$, can be computed using the following lemma.
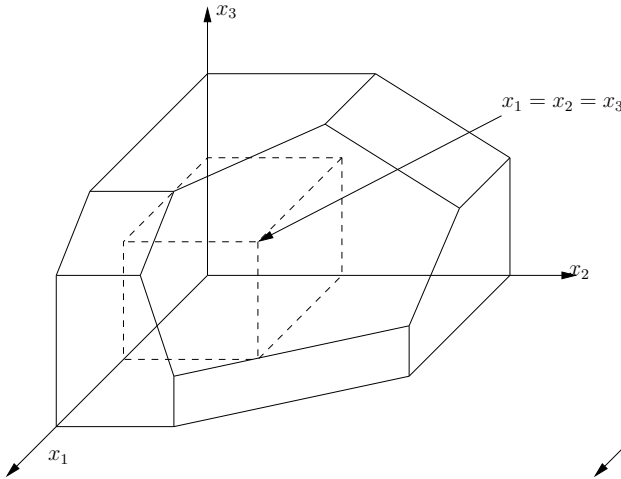
Figure 4.5: All-Equal Rate-Vector Is on the Sum-Capacity Facet
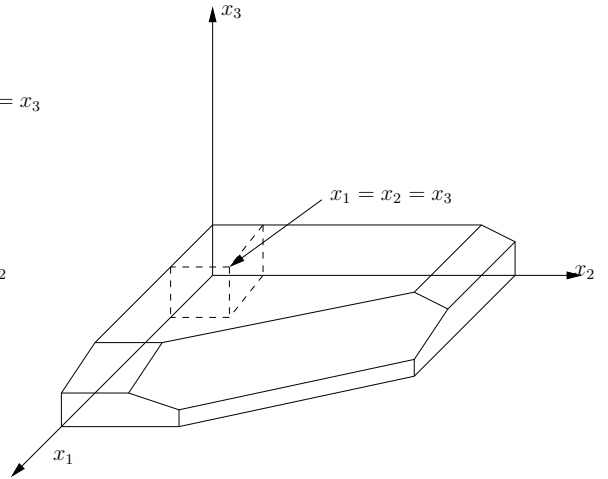
Figure 4.6: All-Equal Rate-Vector Is NOT on the Sum-Capacity Facet

Lemma 4.6. *In the polymatroid $\mathcal{B}(\mathfrak{f}, E)$, define*

$$\underline{\delta} \quad = \quad \max \min_{i \in E} x_i.$$

$$\text{s.t.} \quad (x_1, \ldots, x_a) \in \mathcal{B}(\mathfrak{f}, E). \tag{4.26}$$

Then,

$$\underline{\delta} = \min_{S \subset E, S \neq \emptyset} \frac{\mathfrak{f}(S)}{|S|}. \tag{4.27}$$

Proof. Consider $\mathbf{x} \in \mathcal{B}(\mathfrak{f}, E)$, and let $\sigma = \min_i x_i$. Therefore,

$$\forall S \subset E, \ \sigma |S| \leq \mathbf{x}(S). \tag{4.28}$$

Noting $\forall S \subset E, \ \mathbf{x}(S) \leq \mathfrak{f}(S)$ and using the above inequality, we have

$$\forall S \subset E, \ \sigma |S| \leq \mathfrak{f}(S). \tag{4.29}$$

Consequently, $\sigma \leq \min_{S \subset E, \ S \neq \emptyset} \frac{\mathfrak{f}(S)}{|S|}$. Therefore, $\min_{S \subset E, \ S \neq \emptyset} \frac{\mathfrak{f}(S)}{|S|}$ provides an upper bound on $\min_i x_i$. By selecting $\mathbf{x} = \underline{\delta} \mathbf{1}_a \in \mathcal{B}(\mathfrak{f}, E)$, where $\underline{\delta} = \min_{S \subset E, \ S \neq \emptyset} \frac{\mathfrak{f}(S)}{|S|}$, the upper bound is achieved, and the proof is completed. $\qquad \square$

In minimization (4.27), if the minimizer is not the set E, then $\underline{\delta}$ (the optimal max-min value) is less than $\frac{R_{\text{Sum-Capacity}}}{a}$ ($R_{\text{Sum-Capacity}} = \mathfrak{f}(E)$ is the sum-capacity), and therefore, the ideal fairness is not feasible. For example, in the polymatroid depicted in Fig 4.6, the minimizing set in (4.27) is the set $\{3\}$, and therefore $\underline{\delta} = \mathfrak{f}(\{3\})$.

In the following, a recursive algorithm is proposed to locate a rate vector $\mathbf{x}^*$ on the sum-capacity facet which not only attains the optimal max-min value $\underline{\delta}$, but also

provides fairness among the users which have the rates higher than $\underline{\delta}$. The proposed algorithm partitions the set of active users into $\varsigma + 1$ disjoint subsets, $S^{\langle 0 \rangle}, ..., S^{\langle \varsigma \rangle}$, such that in the i'th subset the rate of all users is equal to $\varrho^{\langle i \rangle}, i = 0, \cdots, \varsigma$, where $\underline{\delta} = \varrho^{\langle 0 \rangle} < \varrho^{\langle 1 \rangle} < \cdots < \varrho^{\langle \varsigma \rangle}$. Starting from $\varrho^{\langle 0 \rangle}$, the algorithm maximizes $\varrho^{\langle i \rangle}$, $i = 1, \cdots, \varsigma$, given that $\varrho^{\langle j \rangle}$'s, $j = 0, \cdots, i - 1$, are already at their maximum possible values. To simplify this procedure, we establish a chain of nested polymatroids, $\mathcal{B}(\mathfrak{f}^{\langle \alpha \rangle}, E^{\langle \alpha \rangle})$, $\alpha = 0, \ldots, \varsigma$, where

$$\mathcal{B}(\mathfrak{f}^{\langle \varsigma \rangle}, E^{\langle \varsigma \rangle}) \subset \mathcal{B}(\mathfrak{f}^{\langle \varsigma - 1 \rangle}, E^{\langle \varsigma - 1 \rangle}) \subset \ldots \subset \mathcal{B}(\mathfrak{f}^{\langle 0 \rangle}, E^{\langle 0 \rangle}) = \mathcal{B}(\mathfrak{f}, E). \qquad (4.30)$$

In this algorithm, we use the result of the following lemma.

Lemma 4.7. *Let $E = \{1, \ldots, a\}$ and $A \subset E$, $A \neq E$. If the set function $\mathfrak{f} : 2^E \longrightarrow \mathcal{R}_+$ is a rank function, then $\mathfrak{h} : 2^{E-A} \longrightarrow \mathcal{R}_+$, defined as*

$$\mathfrak{h}(S) = \mathfrak{f}(S \cup A) - \mathfrak{f}(A), \quad S \subset E - A, \qquad (4.31)$$

is a rank function.

Proof. By direct verification. $\qquad \square$

Using the following algorithm, one can compute the rate-vector $\mathbf{x}^*$.

Algorithm 4.8.

    1. Initialize the iteration index $\alpha = 0$, $E^{\langle 0 \rangle} = E$, and $\mathfrak{f}^{\langle 0 \rangle} = \mathfrak{f}$.

2. *Find $\varrho^{\langle\alpha\rangle}$, where*

$$\varrho^{\langle\alpha\rangle} = \min_{S \subset E^{\langle\alpha\rangle}, S \neq \emptyset} \frac{\mathfrak{f}^{\langle\alpha\rangle}(S)}{|S|}. \tag{4.32}$$

Set $S^{\langle\alpha\rangle}$ equal to the optimizing subset.

3. *For all $i \in S^{\langle\alpha\rangle}$, set $x_i^* = \varrho^{\langle\alpha\rangle}$.*

4. *Define the polymatroid $\mathcal{B}(\mathfrak{f}^{\langle\alpha+1\rangle}, E^{\langle\alpha+1\rangle})$, where*

$$E^{\langle\alpha+1\rangle} = E^{\langle\alpha\rangle} - S^{\langle\alpha\rangle}, \tag{4.33}$$

and $\forall S \subset E^{\langle\alpha+1\rangle}$,

$$\mathfrak{f}^{\langle\alpha+1\rangle}(S) = \mathfrak{f}^{\langle\alpha\rangle}(S \cup S^{\langle\alpha\rangle}) - \mathfrak{f}^{\langle\alpha\rangle}(S^{\langle\alpha\rangle}). \tag{4.34}$$

5. *If $E^{\langle\alpha+1\rangle} \neq \emptyset$, set $\alpha \longleftarrow \alpha + 1$ and move to step 2, otherwise stop.*

This algorithm computes the optimization sets $S^{\langle\alpha\rangle}$, $\alpha = 0, \cdots, \varsigma$ and their corresponding $\varrho^{\langle\alpha\rangle}$, where $E = \bigcup_{j=0}^{\varsigma} S^{\langle j\rangle}$ and $x_i^* \in \{\varrho^{\langle 0\rangle}, \cdots, \varrho^{\langle\varsigma\rangle}\}, i = 1, \cdots, a$.

To provide better insight about the algorithm, let us apply it over the polymatroids depicted in figures 4.5 and 4.6. For the polymatroid in Fig. 4.5, the algorithm results in $\mathbf{x}^* = (\varrho^{\langle 0\rangle}, \varrho^{\langle 0\rangle}, \varrho^{\langle 0\rangle})$ where $\varrho^{\langle 0\rangle} = \frac{\mathfrak{f}(\{1,2,3\})}{3}$. For the polymatroid shown in Fig 4.6, the resulting point is $\mathbf{x}^* = (\varrho^{\langle 1\rangle}, \varrho^{\langle 1\rangle}, \varrho^{\langle 0\rangle})$, where $\varrho^{\langle 0\rangle} = \frac{\mathfrak{f}(\{3\})}{1}$ and $\varrho^{\langle 1\rangle} = \frac{\mathfrak{f}^{\langle 1\rangle}(\{1,2\})}{2} = \frac{\mathfrak{f}(\{1,2,3\}) - \mathfrak{f}(\{3\})}{2}$ (see Fig. 4.7).

In the following, we prove some properties of the vector $\mathbf{x}^*$.

Theorem 4.9. *Assume that Algorithm 4.8 is applied over the polymatroid $\mathcal{B}(\mathfrak{f}, E)$, then*
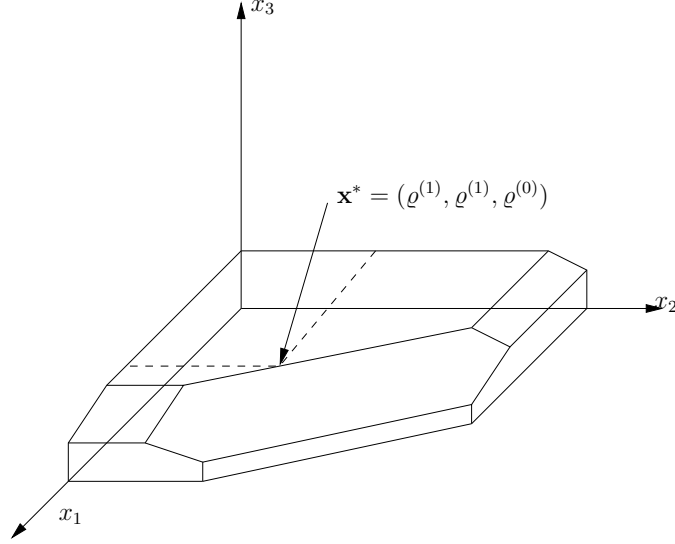
Figure 4.7: The Fairest Rate Vector $\mathbf{x}^*$ on the Sum-Rate Facet of the Polymatroid

(I) $\mathbf{x}^* \in \mathcal{B}(\mathfrak{f}, E)$ *and is located on the sum-capacity facet* $\mathbf{x}(E) = \mathfrak{f}(E)$.

(II) *The minimum entry of the vector* $\mathbf{x}^*$ *attains the optimum value determined by Lemma 4.6 and*

$$\underline{\delta} = \varrho^{\langle 0 \rangle} < \varrho^{\langle 1 \rangle} < \cdots < \varrho^{\langle \varsigma \rangle}. \tag{4.35}$$

Proof. **Part (I):** We show that $\mathbf{x}^* \in \mathcal{B}(\mathfrak{f}, E)$. According to the algorithm, we have $\varrho^{\langle 0 \rangle} = \min_{S \subset E, S \neq \emptyset} \frac{\mathfrak{f}(S)}{|S|}$, where $S^{\langle 0 \rangle}$ is the minimizing set. In addition, $x_i^* = \varrho^{\langle 0 \rangle}$ for all $i \in S^{\langle 0 \rangle}$. It is straight-forward to check that the assigned values for $x_i^*, i \in S^{\langle 0 \rangle}$, do not violate the constraints of the polymatroid $\mathcal{B}(\mathfrak{f}, E)$, expressed in (4.1). By substituting the assigned values for $x_i, i \in S^{\langle 0 \rangle}$, in the constraints of the polymatroid $\mathcal{B}(\mathfrak{f}, E)$, the constraints over the coordinate i, $i \in E - S^{\langle 0 \rangle}$, are updated as follows: from the definition of the polymatroid, we have a set of constraints on $\mathbf{x}(S)$, $S \subset E - S^{\langle 0 \rangle}$, which

has the following format:

$$\forall A \subset S^{\langle 0 \rangle}, \mathbf{x}(S \cup A) \leq \mathfrak{f}^{\langle 0 \rangle}(S \cup A). \tag{4.36}$$

Since $S \cap A = \emptyset$, then $\mathbf{x}(S \cup A) = \mathbf{x}(S) + \mathbf{x}(A)$. Consequently, from (4.36), we have,

$$\forall A \subset S^{\langle 0 \rangle}, \mathbf{x}(S) \leq \mathfrak{f}^{\langle 0 \rangle}(S \cup A) - \mathbf{x}(A). \tag{4.37}$$

Consequently, $\forall \ S \subset E - S^{\langle 0 \rangle}$,

$$\mathbf{x}(S) \leq \min_{A \subset S^{\langle 0 \rangle}} \{\mathfrak{f}^{\langle 0 \rangle}(S \cup A) - \mathbf{x}(A)\}. \tag{4.38}$$

We claim that $\min_{A \subset S^{\langle 0 \rangle}} \{\mathfrak{f}^{\langle 0 \rangle}(S \cup A) - \mathbf{x}(A)\}$ is equal to $\mathfrak{f}^{\langle 0 \rangle}(S \cup S^{\langle 0 \rangle}) - \mathfrak{f}^{\langle 0 \rangle}(S^{\langle 0 \rangle})$. The proof is as follows:

$$\forall A \subset S^{\langle 0 \rangle}, \quad \mathfrak{f}^{\langle 0 \rangle}(S \cup A) - \mathbf{x}(A) \tag{4.39}$$

$$\geq \mathfrak{f}^{\langle 0 \rangle}(S \cup A) - \mathfrak{f}^{\langle 0 \rangle}(A) \tag{4.40}$$

$$\geq \mathfrak{f}^{\langle 0 \rangle}(S \cup S^{\langle 0 \rangle}) - \mathfrak{f}^{\langle 0 \rangle}(S^{\langle 0 \rangle}). \tag{4.41}$$

The first inequality relies on the fact that $\forall A$, $\mathbf{x}(A) \leq \mathfrak{f}^{\langle 0 \rangle}(A)$. The second inequality is proven by using (4.4) and the fact that $A \subset S^{\langle 0 \rangle}$ and $S \cap S^{\langle 0 \rangle} = \emptyset$. It is easy to check that the above inequalities change to equalities for $A = S^{\langle 0 \rangle}$.

Regarding the above statements, for the non-allocated entries of $\mathbf{x}$, we have the following set of constraints,

$$\forall S \subset E - S^{\langle 0 \rangle}, \ \mathbf{x}(S) \leq \mathfrak{f}^{\langle 0 \rangle}(S \cup S^{\langle 0 \rangle}) - \mathfrak{f}^{\langle 0 \rangle}(S^{\langle 0 \rangle}). \tag{4.42}$$

Let us define $E^{\langle 1 \rangle} = E^{\langle 0 \rangle} - S^{\langle 0 \rangle}$, $\mathfrak{f}^{\langle 1 \rangle}(S) = \mathfrak{f}^{\langle 0 \rangle}(S \cup S^{\langle 0 \rangle}) - \mathfrak{f}^{\langle 0 \rangle}(S^{\langle 0 \rangle})$, $\forall S \subset E^{\langle 1 \rangle}$.

By using Lemma 4.7, the set of constraints (4.42) on $E^{\langle 1 \rangle}$ defines the polymatroid $\mathcal{B}(\mathfrak{f}^{\langle 1 \rangle}, E^{\langle 1 \rangle})$, which is a subset of $\mathcal{B}(\mathfrak{f}, E)$. Now, we use the same procedure that is applied for $\mathcal{B}(\mathfrak{f}^{\langle 0 \rangle}, E^{\langle 0 \rangle})$ over $\mathcal{B}(\mathfrak{f}^{\langle 1 \rangle}, E^{\langle 1 \rangle})$, and continue recursively. Therefore, in iteration indexed by α, $\alpha = 0, \ldots, \varsigma$, the rates of a subset of coordinates are determined such that the constraints of the polymatroid $\mathcal{B}(\mathfrak{f}^{\langle \alpha \rangle}, E^{\langle \alpha \rangle})$ are not violated. Since $\mathcal{B}(\mathfrak{f}^{\langle \alpha \rangle}, E^{\langle \alpha \rangle}) \subset \mathcal{B}(\mathfrak{f}, E)$, then $\mathbf{x}^* \in \mathcal{B}(\mathfrak{f}, E)$. Direct verification proves that $\mathbf{x}^*(E) = \mathfrak{f}(E)$.

Part (II): We must show that the smallest entries of $\mathbf{x}^*$ is equal to $\min_{S \subset E} \frac{\mathfrak{f}(S)}{|S|}$. According to the algorithm, for all $i \in E$, we have $x_i^* \in \{\varrho^{\langle 0 \rangle}, ..., \varrho^{\langle \varsigma \rangle}\}$. Furthermore, $\varrho^{\langle 0 \rangle} = \min_{S \subset E} \frac{\mathfrak{f}(S)}{|S|}$.

From the algorithm, we have

$$\varrho^{\langle j \rangle} = \frac{\mathfrak{f}^{\langle j \rangle}(S^{\langle j \rangle})}{|S^{\langle j \rangle}|} = \min_{S \subset E^{\langle j \rangle}} \frac{\mathfrak{f}^{\langle j \rangle}(S)}{|S|} < \frac{\mathfrak{f}^{\langle j \rangle}(S^{\langle j+1 \rangle} \cup S^{\langle j \rangle})}{|S^{\langle j+1 \rangle} \cup S^{\langle j \rangle}|} = \frac{\mathfrak{f}^{\langle j \rangle}(S^{\langle j+1 \rangle} \cup S^{\langle j \rangle})}{|S^{\langle j+1 \rangle}| + |S^{\langle j \rangle}|}. \qquad (4.43)$$

Therefore,

$$\varrho^{\langle j \rangle} < \frac{\mathfrak{f}^{\langle j \rangle}(S^{\langle j+1 \rangle} \cup S^{\langle j \rangle})}{|S^{\langle j+1 \rangle}| + |S^{\langle j \rangle}|} \qquad \Longrightarrow \qquad (4.44)$$

$$\varrho^{\langle j \rangle} < \frac{\mathfrak{f}^{\langle j \rangle}(S^{\langle j+1 \rangle} \cup S^{\langle j \rangle}) - \varrho^{\langle j \rangle}|S^{\langle j \rangle}|}{|S^{\langle j+1 \rangle}|} \qquad \Longrightarrow \qquad (4.45)$$

$$\varrho^{\langle j \rangle} < \frac{\mathfrak{f}^{\langle j \rangle}(S^{\langle j+1 \rangle} \cup S^{\langle j \rangle}) - \mathfrak{f}^{\langle j \rangle}(S^{\langle j \rangle})}{|S^{\langle j+1 \rangle}|} = \varrho^{\langle j+1 \rangle}, \qquad (4.46)$$

where (4.46) relies on LHS of (4.43). Consequently, $\varrho^{\langle 0 \rangle} < \varrho^{\langle 1 \rangle} < \ldots < \varrho^{\langle \varsigma \rangle}$ and the proof is complete. $\qquad \square$

The remaining issue in Algorithm 4.8 is how to compute $\min_{S \subset E, S \neq \emptyset} \frac{\mathfrak{f}(S)}{|S|}$. These

types of problems are known as geometric minimizations. In order to find the minimizer, the smallest value of β is desirable such that there is a set S with $\mathfrak{f}(S) = \beta|S|$. For the special case of single antenna Gaussian multiaccess channels, computing such β is very simple. For the general case, β can be computed by Dinkelbach's discrete Newton method as follows [15].

The algorithm is initialized by setting β equal to $\mathfrak{f}(E)/|E|$, which is an upper bound for optimum β. Then, a minimizer Y of $\mathfrak{f}(S) - \beta|S|$ is calculated, as will be explained later. Since $\mathfrak{f}(E) - \beta|E| = 0$, then $\mathfrak{f}(Y) - \beta|Y| \le 0$. If $\mathfrak{f}(Y) - \beta|Y| = 0$, the current β is optimum. If $\mathfrak{f}(Y) - \beta|Y| < 0$, then we update $\beta = \mathfrak{f}(Y)/|Y|$, which provides an improved upper bound. By repeating this operation, the optimal value of β will eventually be calculated [15]. It is shown that the number of β visited by the algorithm is at most $|E|$ [15].

Using this approach, the minimization problem $\min_{S \subset E, S \ne \emptyset} \frac{\mathfrak{f}(S)}{|S|}$ is changed to $\min_{S \subset E, S \ne \emptyset} \mathfrak{f}(S) - \beta|S|$. By direct verification of (4.4), it is easy to see that $\mathfrak{f}(S) - \beta|S|$ is a submodular function. There have been a lot of research on submodular minimization problems [15, 27, 48]. In [27, 48], the first combinatorial polynomial-time algorithms for solving submodular minimization problems are developed. These algorithms design a strongly polynomial combinatorial algorithm for testing membership in polymatroid polyhedra.

4.4.2 Decomposition of the Time-Sharing Problem

In the following, we take advantage of the special properties of $\mathbf{x}^*$ and polymatroids to break down the time-sharing problem to some lower-dimensional subproblems. In the previous sub-section, a chain of nested polymatroids $\mathcal{B}(\mathfrak{f}^{\langle\alpha\rangle}, E^{\langle\alpha\rangle})$, $\alpha = 0, \ldots, \varsigma$, is introduced, where $\mathcal{B}(\mathfrak{f}^{\langle\alpha-1\rangle}, E^{\langle\alpha-1\rangle}) \subset \mathcal{B}(\mathfrak{f}^{\langle\alpha\rangle}, E^{\langle\alpha\rangle})$ for $\alpha = 1, \ldots, \varsigma$. Since $S^{\langle j\rangle} \subset E^{\langle j\rangle}$ for $j = 0, \ldots, \varsigma$ and regarding the definition of polymatroid, $\mathcal{B}(\mathfrak{f}^{\langle j\rangle}, S^{\langle j\rangle})$, $j = 1, \ldots, \varsigma$, is a polymatroid, which is defined on the dimensions $S^{\langle j\rangle}$. According to the proof of Theorem 4.9, the vector $\varrho^{\langle j\rangle}\mathbf{1}_{|S^{\langle j\rangle}|} \in \mathcal{B}(\mathfrak{f}^{\langle j\rangle}, S^{\langle j\rangle})$ is on the hyperplane $\mathbf{x}(S^{\langle j\rangle}) = \mathfrak{f}(S^{\langle j\rangle})$. Let $\{\boldsymbol{\pi}_{\tau_j}^{\langle j\rangle}, \tau_j = 1, \ldots, |S^{\langle j\rangle}|!\}$ be the set of all permutations of the set $S^{\langle j\rangle}$, and $\boldsymbol{\omega}^{\langle j\rangle}(\boldsymbol{\pi}_{\tau_j}^{\langle j\rangle})$ be the corner point corresponding to the permutation $\boldsymbol{\pi}_{\tau_j}^{\langle j\rangle}$ in the polymatroid $\mathcal{B}(\mathfrak{f}^{\langle j\rangle}, S^{\langle j\rangle})$. Then, there exist the coefficients $0 \leq \lambda_{\tau_j}^{\langle j\rangle} \leq 1$, $\tau_j = 1, \ldots, |S^{\langle j\rangle}|!$, such that

$$\varrho^{\langle j\rangle}\mathbf{1}_{|S^{\langle j\rangle}|} = \sum_{\tau_j=1}^{|S^{\langle j\rangle}|!} \lambda_{\tau_j}^{\langle j\rangle}\boldsymbol{\omega}^{\langle j\rangle}\left(\boldsymbol{\pi}_{\tau_j}^{\langle j\rangle}\right), \tag{4.47}$$

where

$$\sum_{\tau_j=1}^{|S^{\langle j\rangle}|!} \lambda_{\tau_j}^{\langle j\rangle} = 1. \tag{4.48}$$

Note that $E = \bigcup_{j=0}^{\varsigma} S^{\langle j\rangle}$. Consider a permutation $\boldsymbol{\pi}_{\tau_j}^{\langle j\rangle}$ as one of the total $|S^{\langle j\rangle}|!$ permutations of $S^{\langle j\rangle}$, for $j = 0, \cdots, \varsigma$, then the permutation $\boldsymbol{\pi}$ formed by concatenating these permutations, i.e. $\boldsymbol{\pi} = \left(\boldsymbol{\pi}_{\tau_\varsigma}^{\langle\varsigma\rangle}, \cdots, \boldsymbol{\pi}_{\tau_0}^{\langle 0\rangle}\right)$, is a permutation on the set E.

Theorem 4.10. *Consider the permutation* $\boldsymbol{\pi} = \left(\boldsymbol{\pi}_{\tau_\varsigma}^{\langle\varsigma\rangle}, \cdots, \boldsymbol{\pi}_{\tau_0}^{\langle 0\rangle}\right)$ *of the set* E.

(I) The corner point corresponding to the permutation $\boldsymbol{\pi}$ *in the polymatroid* $\mathcal{B}(\mathfrak{f}, E)$

is

$$v_i(\boldsymbol{\pi}) = \omega_i^{\langle j\rangle}(\boldsymbol{\pi}_{\tau_j}^{\langle j\rangle}), \quad \text{for} \quad i \in S^{\langle j\rangle}, \tag{4.49}$$

where $\boldsymbol{\omega}^{\langle j\rangle}(\boldsymbol{\pi}_{\tau_j}^{\langle j\rangle})$ is the corner point of the polymatroid $\mathcal{B}(\mathfrak{f}^{\langle j\rangle}, S^{\langle j\rangle})$ corresponding to the permutation $\boldsymbol{\pi}_{\tau_j}^{\langle j\rangle}$, and $\omega_i^{\langle j\rangle}(\boldsymbol{\pi}_{\tau_j}^{\langle j\rangle})$ denotes the value of $\boldsymbol{\omega}^{\langle j\rangle}(\boldsymbol{\pi}_{\tau_j}^{\langle j\rangle})$ over the dimension i, $i \in S^{\langle j\rangle}$.

(II) The vector $\mathbf{x}^*$ is in the convex hull of the set of corner points corresponding to the following set of permutations

$$\left\{ \left(\boldsymbol{\pi}_{\tau_\varsigma}^{\langle \varsigma\rangle}, \cdots, \boldsymbol{\pi}_{\tau_0}^{\langle 0\rangle} \right), 1 \leq \tau_\varsigma \leq |S^{\langle \varsigma\rangle}|!, \ldots, 1 \leq \tau_0 \leq |S^{\langle 0\rangle}|! \right\}, \tag{4.50}$$

where the coefficient of the corner point corresponding to the permutation $\boldsymbol{\pi} = \left(\boldsymbol{\pi}_{\tau_\varsigma}^{\langle \varsigma\rangle}, \cdots, \boldsymbol{\pi}_{\tau_0}^{\langle 0\rangle} \right)$ is equal to $\lambda_{\tau_\varsigma}^{\langle \varsigma\rangle} \ldots \lambda_{\tau_0}^{\langle 0\rangle}$, i.e.

$$\mathbf{x}^* = \sum_{\tau_\varsigma=1}^{|S^{\langle \varsigma\rangle}|!} \ldots \sum_{\tau_0=1}^{|S^{\langle 0\rangle}|!} \lambda_{\tau_\varsigma}^{\langle \varsigma\rangle} \ldots \lambda_{\tau_0}^{\langle 0\rangle} \boldsymbol{v}\left(\left(\boldsymbol{\pi}_{\tau_\varsigma}^{\langle \varsigma\rangle}, \cdots, \boldsymbol{\pi}_{\tau_0}^{\langle 0\rangle} \right) \right). \tag{4.51}$$

Proof. **Part (I)** From recursive equation (4.34), we can show that

$$\text{For } S \in E - \bigcup_{i=0}^{j-1} S^{\langle i\rangle}, \quad \mathfrak{f}^{\langle j\rangle}(S) = \mathfrak{f}\left(S \cup \left\{ \bigcup_{i=0}^{j-1} S^{\langle i\rangle} \right\} \right) - \mathfrak{f}\left(\left\{ \bigcup_{i=0}^{j-1} S^{\langle i\rangle} \right\} \right). \tag{4.52}$$

Consider the permutation $\boldsymbol{\pi} = \left(\boldsymbol{\pi}_{\tau_\varsigma}^{\langle \varsigma\rangle}, \cdots, \boldsymbol{\pi}_{\tau_0}^{\langle 0\rangle} \right)$. Set $\xi = \sum_{i=1}^{j} |S^{\langle i\rangle}|$. By using (4.5) and (4.52), for $\xi < \kappa \leq \xi + |S^{\langle j+1\rangle}|$, $v_{\pi(\kappa)}(\boldsymbol{\pi})$ is equal to

$$
\begin{aligned}
v_{\pi(\kappa)}(\boldsymbol{\pi}) =\ & \mathfrak{f}\left(\{\pi(1), \ldots, \pi(\kappa)\} \right) - \mathfrak{f}\left(\{\pi(1), \ldots, \pi(\kappa-1)\} \right) \\
=\ & \mathfrak{f}\left(\left\{ \bigcup_{i=0}^{j-1} S^{\langle i\rangle}, \pi(\xi+1) \ldots, \pi(\kappa) \right\} \right) - \mathfrak{f}\left(\left\{ \bigcup_{i=0}^{j-1} S^{\langle i\rangle}, \pi(\xi+1), \ldots, \pi(\kappa-1) \right\} \right) \\
=\ & \mathfrak{f}^{\langle j\rangle}\left(\{\pi(\xi+1) \ldots, \pi(\kappa)\} \right) - \mathfrak{f}^{\langle j\rangle}\left(\{\pi(\xi+1) \ldots, \pi(\kappa-1)\} \right).
\end{aligned}
$$

According to definition of polymatroid and its corner points, the RHS of (4.53) is the value of $\omega_{\pi(\kappa)}^{\langle j \rangle}(\boldsymbol{\pi}^{\langle j \rangle})$ in the corresponding corner point of the polymatroid $\mathcal{B}(\mathfrak{f}^{\langle j \rangle}, S^{\langle j \rangle})$.

Part (II) Since $\sum_{\tau_0=1}^{|S^{\langle 0 \rangle}|!} \lambda_{\tau_0}^{\langle 0 \rangle} = 1$ and by using (4.47) and part (I) of the theorem, it is easy to verify that the ith, $i \in S^{\langle 0 \rangle}$, entry of

$$\sum_{\tau_0=1}^{|S^{\langle 0 \rangle}|!} \lambda_{\tau_0}^{\langle 0 \rangle} \boldsymbol{v}\big(\boldsymbol{\pi}_{\tau_\varsigma}^{\langle \varsigma \rangle}, \ldots, \boldsymbol{\pi}_{\tau_0}^{\langle 0 \rangle}\big) \tag{4.53}$$

is equal to $\varrho^{\langle 0 \rangle}$. Similarly, the entry i, $i \in S^{\langle 1 \rangle}$, of

$$\sum_{\tau_1=1}^{|S^{\langle 1 \rangle}|!} \lambda_{\tau_1}^{\langle 1 \rangle} \sum_{\tau_0=1}^{|S^{\langle 0 \rangle}|!} \lambda_{\tau_0}^{\langle 0 \rangle} \boldsymbol{v}\big(\boldsymbol{\pi}_{\tau_\varsigma}^{\langle \varsigma \rangle}, \ldots, \boldsymbol{\pi}_{\tau_0}^{\langle 0 \rangle}\big), \tag{4.54}$$

is equal to $\varrho^{\langle 1 \rangle}$, while the entry i, $i \in S^{\langle 0 \rangle}$, remains $\varrho^{\langle 0 \rangle}$. By continuing this procedure, part (II) of the algorithm is proven. $\qquad\square$

Regarding the above statements, the problem of finding time-sharing coefficients is decomposed to some lower-dimensional subproblems. In each sub-problem, the objective is to find the coefficients of the time-sharing among the corner points of the polymatroid $\mathcal{B}(\mathfrak{f}^{\langle j \rangle}, S^{\langle j \rangle})$, $j = 0, \ldots, \varsigma$, to attain $\varrho^{\langle j \rangle} \mathbf{1}_{|S^{\langle j \rangle}|}$. In this part, we present an algorithm which finds the coefficients of the time-sharing over the corner points of a general polymatroid $\mathcal{B}(\mathfrak{f}, E)$ to attain a vector $\mathbf{x}$ located on the face of the polymatroid.

Algorithm 4.11.

1. Initialize $\alpha = 1$, $\boldsymbol{\omega}_1 = \boldsymbol{v}(\boldsymbol{\pi}^*)$ (the fairest corner point obtained by Algorithm 4.3).

2. *Solve the linear optimization problem*

$$\max \varepsilon$$

$$s.t. \quad \sum_{i=1}^{\alpha} \hat{\mu}_i \boldsymbol{\omega}_i - \mathbf{x} \geq \varepsilon$$

$$0 \leq \hat{\mu}_i \leq 1 \tag{4.55}$$

Let $\hat{\mu}_i^{\alpha}$, $i = 1, \ldots, \alpha$ be the optimizing coefficients.

3. *If $\mathbf{x} = \sum_{i=1}^{\alpha} \hat{\mu}_i^{\alpha} \boldsymbol{\omega}_i$, Stop.*

4. *$\alpha \longleftarrow \alpha + 1$. Set $\mathbf{e} = \mathbf{x} - \sum_{i=1}^{\alpha} \hat{\mu}_i^{\alpha} \boldsymbol{\omega}_i$ and determine the permutation $\boldsymbol{\pi}$ for which*

   $\mathbf{e}_{\pi(1)} \geq \mathbf{e}_{\pi(2)} \geq \ldots \geq \mathbf{e}_{\pi(|E|)}$. Set $\boldsymbol{\omega}_{\alpha} = \boldsymbol{v}(\boldsymbol{\pi})$ and move to step 2.

The idea behind the algorithm is as follows. In each step, the time-sharing among some corner points is performed. If the resulting vector is equal to $\mathbf{x}$, the answer is obtained; otherwise a permutation $\boldsymbol{\pi}$ is determined such that $\mathbf{e}_{\pi(1)} \geq \mathbf{e}_{\pi(2)} \geq \ldots \geq \mathbf{e}_{\pi(|E|)}$, where the error vector $\mathbf{e}$ represents the difference between the vector $\mathbf{x}$ and resulting vector from time-sharing. We can compensate the error vector $\mathbf{e}$ by including an appropriate corner point in the set of corner points participating in time-sharing. Clearly, the best one to be included is the one which has the highest possible rate for user $\pi(1)$ and lowest possible rate for user $\pi(|E|)$. Apparently, this corner point is $\boldsymbol{v}(\boldsymbol{\pi})$, computed by Algorithm 4.11.

Note that Algorithm 4.11 can be applied over the sub-polymatroids $\mathcal{B}(\mathfrak{f}^{\langle j \rangle}, S^{\langle j \rangle})$, $j = 0, \ldots, \varsigma$, to attain $\varrho^{\langle j \rangle} \mathbf{1}_{|S^{\langle j \rangle}|}$ or directly applied over the original polymatroid to

attain $\mathbf{x}^*$. If a and $|S^{\langle j \rangle}|$ are relatively small numbers, the decomposition method has less complexity, otherwise applying Algorithm 4.11 over the original problem is less complex.

4.4.3 Decomposition of Rate-Splitting Approach

As mentioned, an alternative approach to achieve any rate-vector on the sum-capacity facet of MAC is *rate splitting* [21, 45]. This method is based on splitting all input sources except one into two parts, and treating each spilt input as two virtual inputs (or two virtual users). Thus, there are at most $2a - 1$ virtual users. It is proven that by splitting the sources appropriately and successively decoding virtual users in a suitable order, any point on the sum-capacity facet can be attained.

Similar to the time-sharing part, we prove that to attain the rate vector $\mathbf{x}^*$, the rate-splitting procedure can be decomposed into some lower-dimensional subproblems. Consider a MAC, where the capacity region is represented by polymatroid $\mathcal{B}(\mathfrak{f}, E)$ and the vector $\mathbf{x}^*$, derived in Algorithm 4.8, is on its face. Assume that the users in the set $S^{\langle j \rangle}$ are decoded before the set of users in $\{S^{\langle j-1 \rangle}, S^{\langle j-2 \rangle}, \ldots, S^{\langle 0 \rangle}\}$ and after the users in the set $\{S^{\langle \varsigma \rangle}, \ldots, S^{\langle j+2 \rangle}, S^{\langle j+1 \rangle}\}$ .Therefore, by similar discussion used in (4.36) to (4.42), we conclude that the rate of the users in the set $S^{\langle j \rangle}$ is characterized by the polymatroid $\mathcal{B}(\mathfrak{f}^{\langle j \rangle}, S^{\langle j \rangle})$, where the rate-vector $\varrho^{\langle j \rangle} \mathbf{1}_{|S^{\langle j \rangle}|}$ is on its face. Regarding the results presented in [21,45], we can attain the rate-vector $\varrho^{\langle j \rangle} \mathbf{1}_{|S^{\langle j \rangle}|}$ by properly splitting

the sources of all inputs, except for one, in the set $S^{\langle j \rangle}$ to form $2|S^{\langle j \rangle}| - 1$ virtual users and by choosing the proper order of the decoding of the virtual users. Consequently, using Algorithm 4.12 (below), we achieve the rate-vector $\mathbf{x}^*$ in the original polymatroid.

Algorithm 4.12.

1. *Apply rate-splitting approach to attain the rate-vector $\varrho^{\langle j \rangle} \mathbf{1}_{|S^{\langle j \rangle}|}$ on the face of the polymatroid $\mathcal{B}(\mathfrak{f}^{\langle j \rangle}, S^{\langle j \rangle})$, for $j = 0, \ldots, \varsigma$. Therefore, for each j, $0 \leq j \leq \varsigma$, at most $2|S^{\langle j \rangle}| - 1$ virtual users are specified with a specific order of decoding.*

2. *Starting from $j = \varsigma$, decode the virtual users in the set $S^{\langle j \rangle}$ in the order found in Step 1. Set $j \leftarrow j - 1$. Follow the procedure until $j < 0$.*

4.5   Conclusion

We considered the problem of fairness for a class of systems for which a subset of the capacity region forms a polymatroid structure. The main purpose is to find a point on the sum-capacity facet which satisfies a notion of fairness among active users. This problem is addressed in cases where the complexity of achieving interior points is not feasible, and where the complexity of achieving interior points is feasible. For the first case, the corner point for which the minimum rate of the active users is maximized (max-min corner point) is desired for signaling. A simple greedy algorithm is introduced to find the optimum max-min corner point. For the second case, the

polymatroid properties are exploited to locate a rate-vector on the sum-capacity facet which is optimally fair in the sense that the minimum rate among all users is maximized (max-min rate). In the case that the rate of some users can not increase further (attain the max-min value), the algorithm recursively maximizes the minimum rate among the rest of the users. It is shown that the problems of deriving the time-sharing coefficients and rate-splitting scheme can be solved by decomposing the problem to some lower-dimensional subproblems. In addition, a fast algorithm to compute the time-sharing coefficients to attain a general point on the sum-capacity facet is proposed.

Chapter 5

Optimal Order of Decoding in Interference Channels

5.1 Introduction

Wireless technology has been advancing at an exponential rate, due to increasing expectations for multi-media services. This, in turn, necessitates the development of novel techniques of signaling with high spectral efficiency. Channel sharing is known as an effective scheme to increase the spectral efficiency and coverage in the wireless systems. The main source of impairment in such systems is the interference among the links. These systems are known with the general name of interference channels.

The interference channel was first introduced by Shannon [51]. In [4], it is shown that in the Gaussian interference channels, very strong interference amounts to no inter-

ference at all. In [8, 22, 47], the result of [4] is extended to general discrete interference channels with strong interference. In [5, 46], the capacity of degraded interference channels is investigated. The best result on the capacity region of the interference channels is introduced in [22]. In the scheme presented in [22], each transmitter splits its message into two independent massages, one is private which is only decodable by the intended receiver and the other is common which is decodable at both receivers.

A lot of research efforts have been devoted to the problem of fairness in the interference channels. In [1], K-user Gaussian interference channels without any constraint on the transmit powers are considered and the maximum signal-to-interference-plus-noise-ratio (SINR) that all the transmitters can attain simultaneously is computed. The result in [1] is formulated as the inverse of the Perron-Frobenius eigenvalue (see [25]) of a non-negative matrix. Recently in [41], the result of [1] is generalized to the case where the power of the transmitters are constrained. In [14], the problem of spectrum sharing in unlicensed bands is investigated. It is shown that in a K-user interference channel, any rate vector inside the rate region is achievable with a piece-wise constant power allocation over $2K$ bandwidth intervals. In addition, it is investigated whether fairness and efficiency can be attained if the users follow a selfish spectrum sharing strategy. Generally in the literature, including [1, 14, 41], it is assumed that each receiver only decodes the data of the designated transmitter, while the signals coming from other transmitters are treated as interference.

In this chapter, we consider a K-user memoryless interference channel, where each

receiver sequentially decodes the data of a subset of transmitters before it decodes the data of the designated transmitter. Since part of the interference is canceled out, this system can potentially achieve higher data rate. In this system, the data rate of each transmitter depends on (i) the subset of receivers which decode the data of that transmitter, (ii) the decoding order employed at each receiver which decodes the data of that transmitter. The main objective of this chapter is to find the set of transmitters which are decoded at each receiver and the corresponding order of decoding such that the minimum rate of the users is maximized. A simple greedy algorithm is proposed and proven to be optimal. We established similar result for the memoryless multi-access channels in [40].

5.2   Problem Formulation

We focus on a K-user memoryless interference channel modeled by

$$\Pr(y_1, y_2, \ldots, y_K | x_1, x_2, \ldots, x_K). \tag{5.1}$$

It is assumed that user t, $t \in E = \{1, 2, \ldots, K\}$, utilizes the codebook $\mathcal{C}^{[t]}$, with the input distribution $\Pr(x_t)$. Receivers have the possibility of successive decoding. Each receiver decodes the data of some of the users in a specific order and then it decodes the data of the designated transmitter. For the sake of brevity, we say "user t is decoded at receiver r", instead of saying "the data of the user t is decoded at receiver r".

The order of decoding at receiver r is denoted by the permutation

$\boldsymbol{\pi}^{[r]} = (\pi^{[r]}(1), \pi^{[r]}(2), \ldots, \pi^{[r]}(K))$ of the set E. Receiver r first decodes user $\pi^{[r]}(K)$, then user $\pi^{[r]}(K-1)$, and so forth until it decodes the data of the designated transmitter (See Fig. 5.1). In the permutation $\boldsymbol{\pi}^{[r]}$, if $l > i$ ($l < i$), we say user $\pi^{[r]}(l)$ is located before (after) user $\pi^{[r]}(l)$, which means that at receiver r, user $\pi^{[r]}(l)$ is decoded before (after) user $\pi^{[r]}(i)$. Apparently, the users located after user r in the permutation $\boldsymbol{\pi}^{[r]}$ are not decoded at receiver r. The orders of decoding at all receivers, i.e., $\boldsymbol{\pi}^{[1]}, \boldsymbol{\pi}^{[2]}, \ldots, \boldsymbol{\pi}^{[K]}$, are denoted by Π.
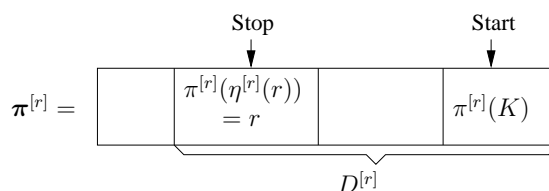

Figure 5.1: Order of Decoding at Receiver r

Defintion 5.1. *The vector $\boldsymbol{\eta}^{[t]}$ is defined such that $\eta^{[t]}(r)$ shows the position of user t in $\boldsymbol{\pi}^{[r]}$, therefore,*

$$\pi^{[r]}(\eta^{[t]}(r)) = t.$$

Defintion 5.2. *The set $D^{[r]}$ is defined as the set of users which are decoded at receiver r, i.e.,*

$$D^{[r]} = \{\pi^{[r]}(\eta^{[r]}(r)), \pi^{[r]}(\eta^{[r]}(r) + 1), \ldots, \pi^{[r]}(K)\}. \tag{5.2}$$

Note that $\pi^{[r]}(\eta^{[r]}(r))$ is equal to r, which is the last user, decoded at receiver r. The users located after user r in $\boldsymbol{\pi}^{[r]}$ are not decoded at receiver r.

Defintion 5.3. *The set $E^{[t]}$ is defined as the set of receivers which decode user t. Apparently, $t \in E^{[t]}$.*

Receiver r and the transmitter in $D^{[r]}$ can be considered as a multi-access channel, while the contributions of the users in $E - D^{[r]}$ are treated as interference. Regarding the order of decoding applied at receiver r, the rate of user t, $t \in D^{[r]}$, is upper-bounded by

$$\vartheta_t \leq I\big(y_r; x_t | x_{\pi^{[r]}(\eta^{[t]}(r)+1)}, x_{\pi^{[r]}(\eta^{[t]}(r)+2)}, \dots, x_{\pi^{[r]}(K)}\big). \tag{5.3}$$

Note that $\{x_{\pi^{[r]}(\eta^{[t]}(r)+1)}, x_{\pi^{[r]}(\eta^{[t]}(r)+2)}, \dots, x_{\pi^{[r]}(K)}\}$ is the set of users decoded before user t at receiver r.

Therefore, if the decoding orders Π are employed at the receivers, the maximum possible value for ϑ_t, denoted by $\vartheta_t(\Pi)$, is obtained by,

$$\vartheta_t(\Pi) = \min_{r,\ r \in E^{[t]}} I\big(y_r; x_t | x_{\pi^{[r]}(\eta^{[t]}(r)+1)}, x_{\pi^{[r]}(\eta^{[t]}(r)+2)}, \dots, x_{\pi^{[r]}(K)}\big). \tag{5.4}$$

Example Consider a 3-user memoryless interference channel, where the order of decoding is as follows:

$$\boldsymbol{\pi}^{[1]} = (2, 1, 3) \tag{5.5}$$

$$\boldsymbol{\pi}^{[2]} = (3, 1, 2) \tag{5.6}$$

$$\boldsymbol{\pi}^{[3]} = (1, 3, 2) \tag{5.7}$$

Therefore, receiver one first decode the data of transmitter three and then its own data, i.e. $D^{[1]} = \{1, 3\}$. Receiver two just decode its own data (sent by transmitter two),

i.e. $D^{[2]} = \{2\}$. Receiver three first decodes the data of transmitter two, then decodes

its own data. i.e. $D^{[3]} = \{3, 2\}$. Consequently, transmitter one is only decoded at

receiver one. i.e. $E^{[1]} = \{1\}$, transmitter two is decoded at receiver two and three, i.e

$E^{[2]} = \{2, 3\}$, and transmitter three is decoded at receiver one and three $E^{[3]} = \{1, 3\}$.

Therefore, the rate of the users are obtained by,

$$\vartheta_1(\Pi) = I(y_1; x_1 | x_3), \tag{5.8}$$

$$\vartheta_2(\Pi) = \min\left\{ I(y_2; x_2), I(y_3; x_2) \right\}, \tag{5.9}$$

$$\vartheta_3(\Pi) = \min\left\{ I(y_1; x_3), I(y_3; x_3 | x_2) \right\}. \tag{5.10}$$

Note that since at receiver one, user three is decoded before user one, it is helpful for

user one in terms of reducing the interference and increasing the data rate. Whereas,

it is restrictive for user three by imposing extra condition on the data rate of this user

(user three must be decodable at receiver one).

The objective of this chapter is to find the optimal decoding orders $\pi^{[t]}$, $t = 1, \ldots, K$,

such that the minimum of $\vartheta_t(\Pi)$, $t = 1, \ldots, K$, is maximized.

Note that there are $\left(\sum_{i=1}^{K} \frac{K!}{i!} \right)^K$ possible choices for the decoding orders, and it is

prohibitively complex to find the optimal answer through the exhaustive search.

We define the set function $\mathfrak{f}^{[r]}$ as

$$\mathfrak{f}^{[r]}(S) = I\left(y_r; \{x_i, i \in S\} | \{x_i, i \in S^c\}\right), \ \forall S \subset E. \tag{5.11}$$

It is proven that $\mathfrak{f}^{[r]}(S)$ is a rank function as [59] (see Definition 4.1). In addition, it is

easy to see that (5.3) and (5.4) are respectively rewritten as

$$\vartheta_t \leq \mathfrak{f}^{[r]}\big(x_{\pi^{[r]}(1)}, x_{\pi^{[r]}(2)}, \ldots, x_{\pi^{[r]}(\eta^{[t]}(r))}\big) - \mathfrak{f}^{[r]}\big(x_{\pi^{[r]}(1)}, x_{\pi^{[r]}(2)}, \ldots, x_{\pi^{[r]}(\eta^{[t]}(r)-1)}\big). \quad (5.12)$$

and

$$\vartheta_t(\Pi) = \min_{r, \ r \in E^{[t]}} \quad (5.13)$$

$$\mathfrak{f}^{[r]}\big(x_{\pi^{[r]}(1)}, x_{\pi^{[r]}(2)}, \ldots, x_{\pi^{[r]}(\eta^{[t]}(r))}\big) - \mathfrak{f}^{[r]}\big(x_{\pi^{[r]}(1)}, x_{\pi^{[r]}(2)}, \ldots, x_{\pi^{[r]}(\eta^{[t]}(r)-1)}\big).$$

5.3   Algorithm

In this section, we develop an algorithm to specify the optimal decoding orders. In the proposed algorithm, the decoding order for each receiver is determined in a greedy fashion, independent of the decoding orders selected for the other receivers. While this algorithm has a very low complexity, we prove that the resulting decoding orders are optimal.

Algorithm 5.4.

For each receiver r, $r \in E$,

1. Set $\alpha = K$, $D^{*[r]} = \varnothing$.

2. Set $\pi^{*[r]}(\alpha)$ as

$$\pi^{*[r]}(\alpha) = \arg \min_{z \in E, z \notin \mathcal{S}} \mathfrak{f}^{[r]}\big(E - D^{*[r]} - \{z\}\big). \quad (5.14)$$

3. *Set $D^{*[r]} \longleftarrow D^{*[r]} \cup \{\pi^{*[r]}(\alpha)\}$ and $\alpha \longleftarrow \alpha - 1$. If $\alpha \geq 1$ and $\pi^{*[r]}(\alpha + 1) \neq t$,*

   then go to step two, otherwise go to the next step.

4. *If $\alpha \neq 0$, randomly allocate the entries of $E - D^{*[r]}$ to $\pi^{[r]}(1), \pi^{[r]}(2), \ldots, \pi^{[r]}(\alpha)$.*

The following theorem proves the optimality of the proposed algorithm.

Theorem 5.5. *Let $\big(\vartheta_1(\Pi^*), \vartheta_2(\Pi^*), \ldots, \vartheta_K(\Pi^*)\big)$ be the rate vector corresponding to the decoding orders $\pi^{*[1]}, \pi^{*[2]}, \ldots, \pi^{*[K]}$. Then for the rate vector $\big(\vartheta_1(\Pi), \vartheta_2(\Pi), \ldots, \vartheta_K(\Pi)\big)$ corresponding to any decoding orders $\pi^{[1]}, \pi^{[2]}, \ldots, \pi^{[K]}$, we have*

$$\min_i \vartheta_i(\Pi^*) \geq \min_i \vartheta_i(\Pi). \tag{5.15}$$

Proof. Let $\boldsymbol{\eta}^{*[r]}$ and $E^{[*r]}$ respectively be $\boldsymbol{\eta}^{[r]}$ and $E^{[r]}$ corresponding to the decoding orders obtained by the algorithm. Assume that user $\hat{t}$ has the minimum rate among the users, where the decoding orders $\boldsymbol{\pi}^{*[1]}, \boldsymbol{\pi}^{*[2]}, \ldots, \boldsymbol{\pi}^{*[K]}$ are employed at the receivers. Therefore, regarding (5.13), $\exists \hat{r} \in E^{[*\hat{t}]}$ such that

$$\vartheta_{\hat{t}}(\Pi^*) = \mathfrak{f}^{[\hat{r}]}\big(x_{\pi^{*[\hat{r}]}(1)}, x_{\pi^{*[\hat{r}]}(2)}, \ldots, x_{\pi^{[*\hat{r}]}(\eta^{[*\hat{t}]}(\hat{r}))}\big) -$$

$$\mathfrak{f}^{[\hat{r}]}\big(x_{\pi^{[*\hat{r}]}(1)}, x_{\pi^{[*\hat{r}]}(2)}, \ldots, x_{\pi^{[*\hat{r}]}(\eta^{[*\hat{t}]}(\hat{r})-1)}\big) \tag{5.16}$$

In other words, among the receives which decode user $\hat{t}$, the receiver $\hat{r}$ imposes the dominant upper-bound on the data rate of the user $\hat{t}$. For now, we assume that $\hat{t} \neq \hat{r}$. Similar arguments are used to prove the optimality of the algorithm for the case that $\hat{t} = \hat{r}$.

In what follows, we prove that if the decoding orders $\boldsymbol{\pi}^{*[1]}, \boldsymbol{\pi}^{*[2]}, \ldots, \boldsymbol{\pi}^{*[K]}$ are permuted to generate new decoding orders, then the minimum rate of users is not greater than $\vartheta_{\hat{t}}(\Pi^*)$.

Case 1. *Choosing arbitrary permutations for* $\boldsymbol{\pi}^{[l]}, l \in E, l \neq \hat{r}$: Assume that arbitrary decoding orders are chosen for the receivers $l, l \in E$ and $l \neq \hat{r}$, while the user $\hat{r}$ is employed $\boldsymbol{\pi}^{*[\hat{r}]}$ as the decoding order. Then user $\hat{t}$ is still decoded at receiver $\hat{r}$, in the order determined by $\pi^{*[\hat{r}]}$. Therefore, according to (5.13), the rate of user $\hat{t}$ is still upper-bounded by the right-hand side of (5.16), which is $\vartheta_{\hat{t}}(\Pi^*)$. Consequently, if the new decoding orders are employed, the minimum rate of the users is less than or equal to $\vartheta_{\hat{t}}(\Pi^*)$.

Before starting the other cases, we define two sets:

- The set of users located after user $\hat{t}$ in the permeation $\pi^{*[\hat{r}]}$,

$$\underline{\Phi}^{*[\hat{r}]} = \{\pi^{*[\hat{r}]}(1), \ldots, \pi^{*[\hat{r}]}(\eta^{[*\hat{t}]}(\hat{r}) - 1)\}. \tag{5.17}$$

  Note that $\hat{r} \in \underline{\Phi}^{*[\hat{r}]}$. In addition, some of the users in $\underline{\Phi}^{*[\hat{r}]}$ are not decoded at receiver $\hat{r}$.

- The set of users decoded before user $\hat{t}$ at receiver $\hat{r}$ according to the permutation $\pi^{*[\hat{r}]}$:

$$\underline{\Psi}^{*[\hat{r}]} = \{\pi^{*[\hat{r}]}(\eta^{[*\hat{t}]}(\hat{r}) + 1), \ldots, \pi^{*[\hat{r}]}(K)\} \tag{5.18}$$

Therefore, according to (5.16), we have

$$\vartheta_{\hat{t}}(\Pi^*) = \mathfrak{f}^{[\hat{r}]}(\underline{\Phi}^{*[\hat{r}]} \cup \{\hat{t}\}) - \mathfrak{f}^{[\hat{r}]}(\underline{\Phi}^{*[\hat{r}]}). \tag{5.19}$$

Case 2. *Permutation in $\underline{\Phi}^{*[\hat{r}]}$ and $\underline{\Psi}^{*[\hat{r}]}$, choosing arbitrary permutations for $\boldsymbol{\pi}^{[l]}$, $l \in E, l \neq \hat{r}$ (see Fig. 5.2):* Assume that the order of users in $\underline{\Phi}^{*[\hat{r}]}$ and $\underline{\Psi}^{*[\hat{r}]}$ are permuted to generate a new decoding order $\boldsymbol{\pi}^{[\hat{r}]}$ for receiver $\hat{r}$. Note that in the new permutation $\boldsymbol{\pi}^{[\hat{r}]}$, the set of users located after and before user $\hat{t}$ are still $\underline{\Phi}^{*[\hat{r}]}$ and $\underline{\Psi}^{*[\hat{r}]}$. Also assume that for the rest of receivers, arbitrary decoding orders are chosen. In this case, in $\boldsymbol{\pi}^{[\hat{r}]}$, user $\hat{r}$ is still located after user $\hat{t}$ and therefore, user $\hat{t}$ is decoded at receiver $\hat{r}$. In addition, according to (5.13), the rate of user $\hat{t}$ is still less than $\mathfrak{f}^{[\hat{r}]}(\underline{\Phi}^{*[\hat{r}]} \cup \{\hat{t}\}) - \mathfrak{f}^{[\hat{r}]}(\underline{\Phi}^{*[\hat{r}]})$, to be decodable at receiver $\hat{r}$. Therefore, if the new decoding orders are employed, the minimum rate of the users is less that or equal to $\vartheta_{\hat{t}}(\Pi^*)$.
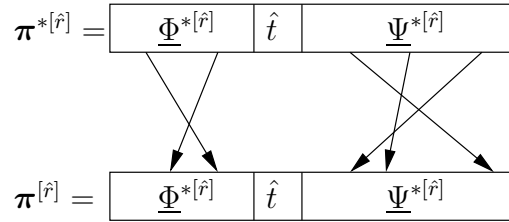

Figure 5.2: Case 2. Permutation in $\underline{\Phi}^{*[\hat{r}]}$ and $\underline{\Psi}^{*[\hat{r}]}$.

Case 3. *Moving a subset of users from $\underline{\Psi}^{*[\hat{r}]}$ to $\underline{\Phi}^{*[\hat{r}]}$, choosing arbitrary permutations for $\boldsymbol{\pi}^{[l]}$, $l \in E, l \neq \hat{r}$ (See Fig 5.3):* Assume a set $\underline{\Upsilon}$ of users, $\underline{\Upsilon} \subset \underline{\Psi}^{*[\hat{r}]}$, is moved from $\underline{\Psi}^{*[\hat{r}]}$ to $\underline{\Phi}^{*[\hat{r}]}$ to generate a new decoding order $\boldsymbol{\pi}^{[\hat{r}]}$ for receiver $\hat{r}$. Note that in the permutation $\boldsymbol{\pi}^{[\hat{r}]}$, the position of user $\hat{t}$ is still before user $\hat{r}$, which means that user $\hat{t}$

is decoded at receiver $\hat{r}$. Assume that arbitrary permutations are chosen for the other receivers. According to (5.13), if the new decoding orders are employed, the rate of user $\hat{t}$ is less than or equal to,

$$\vartheta_{\hat{t}}(\Pi) \leq \mathfrak{f}(\underline{\Phi}^{*[\hat{r}]} \cup \underline{\Upsilon} \cup \{\hat{t}\}) - \mathfrak{f}(\underline{\Phi}^{*[\hat{r}]} \cup \underline{\Upsilon}), \tag{5.20}$$

to be decodable at receiver $\hat{r}$, regardless of the decoding orders chosen for the other receivers.

Using (4.4), we have,

$$\mathfrak{f}(\underline{\Phi}^{*[\hat{r}]} \cup \{\hat{t}\}) + \mathfrak{f}(\underline{\Phi}^{*[\hat{r}]} \cup \underline{\Upsilon}) \geq$$

$$\mathfrak{f}(\underline{\Phi}^{*[\hat{r}]} \cup \underline{\Upsilon} \cup \{\hat{t}\}) + \mathfrak{f}(\underline{\Phi}^{*[\hat{r}]}). \tag{5.21}$$

Using (5.19), (5.20), and (5.21), we conclude that $\vartheta_{\hat{t}}(\Pi) \leq \vartheta_{\hat{t}}(\Pi^*)$, and therefore, the minimum rate of the users in the new decoding orders is less than or equal to $\vartheta_{\hat{t}}(\Pi^*)$.

Note that permuting the users located before (or after) user $\hat{t}$ in $\boldsymbol{\pi}^{[\hat{r}]}$ does not increase the rate of user $\hat{t}$.
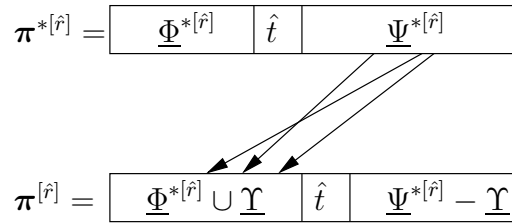

Figure 5.3: Case 3. Moving a set of users from $\underline{\Psi}^{*[\hat{r}]}$ to the set $\underline{\Phi}^{*[\hat{r}]}$.

Case 4. *Moving one or more users from the set $\underline{\Phi}^{*[\hat{r}]}$ to the set $\underline{\Psi}^{*[\hat{r}]}$, with or without moving some users from the set $\underline{\Psi}^{*[r]}$ to the set $\underline{\Phi}^{*[\hat{r}]}$, choosing arbitrary permutations*

for $\boldsymbol{\pi}^{[l]}$*,* $l \in E, l \neq \hat{r}$ *(See Fig 5.4)*: Assume that one or more users move from $\underline{\Phi}^{*[\hat{r}]}$ to $\underline{\Psi}^{*[\hat{r}]}$ (with or without moving some users from the set $\underline{\Psi}^{*[\hat{r}]}$ to the set $\underline{\Phi}^{*[\hat{r}]}$) to generate the new permutation $\boldsymbol{\pi}^{[\hat{r}]}$. As depicted in Fig. 5.4, assume that the user ν is positioned last in the permutation $\boldsymbol{\pi}^{[\hat{r}]}$ among the users moved from $\underline{\Phi}^{*[\hat{r}]}$ to $\underline{\Psi}^{*[\hat{r}]}$ (user $\pi(1)$ is positioned first and user $\pi(K)$ is positioned last in the permutation $\boldsymbol{\pi}$). In the new permutation, user ν is located before user $\hat{r}$, which means that this user is decoded at receiver $\hat{r}$, otherwise, user ν is indeed user $\hat{r}$ which is apparently decoded at receiver $\hat{r}$.
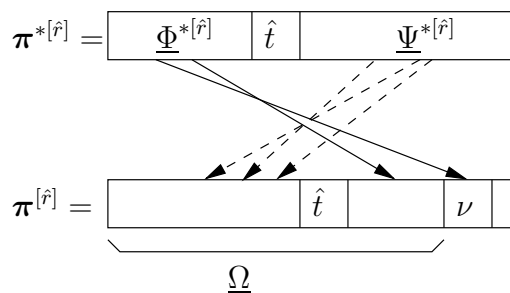

Figure 5.4: Case 4. Moving one or more users from the set $\underline{\Phi}^{*[\hat{r}]}$ to the set $\underline{\Psi}^{*[\hat{r}]}$ (with or without moving some users from the set $\underline{\Psi}^{*[\hat{r}]}$ to the set $\underline{\Phi}^{*[\hat{r}]}$).

Let $\underline{\Omega}$ be the set of users located after the user ν in the permutation $\boldsymbol{\pi}^{[\hat{r}]}$. Using (5.13), and since ν is decoded at receiver $\hat{r}$, the rate of user ν is upper-bounded by,

$$\vartheta_\nu(\Pi) \leq \mathsf{f}^{[\hat{r}]}(\underline{\Omega} \cup \{\nu\}) - \mathsf{f}^{[\hat{r}]}(\underline{\Omega}), \tag{5.22}$$

to be decodable at receiver $\hat{r}$. It is clear that,

$$\{\hat{t}\} \cup \underline{\Phi}^{*[\hat{r}]} - \{\nu\} \subset \underline{\Omega}. \tag{5.23}$$

Using (4.4) with $S = \underline{\Phi}^{*[\hat{r}]} \cup \{\hat{t}\}$ and $T = \underline{\Omega}$, and regarding (5.23), we have,

$$\mathfrak{f}^{[\hat{r}]}(\underline{\Omega} \cup \{\nu\}) - \mathfrak{f}^{[\hat{r}]}(\underline{\Omega})$$

$$\leq \mathfrak{f}^{[\hat{r}]}(\underline{\Phi}^{*[\hat{r}]} \cup \{\hat{t}\}) - \mathfrak{f}^{[\hat{r}]}(\underline{\Phi}^{*[\hat{r}]} \cup \{\hat{t}\} - \{\nu\}). \tag{5.24}$$

On the other hand, user ν is in the set $\underline{\Phi}^{*[\hat{r}]}$ in permutation $\boldsymbol{\pi}^{*[\hat{r}]}$. It means that in Step 2 of the algorithm, this user has been compared with other users in the set $\underline{\Phi}^{*[\hat{r}]} \cup \{\hat{t}\}$ to be located in the position $\eta^{*[\hat{t}]}(\hat{r})$ of the permutation $\boldsymbol{\pi}^{*[\hat{r}]}$, but user $\hat{t}$ has been chosen for the position, i.e., $\mathfrak{f}^{[\hat{r}]}\left(\underline{\Phi}^{*[\hat{r}]} \cup \{\hat{t}\} - \{\hat{t}\}\right) \leq \mathfrak{f}^{[\hat{r}]}\left(\underline{\Phi}^{*[\hat{r}]} \cup \{\hat{t}\} - \{\nu\}\right)$, therefore,

$$\mathfrak{f}^{[\hat{r}]}\left(\underline{\Phi}^{*[\hat{r}]}\right) \leq \mathfrak{f}^{[\hat{r}]}\left(\underline{\Phi}^{*[\hat{r}]} \cup \{\hat{t}\} - \{\nu\}\right). \tag{5.25}$$

Using (5.19), (5.22), (5.24), and (5.25), we conclude that $v_\nu(\Pi) \leq v_{\hat{t}}(\Pi^*)$, regardless of the decoding orders chosen for the other receivers. Therefore, if the new decoding orders are employed, the minimum rate of the users is less than or equal to $\vartheta_{\hat{t}}(\Pi^*)$. Note that permuting of the users located before (or after) user ν in $\boldsymbol{\pi}^{[\hat{r}]}$ does not increase the rate of user ν. $\qquad\square$

5.3.1 Special Case: Gaussian Interference Channels

A Gaussian interference channel, including K users, is represented by the gain matrix $\mathbf{G} = [g_{rt}]_{K \times K}$ where g_{rt} is the power gain from transmitter t to receiver r. A white Gaussian noise with zero mean and variance σ_r^2 is added to the received signal at receiver

r terminal. In this case, $\mathfrak{f}^{[r]}$, defined in (5.11), is written as

$$\mathfrak{f}^{[r]}(S) = \log_2 \left(\sigma_r^2 + \sum_{t \in S} g_{rt} p_t \right),$$ (5.26)

where p_t denotes the power of transmitter t.

We can show that Algorithm 5.4 simplifies as follows. The set of users decoded at receiver r, $D^{*[r]}$, is equal to

$$D^{*[r]} = \{t \; : \; g_{rt} p_t \geq g_{rr} p_r\}.$$ (5.27)

At receiver r, user i is decoded before user t if $g_{ri} p_i \geq g_{rt} p_t$. Therefore, to obtain the optimal decoding order for receiver r, we sort $g_{ri} p_i$, $i \in E$, decreasingly. The optimal decoding order for receiver r, i.e., $\boldsymbol{\pi}^{[*r]}$ is such that,

$$g_{r\pi^{[*r]}(K)} p_{\pi^{[*r]}(K)} \geq g_{r\pi^{[*r]}(K-1)} p_{\pi^{[*r]}(K-1)} \geq \ldots \geq g_{rr} p_r.$$ (5.28)

In addition, the set of receivers which decode user t, i.e., $E^{*[t]}$ is derived as,

$$E^{*[t]} = \{r \; : \; g_{rt} p_t \geq g_{rr} p_r\}.$$ (5.29)

In this case, the rate of user t is obtained by

$$\vartheta_t(\Pi^*) = \min_{r, r \in E^{*[t]}} \log_2 \left(1 + \frac{g_{rt} p_t}{\sigma_r^2 + \sum_{i : g_{rt} p_t > g_{ri} p_i} g_{ri} p_i} \right).$$ (5.30)

5.4 Conclusion

In this chapter, a K-user memoryless interference channel is considered where each receiver sequentially decodes the data of a subset of transmitters before it decodes

the data of the designated transmitter. Therefore, the data rate of each transmitter depends on (i) the subset of receivers which decode the data of that transmitter, (ii) the decoding order, employed at each of these receivers. In this chapter, a greedy algorithm is developed to find the users which are decoded at each receiver and the corresponding decoding order such that the minimum rate of the users is maximized. It is proven that the proposed algorithm is optimal.

Chapter 6

Conclusion and Future Research

This dissertation focuses on the problem of signaling and fairness for the MIMO multi-user systems.

In Chapter Two, a simple signaling method for broadcast channels with multiple transmit multiple receive antennas is proposed. In this method, for each user, the direction in which the user has the maximum gain is determined. The best user in terms of the largest gain is selected. The corresponding direction is used as the modulation vector (MV) for the data stream transmitted to the selected user. The algorithm proceeds in a recursive manner where in each step, the search for the best direction is performed in the null space of the previously selected MVs. It is demonstrated that with the proposed method, each selected MV has no interference on the previously selected MVs. Dirty paper coding is used to cancel the remaining interference. To analyze the performance of the scheme, an upper-bound on the outage probability

134

of each sub-channel is derived which is used to establish the diversity order and the asymptotic sum-rate of the scheme. It is shown that the diversity order of the jth data stream, $1 \leq j \leq M$, is equal to $N(M - j + 1)(K - j + 1)$, where M, N, and K indicate the number of transmit antennas, the number of receive antennas, and the number of users, respectively. Furthermore, it is proven that the throughput of this scheme scales as $M \log \log(K)$ and asymptotically $(K \longrightarrow \infty)$ tends to the sum-capacity of the MIMO broadcast channel. The simulation results indicate that the achieved sum-rate is close to the sum-capacity of the underlying broadcast channel.

Chapter three presents a new scenario of data communication for a multiple-antenna system with two transmitters and two receivers in which each receiver receives data from both transmitters (X-Channels). In this scenario, it is assumed that each transmitter is unaware of the other transmitter's data (non-cooperative scenario). This system can be considered as a combination of two broadcast channels (from the transmitters' points of view) and two multi-access channels (from the receivers' points of view). Taking advantage of both perspectives, two signaling schemes for such a scenario are developed. In these schemes, some linear filters are employed at the transmitters and at the receivers which decompose the system into either two non-interfering multi-antenna broadcast sub-channels or two non-interfering multi-antenna multi-access sub-channels. The main objective in the design of the filters is to exploit the structure of the channel matrices to achieve the highest multiplexing gain (MG). It is shown that the proposed non-cooperative signaling schemes outperform other known non-cooperative schemes

in terms of the achievable MG. In particular, it is shown that in some specific cases, the achieved MG is the same as the MG of the system if full cooperation is provided either between the transmitters or between the receivers.

Chapter four investigates the problem of fairness in a wide class of multi-user systems for which a subset of capacity region, including the corner points and the sum-capacity facet, has a special structure known as polymatroid. Multi-access channels with fixed input distributions and multiple-antenna broadcast channels are examples of such systems. Any interior point of the sum-capacity facet can be achieved by time-sharing among corner points or by an alternative method known as *rate-splitting*. The main purpose of this part is to find a point on the sum-capacity facet which satisfies a notion of fairness among active users. This problem is addressed in two cases: (i) where the complexity of achieving interior points is not feasible, and (ii) where the complexity of achieving interior points is feasible. For the first case, the corner point for which the minimum rate of the active users is maximized (max-min corner point) is desired for signaling. A simple greedy algorithm is introduced to find the optimum max-min corner point. For the second case, the polymatroid properties are exploited to locate a rate-vector on the sum-capacity facet which is optimally fair in the sense that the minimum rate among all users is maximized (max-min rate). In the case that the rate of some users can not increase further (attain the max-min value), the algorithm recursively maximizes the minimum rate among the rest of the users. It is shown that the problems of deriving the time-sharing coefficients or rate-spitting scheme can be solved

by decomposing the problem to some lower-dimensional subproblems. In addition, a fast algorithm to compute the time-sharing coefficients to attain a general point on the sum-capacity facet is proposed.

In chapter five, a K-user memoryless interference channel is considered where each receiver sequentially decodes the data of a subset of transmitters before it decodes the data of the designated transmitter. Therefore, the data rate of each transmitter depends on (i) the subset of receivers which decode the data of that transmitter, (ii) the decoding order, employed at each of these receivers. In this chapter, a greedy algorithm is developed to find the users which are decoded at each receiver and the corresponding decoding order such that the minimum rate of the users is maximized. It is proven that the proposed algorithm is optimal.

6.1   Future Research Directions

The dissertation can be continued in several directions as briefly explained in what follows.

In the signaling scheme, presented in chapter two, it is assumed that the channel state information or the best modulation vectors are perfectly available at the transmitter. An extension to this work is to consider the effect of quantizing the channel state information for the practical scenarios where the feedback channels have limited capacity. The main objective would be to find the performance degradation of the

proposed scheme as a function of the number of quantizing levels.

In chapter two, it is shown that in a limited SNR, the difference between the sum-capacity of the system and the sum-rate of the proposed scheme diminishes as the number of users increases. An insightful direction to extend this work is to compute the difference of the sum-capacity and the sum-rate where the number of users is limited and SNR is high. The derived multiplexing gain of the scheme shows that the curve of the sum-rate versus SNR and the curve of the sum-capacity versus SNR have the same slope in the high SNR. Computing the power offset of the proposed scheme along with the derived multiplexing gain provides a complete picture from the performance of the scheme in the high SNR regime.

As mentioned in chapter three, the X channel can be considered as the building block of a system with two transmitters, two relay nodes, and two receivers, where each relay node retransmits the data of the two transmitters. Investigating the achievable region and signaling schemes for such relay channel is an interesting direction for future research.

In chapter five, the optimal order of decoding is derived where the receivers have the possibility of successive decoding. A fruitful future work is to derive the optimal power allocation to attain a specific rate vector for both cases of single-antenna and multiple-antenna interference channels.

Appendix A

Some Results from the Theory of

Order Statistics

Let $z_1, z_2, \ldots, z_K$ be i.i.d random variables with a common CDF $F(.)$ and probability density function $f(.)$. Let $F_{j:K}(.)$ denote the CDF of the jth largest variable, $z^{\{j\}} = j^{th} \max\{z_1, \ldots, z_K\}$. Then, we have the following lemmas and theorems.

Lemma A.1. *[9, Chapter 2, Page 8]*

$$F_{j:K}(z) = \Pr(z^{\{j\}} \leq z) = \sum_{i=K-j+1}^{K} \binom{K}{i} F^i(z)[1 - F(z)]^{K-i}. \qquad (A.1)$$

When $K \longrightarrow \infty$, the following theorem characterizes the limiting distribution of $F_{j:K}(.)$.

Theorem A.2. *[55, Smirnov, 1949] Assume that there exists the sequence of normal-*

izing constants $a_i > 0$ and b_i, $i = 1, \ldots, K$, such that

$$\lim_{K \longrightarrow \infty} F_{j:K}(a_K z + b_K) = \tilde{\Upsilon}^{\{j\}}(z). \tag{A.2}$$

Then, $\tilde{\Upsilon}^{\{j\}}(z)$ has the following form:

$$\tilde{\Upsilon}^{\{j\}}(z) = \Lambda(z) \sum_{i=0}^{j-1} \frac{\{-\log[\Lambda(z)]\}^i}{i!}, \tag{A.3}$$

where $\Lambda(z)$ belongs to one of the following three types of functions:

$$\text{Type (i)} \quad \Lambda_1(z) = \begin{cases} 0 & z \le 0 \\ \\ \exp(-z^{-\tilde{\epsilon}}) & z > 0, \tilde{\epsilon} > 0 \end{cases} \tag{A.4}$$

$$\text{Type (ii)} \quad \Lambda_2(z) = \begin{cases} \exp(-(-z)^{\tilde{\epsilon}}) & z \le 0, \tilde{\epsilon} > 0 \\ \\ 1 & z > 0 \end{cases} \tag{A.5}$$

$$\text{Type (iii)} \quad \Lambda_3(z) = \exp(-e^{-z}). \tag{A.6}$$

The following theorem gives the necessary and sufficient condition for distribution $F(z)$ to belong to the domain of attraction of one of the three limiting forms.

Theorem A.3. *[55] Suppose $a_K > 0$ and b_K are sequences of real numbers. For distribution function $F_{j:K}$ and $\Lambda_l(z)$, where j is a fixed natural number, we have*

$$\lim_{K \longrightarrow \infty} F_{j:K}(a_K z + b_K) = \tilde{\Upsilon}_l^{\{j\}}(z) = \Lambda_l(z) \sum_{i=0}^{j-1} \frac{\{-\log[\Lambda_l(z)]\}^i}{i!}, \tag{A.7}$$

if and only if

$$\lim_{K \longrightarrow \infty} K\left[1 - F(a_K z + b_K)\right] = -\log[\Lambda_l(z)]. \tag{A.8}$$

The following theorem determines the rate of the convergence to the limiting distributions.

Theorem A.4. *[11, Dziubdziela, 1974] Assume $F(z)$ with normalizing sequences a_K and b_K is in the domain of attraction of type l limiting distribution, $l \in \{1, 2, 3\}$. If $\frac{1}{2} < F(a_K z + b_K) < 1$ and $-\log[\Lambda_l(z)] < \infty$, then for natural number j,*

$$\left| F_{j:K}(a_K z + b_K) - \tilde{\Upsilon}_l^{\{j\}}(z) + \frac{1}{2}K\tilde{\delta}_K^2 g(j, K\tilde{\delta}_K) \right| \le$$

$$\frac{1}{2}\pi \exp(2K\tilde{\delta}_K)K\tilde{\delta}_K^3 \left[\frac{4}{3(1 - 2\tilde{\delta}_K)} + \left(\frac{16}{9}K\tilde{\delta}_K^3 \frac{1}{(1 - 2\tilde{\delta}_K)^2} + \right.\right.$$

$$\left.\left. +\frac{8}{3}K\tilde{\delta}_K^2 \frac{1}{1 - 2\tilde{\delta}_K} + K\tilde{\delta}_K \right) \exp\left(K\tilde{\delta}_K^2 \left\{ 1 + \frac{4}{3}\tilde{\delta}_K \frac{1}{1 - 2\tilde{\delta}_K} \right\} \right) \right] + \Theta(z), \quad (A.9)$$

where

$$\Theta(z) = \left| \frac{1}{(j-1)!} \int_{K\tilde{\delta}_K}^{-\log[\Lambda_l(z)]} \varpi^{j-1} \exp(-\varpi)d\varpi \right|, \quad (A.10)$$

and

$$\tilde{\delta}_K(z) = 1 - F(a_K z + b_K), \quad (A.11)$$

and

$$g(z, \tilde{\vartheta}) = \begin{cases} 0 & z \le 0 \\ \exp(-\tilde{\vartheta}) & 0 < z \le 1 \\ \exp(-\tilde{\vartheta}) \left(\frac{\tilde{\vartheta}^{\mu+1}}{(\mu+1)!} - \frac{\tilde{\vartheta}^{\tilde{\mu}}}{(\tilde{\mu})!} \right) & \tilde{\mu} + 1 < z \le \tilde{\mu} + 2 \quad \tilde{\mu} = 0, 1, 2, \ldots \end{cases} \quad (A.12)$$

In the following lemma, we apply the above theorems for a specific distribution which is used throughout this chapter.

Lemma A.5. *Let* $z_1, z_2, \ldots, z_K$ *be* K *i.i.d random variables with a common CDF*

$$F(z) = 1 - \frac{1}{\tilde{\beta}} z^{\tilde{\alpha}} e^{-z} \quad \tilde{\alpha} \geq 0, \tilde{\beta} > 0, \tag{A.13}$$

then,

- *Distribution function* $F(z)$ *is in the domain of attraction of type (iii) limiting distribution with normalizing sequences*

$$a_K = 1, \tag{A.14}$$

$$b_K = \log\left(\frac{K}{\tilde{\beta}}\right) - \tilde{\alpha} \log\log\left(\frac{K}{\tilde{\beta}}\right). \tag{A.15}$$

- *If* $z^{\{j\}}$ *denotes the* j^{th} *largest random variable, then,*

$$\Pr\left\{ b_K - \log\log(\sqrt{K}) \leq z^{\{j\}} \leq b_K + \log\log(\sqrt{K}) \right\} \geq 1 - O\left(\frac{1}{\log K}\right). \tag{A.16}$$

Proof. **Part One:**

Using a_K and b_K, defined in (A.14) and (A.15), we have

$$\lim_{K \longrightarrow \infty} K(1 - F(a_K z + b_K)) = K \frac{1}{\tilde{\beta}} (a_K z + b_K)^{-\tilde{\alpha}} \exp(-a_K z - b_K) =$$

$$\lim_{K \longrightarrow \infty} K \frac{1}{\tilde{\beta}} \left[z + \log\left(\frac{K}{\tilde{\beta}}\right) - \tilde{\alpha} \log\log\left(\frac{K}{\tilde{\beta}}\right) \right]^{-\tilde{\alpha}} \exp\left[-z - \log\left(\frac{K}{\tilde{\beta}}\right) + \tilde{\alpha} \log\log\left(\frac{K}{\tilde{\beta}}\right) \right] =$$

$$\lim_{K \longrightarrow \infty} \exp(-z) \left[z + \log\left(\frac{K}{\tilde{\beta}}\right) - \tilde{\alpha} \log\log\left(\frac{K}{\tilde{\beta}}\right) \right]^{-\tilde{\alpha}} \left[\log\left(\frac{K}{\tilde{\beta}}\right) \right]^{\tilde{\alpha}} =$$

$$= \exp(-z) = -\log[\Lambda_3(z)]. \tag{A.17}$$

Therefore, regarding Theorem A.3, the distribution (A.13) is in the domain of attraction of type (iii) limiting distribution.

Part Two:

Substituting $\log\log(\sqrt{K})$ and $-\log\log(\sqrt{K})$ in $\tilde{\Upsilon}_3^{\{j\}}(z)$, defined in (A.7), we obtain

$$\tilde{\Upsilon}_3^{\{j\}}\left(\log\log\sqrt{K}\right) = \exp\left(-\frac{1}{\log\sqrt{K}}\right)\sum_{i=0}^{j-1}\frac{1}{i!\log^i\sqrt{K}} = 1 - O\left(\frac{1}{\log K}\right), \qquad \text{(A.18)}$$

and

$$\tilde{\Upsilon}_3^{\{j\}}\left(-\log\log\sqrt{K}\right) = \frac{1}{\sqrt{K}}\sum_{i=0}^{j-1}\frac{\log^i\sqrt{K}}{i!} = O\left(\frac{\log^j\sqrt{K}}{\sqrt{K}}\right). \qquad \text{(A.19)}$$

Therefore,

$$\tilde{\Upsilon}_3^{\{j\}}\left(\log\log\sqrt{K}\right) - \tilde{\Upsilon}_3^{\{j\}}\left(-\log\log\sqrt{K}\right) \geq 1 - O\left(\frac{1}{\log K}\right). \qquad \text{(A.20)}$$

In the following, we apply Theorem A.4 to find out how $F_{j:K}(z)$ is close to limiting distribution $\tilde{\Upsilon}_3^{\{j\}}(z)$ at $z = \log\log\sqrt{K}$ and $z = -\log\log\sqrt{K}$. To simplify the derivation, we first calculate some terms appeared in Theorem A.4 at these two points.

Using (A.11), (A.14), and (A.15), for $F(z)$ in (A.13), we obtain

$$\tilde{\delta}_K(z) = 1 - F(a_K z + b_K) = \frac{e^{-z}}{K}\left[1 + O\left(\frac{1}{\log K}\right)\right]. \qquad \text{(A.21)}$$

Therefore,

$$\tilde{\delta}_K\left(\log\log\sqrt{K}\right) = \frac{1}{K\log\sqrt{K}}\left[1 + O\left(\frac{1}{\log K}\right)\right], \qquad \text{(A.22)}$$

and

$$\tilde{\delta}_K\left(-\log\log\sqrt{K}\right) = \frac{\log\sqrt{K}}{K}\left[1 + O\left(\frac{1}{\log K}\right)\right]. \qquad \text{(A.23)}$$

It is easy to show that $\Theta(z)$ in (A.10) is equal to,

$$\Theta(z) = \left|\exp[-K\tilde{\delta}_K(z)]\sum_{i=0}^{j-1}\frac{[K\tilde{\delta}_K(z)]^i}{i!} - \tilde{\Upsilon}_3^{\{j\}}(z)\right|. \qquad \text{(A.24)}$$

On the other hand, using (A.22), we obtain

$$\exp[-K\tilde{\delta}_K(\log \log \sqrt{K})] = 1 - O\left(\frac{1}{\log K}\right), \qquad (A.25)$$

and using (A.22), we obtain

$$\exp[-K\tilde{\delta}_K(-\log \log \sqrt{K})] = O\left(\frac{1}{\sqrt{K}}\right). \qquad (A.26)$$

Consequently, using (A.18), (A.22), (A.24) and (A.25), we have

$$\Theta\left(\log \log \sqrt{K}\right) = O\left(\frac{1}{\log K}\right), \qquad (A.27)$$

and using (A.19), (A.23), (A.24) and (A.26), we have

$$\Theta\left(-\log \log \sqrt{K}\right) = O\left(\frac{\log^j \sqrt{K}}{\sqrt{K}}\right). \qquad (A.28)$$

Regarding (A.12), we have,

$$g(j, K\tilde{\delta}_K(z)) = \begin{cases} \exp(-K\tilde{\delta}_K(z)) & j = 1 \\ \exp(-K\tilde{\delta}_K(z))\left(\frac{[K\tilde{\delta}_K(z)]^{j-1}}{(j-1)!} - \frac{[K\tilde{\delta}_K(z)]^{j-2}}{(j-2)!}\right) & j \geq 2 \end{cases} \qquad (A.29)$$

Therefore, using (A.22), we obtain,

$$K\tilde{\delta}_K^2(\log \log \sqrt{K})g\left(j, K\tilde{\delta}_K(\log \log \sqrt{K})\right) = o\left(\frac{1}{K}\right), \qquad (A.30)$$

and using (A.23), we obtain,

$$K\tilde{\delta}_K^2(-\log \log \sqrt{K})g\left(j, K\tilde{\delta}_K(-\log \log \sqrt{K})\right) = o\left(\frac{1}{K}\right). \qquad (A.31)$$

Applying Theorem A.4 for $z = \log\log\sqrt{K}$, and using (A.22), (A.27), and (A.30), we have

$$\left| F_{j:K}(\log\log\sqrt{K} + b_K) - \tilde{\Upsilon}_3^{\{j\}}(\log\log\sqrt{K}) + o\left(\frac{1}{K}\right)\right| \leq O\left(\frac{1}{\log K}\right). \qquad \text{(A.32)}$$

Similarly, Applying Theorem A.4 for $z = -\log\log\sqrt{K}$, and using (A.23), (A.28), and (A.31), we have

$$\left| F_{j:K}(-\log\log\sqrt{K} + b_K) - \tilde{\Upsilon}_3^{\{j\}}(-\log\log\sqrt{K}) + o\left(\frac{1}{K}\right)\right| \leq O\left(\frac{\log^j\sqrt{K}}{\sqrt{K}}\right). \quad \text{(A.33)}$$

Using (A.20), (A.33), and (A.32), we obtain

$$\left| F_{j:K}\left(\log\log\sqrt{K} + b_K\right) - F_{j:K}\left(-\log\log\sqrt{K} + b_K\right)\right| \geq 1 - O\left(\frac{1}{\log K}\right). \quad \text{(A.34)}$$

Since $F_{j:K}(.)$ denotes CDF of $z^{\{j\}}$, (A.34) results in (A.16). $\qquad\square$

Appendix B

$G_{\tilde{m},\tilde{n}}(z)$ for Small z

In chapter two, Lemma 2.3, the distribution of the largest eigenvalue of a Wishart matrix $G_{\tilde{m},\tilde{n}}(z)$, is presented. In this appendix, we obtain the behavior of $G_{\tilde{m},\tilde{n}}(z)$ for the small values z.

By substituting the Taylor expansion of e^z and e^{-z} into (2.20),

$$
\gamma(n+1, z) =
$$

$$
n!\left(1 - e^{-z}\sum_{m=1}^{n}\frac{z^m}{m!}\right) = n!e^{-z}\left(e^z - \sum_{m=1}^{n}\frac{z^m}{m!}\right)
$$

$$
= n!\left(1 - z + \frac{z^2}{2!} - \frac{z^3}{3!} + \cdots\right)\left(\sum_{m=1}^{\infty}\frac{z^m}{m!} - \sum_{m=1}^{n}\frac{z^m}{m!}\right)
$$

$$
= n!\left(1 - z + \frac{z^2}{2!} - \frac{z^3}{3!} + \cdots\right)\left(\sum_{m=n+1}^{\infty}\frac{z^m}{m!}\right)
$$

$$
= \frac{z^{n+1}}{n+1}(1 + O(z)). \tag{B.1}
$$

Substituting (B.1) in (2.19), we have,

$$\overline{\boldsymbol{\Psi}} = \left[\frac{z^{m-n+p+q-1}}{m-n+p+q-1}(1+O(z)) \right]^{n\times n}_{(p,q)}. \tag{B.2}$$

It is known that if a column or row of a matrix is multiplied by variable z, the

determinant of the resulting matrix is z times the determinant of the original matrix.

Using this property, first, we factor z^{m-n+q} from column q, $0 \le q \le n$ of the $\overline{\boldsymbol{\Psi}}$,

and then we factor z^{p-1} from row p, $1 \le p \le n$. The remaining matrix is equal to

$\left[\frac{1}{m-n+p+q-1}(1+O(z)) \right]^{n\times n}_{(p,q)}$, and the power of z outside the determinant is equal to

$$\sum_{q=1}^{n}(m-n+q) + \sum_{p=1}^{n}(p-1) = mn. \tag{B.3}$$

Therefore,

$$\det(\overline{\boldsymbol{\Psi}}) = z^{mn}\det\left(\left[\frac{1}{m-n+p+q-1}(1+O(z)) \right]^{n\times n}_{(p,q)} \right). \tag{B.4}$$

By substituting (B.4) into (2.18), we have

$$G_{\tilde{m},\tilde{n}}(z) =$$

$$\frac{z^{mn}}{\prod_{k=1}^{n}\Gamma(m-k+1)\Gamma(n-k+1)}\det\left(\left[\frac{1}{m-n+p+q-1}(1+O(z)) \right]^{n\times n}_{(p,q)} \right) \tag{B.5}$$

According to (B.5), the coefficient of the smallest degree of z is equal to

$$c = \frac{1}{\prod_{k=1}^{n}\Gamma(m-k+1)\Gamma(n-k+1)}\det\left(\left[\frac{1}{m-n+p+q-1} \right]^{n\times n}_{(p,q)} \right). \tag{B.6}$$

We apply the following formula to calculate the determinant in (B.6) (see [44, p. 92,

Problem 3])

$$\det\left(\left[\frac{1}{x_p + y_q}\right]_{(p,q)}\right) = \frac{\prod_{q>p}(x_q - x_p)(y_q - y_p)}{\prod_{p,q}(x_p + y_q)}, \tag{B.7}$$

where x_p and y_q depend only on p and q, respectively. Substituting $x_p = m - n + p - 1$ and $y_q = q$ in (B.7), we compute the determinant term in (B.6), resulting in

$$\lim_{z\to 0} G_{\tilde{m},\tilde{n}}(z) = c_{\tilde{m},\tilde{n}} z^{\tilde{m}\tilde{n}}, \tag{B.8}$$

where $c_{\tilde{m},\tilde{n}}$ is equal to

$$c_{\tilde{m},\tilde{n}} = \frac{\prod_{\hat{\zeta}=1}^{n-1}(n - \hat{\zeta})!}{\prod_{k=1}^{n}(m - k)!\prod_{\hat{\zeta}=1}^{n}(m - n + \hat{\zeta})^{\hat{\zeta}}(m + n - \hat{\zeta})^{\hat{\zeta}}}, \tag{B.9}$$

where $n = \min\{\tilde{m}, \tilde{n}\}$ and $m = \max\{\tilde{m}, \tilde{n}\}$.

Appendix C

$G_{\tilde{m},\tilde{n}}(z)$ for Large z

In this appendix, we obtain the behavior of $G_{\tilde{m},\tilde{n}}(z)$, the distribution of the largest eigenvalue of a Wishart matrix (see Lemma 2.3) for the large values of z.

By using (2.20), the determinant of matrix $\overline{\boldsymbol{\Psi}}$ in (2.19) has the following structure:

$$\det(\overline{\boldsymbol{\Psi}}) =$$

$$\det\left([\gamma(m-n+p+q-1,z)]_{(p,q)}^{n\times n}\right) =$$

$$\tilde{\varphi}_0 + \tilde{\varphi}_1(z)e^{-z} + \tilde{\varphi}_2(z)e^{-2z} + \cdots + \tilde{\varphi}_n(z)e^{-nz}, \qquad (\text{C.1})$$

where $\tilde{\varphi}_0$ is a constant number, and $\tilde{\varphi}_i(z)$, $i = 1, \cdots, n$ are polynomials. Therefore, when $z \to \infty$,

$$\det(\overline{\boldsymbol{\Psi}}) \to \tilde{\varphi}_0 + \tilde{\kappa}z^{\tilde{\iota}}e^{-z}, \qquad (\text{C.2})$$

where $\tilde{\iota}$ is the degree of $\tilde{\varphi}_1(z)$, and $\tilde{\kappa}$ is the coefficient of $z^{\tilde{\iota}}$ in $\tilde{\varphi}_1(z)$. In the following, we determine $\tilde{\varphi}_0$, $\tilde{\kappa}$, and $\tilde{\iota}$.

149

Computing $\tilde{\varphi}_0$: Using the expansion (2.20), it is easy to verify that

$$\lim_{z\to\infty} \gamma(m - n + p + q - 1, z) = (m - n + p + q - 2)!. \tag{C.3}$$

Regarding (C.1) and (C.3) ,

$$\tilde{\varphi}_0 = \lim_{z\to\infty} \det(\overline{\boldsymbol{\Psi}}) = \det\left([(m - n + p + q - 2)!]_{(p,q)}^{n\times n}\right). \tag{C.4}$$

On the other hand, since $G_{\tilde{m},\tilde{n}}(z)$ is the CDF of a random variable, $\lim_{z\to\infty} G_{\tilde{m},\tilde{n}}(z) = 1$.

Substituting (C.4) in (2.18), we have

$$\lim_{z\to\infty} G_{\tilde{m},\tilde{n}}(z) = \frac{\det\left([(m - n + p + q - 2)!]_{(p,q)}^{n\times n}\right)}{\prod_{k=1}^{n} \Gamma(m - k + 1)\Gamma(n - k + 1)} = 1. \tag{C.5}$$

Considering (C.4) and (C.5), we obtain

$$\tilde{\varphi}_0 = \prod_{k=1}^{n} \Gamma(m - k + 1)\Gamma(n - k + 1). \tag{C.6}$$

Computing $\tilde{\kappa}$, and $\tilde{\iota}$: Applying the method of *expansion by minors*, we expand the

determinant of $\overline{\boldsymbol{\Psi}}$ in (2.19), based on the last row of the matrix. It is evident that the

largest power of z in $\tilde{\varphi}_1(z)$ is determined by $\Psi(n, n)$, multiplied by the constant term

of its cofactor. By using (2.19) and (2.20), it is easy to show that this term is equal to

$$\det\left([(m - n + p + q - 2)!]_{(p,q)}^{(n-1)\times(n-1)}\right) \gamma(m + n - 1, z), \tag{C.7}$$

where $\gamma(m+n-1, z)$ is entry (n, n) of matrix $\overline{\boldsymbol{\Psi}}$, and $\det\left([(m - n + p + q - 2)!]_{(p,q)}^{(n-1)\times(n-1)}\right)$

is the constant part of its cofactor. Using (2.20), we obtain

$$\gamma(m + n - 1, z) = (m + n - 2)! - z^{m+n-2}e^{-z}\left(1 + O(z^{-1})\right). \tag{C.8}$$

By rewriting (C.5), we obtain

$$\det\left([(m-n+p+q-2)!]_{(p,q)}^{n\times n}\right) = \prod_{k=1}^{n}\Gamma(m-k+1)\Gamma(n-k+1). \qquad \text{(C.9)}$$

By substituting $m-1$ for m and $n-1$ for n in (C.9),

$$\det\left([(m-n+p+q-2)!]_{(p,q)}^{(n-1)\times(n-1)}\right) = \prod_{k=1}^{n-1}\Gamma(m-k)\Gamma(n-k). \qquad \text{(C.10)}$$

Considering (C.7), (C.8), and (C.10), we have

$$\tilde{\kappa} = -\prod_{k=1}^{n-1}\Gamma(m-k)\Gamma(n-k), \qquad \text{(C.11)}$$

and,

$$\tilde{\iota} = m+n-2. \qquad \text{(C.12)}$$

Using (C.2), (C.6), (C.11), (C.12), and (2.18), we have,

$$G_{\tilde{m},\tilde{n}}(z) = 1 - \frac{e^{-z}z^{m+n-2}}{(m-1)!(n-1)!}\left(1+O(z^{-1}e^{-z})\right), \qquad \text{(C.13)}$$

Since $m = \max\{\tilde{m},\tilde{n}\}$ and $n = \min\{\tilde{m},\tilde{n}\}$, we have

$$G_{\tilde{m},\tilde{n}}(z) = 1 - \frac{e^{-z}z^{\tilde{m}+\tilde{n}-2}}{(\tilde{m}-1)!(\tilde{n}-1)!}\left(1+O(z^{-1}e^{-z})\right). \qquad \text{(C.14)}$$

Bibliography

[1] J.M. Aein. Power balancing in systems employing frequency reuse. In *Comsat Tech. Rev.*, volume 3, 1973.

[2] R. Ahlswede. Multiway communication channels. In *Proc. 2nd. Int. Symp. Information Theory*, pages 23–52, Arminian S.S.R. Prague, 1971.

[3] G. Caire and S. Shamai. On the achievable throughput of a multiantenna Gaussian broadcast channel. *IEEE Trans. Inform. Theory*, IT-49:1691–1706, July 2003.

[4] A. Carleial. A case where interference does not reduce capacity (corresp.). *IEEE Trans. Inform. Theory*, IT-21:569– 570, 1975.

[5] A. B. Carleial. Interference channels. *IEEE Trans. Inform. Theory*, IT-24:60–70, Jan. 1978.

[6] L.U. Choi and R.D. Murch. A transmit preprocessing technique for multiuser MIMO systems using a decomposition approach. *IEEE Transactions on Communications*, 3:20–24, Jan. 2004.

[7] M. Costa. Writing on dirty paper. *IEEE Trans. Inform. Theory*, 29:439–441, May 1983.

[8] M. Costa and A.E. Gamal. The capacity region of the discrete memoryless interference channel with strong interference (corresp.). *IEEE Trans. Inform. Theory*, IT-33:710– 711, 1987.

[9] H. A. David. *Order Statistics*. John Wiley and Sons, Inc, New York, second edition, 1980.

[10] N. Devroye and M. Sharif. The multiplexing gain of MIMO X-channels with partial transmit side-information. In *International Symposium on Information Theory (ISIT)*, Nice-France, July 2007. To be published.

[11] W. Dziubdziela. On convergence rates in the limit laws of extreme order statistics. In *Trans. 7th Prague Conference and 1974 European Meeting of Statisticians*, volume B, pages 119–127, 1974.

[12] U. Erez, S. Shamai, and R. Zamir. Capacity and lattice-strategies for cancelling known interference. *IEEE Trans. Inform. Theory*, IT-51:3820 – 3833, Nov. 2005.

[13] U. Erez and S. ten Brink. Approaching the dirty paper limit in canceling known interference. In *Allerton Conf. Commun., Contr., and Computing*, Oct. 2003.

[14] R. Etkin, A. Parekh, and David Tse. Spectrum sharing for unlicensed bands. *IEEE JSAC Special Issue on Adaptive, Spectrum Agile and Cognitive Wireless Networks*, (April), 2007. To appear.

[15] L. Fleischer and S. Iwata. A push-relabel framework for submodular function minimization and applications to parametric optimization. *Discrete Applied Mathematics*, 131(2):311–322, 2003.

[16] G. J. Foschini, H. Huang, K. Karakayali, R. A. Valenzuela, and S. Venkatesan. The value of coherent base station coordination. In *Conference on Information Sciences and Systems (CISS)*, March 2005.

[17] G. J. Foschini. Layered space-time architecture for wireless communication in a fading environment when using multi-element antennas. *Bell Labs Tech. J.*, pages 41–59, Autumn 1996.

[18] G. J. Foschini and M. J. Gans. On limits of wireless communications in a fading environment when using multiple antennas. *Wireless Personal Commun.*, 6:311–335, 1998.

[19] R. G. Gallager. *Information Theory and Reliable Communication*. John Wiley & Sons, New York, 1968.

[20] A. Goldsmith. *Wireless Communications*. Cambridge University Press, first edition, 2005.

[21] A.J. Grant, B. Rimoldi, R.L. Urbanke, and P.A. Whiting. Rate-splitting multiple access for discrete memoryless channels. *IEEE Trans. Inform. Theory*, IT-47:873–890, March 2001.

[22] T. S. Han and K. Kobayashi. A new achievable rate region for the interference channel. *IEEE Trans. Inform. Theory*, IT-27:49–6o, Jan. 1981.

[23] Z. Han, Z. Ji, and K.J.R. Liu. Fair multiuser channel allocation for OFDMA networks using Nash bargaining solutions and coalitions. *IEEE Transactions on Communications*, 53:1366–1376, Aug 2005.

[24] S.V. Hanly and D.N.C Tse. Multiaccess fading channels. II. delay-limited capacities. *IEEE Trans. Inform. Theory*, IT-44:2816–2831, Nov. 1998.

[25] R.G. Horn and C.A. Johnson. *Matrix Analysis*. Cambridge University Press, 1985.

[26] A. Host-Madsen. Capacity bounds for cooperative diversity. *IEEE Trans. Inform. Theory*, IT-52:1522– 1544, 2006.

[27] S. Iwata, L. Fleischer, and S. Fujishige. A combinatorial strongly polynomial time algorithm for minimizing submodular functions. *Journal of ACM*, 48(4):761–777, 2001.

[28] S. A. Jafar. Degrees of freedom in distributed mimo communications. In *IEEE Communication Theory Workshop*, 2005.

[29] S.A. Jafar. Degrees of freedom on the MIMO X channel - the opti-mality of the MMK scheme. Technical report, Sept. 2006. available at http://arxiv.org/abs/cs.IT/0607099.

[30] N. Jindal. High SNR analysis of MIMO broadcast channels. In *International Symposium on Information Theory (ISIT)*, pages 2310– 2314, Adelaide, Australia, Sept. 2005.

[31] M. Kang and M.-S. Alouini. Largest eigenvalue of complex Wishart matrices and performance analysis of MIMO mrc systems. *IEEE Journal on Selected Areas in Communications*, 21:418–426, April 2003.

[32] F.P. Kelly. Charging and rate control for elastic traffic. *European Transactions on Telecommunications*, 8:33–37, 1997.

[33] C. G. Khatri. Distribution of the largest or the smallest characteristic root under null hyperthesis concerning complex multivariate normal populations. *Ann. Math. Stat.*, 35:1807–1810, 1964.

[34] R. Knopp and P. Humblet. Information capacity and power control in single cell multiuser communications. In *Proc. IEEE Int. Computer Conf. (ICC 95)*, Seattle, WA, June 1995.

[35] H. Liao. *Multiple access channels*. PhD thesis, Dep. Elec. Eng., Univ. of Hawaii., 1972.

[36] A. Lozano, A.M. Tulino, and S Verdu. High-SNR power offset in multiantenna communication. *IEEE Trans. Inform. Theory*, IT-51:4134– 4151, 2005.

[37] M. A. Maddah-Ali, M. Ansari, and Amir K. Khandani. An efficient signaling scheme for MIMO broadcast systems: Design and performance evaluation. *IEEE Trans. Inform. Theory*, July 2005. Submitted for Publication.

[38] M. A. Maddah-Ali, S. A. Motahari, and Amir K. Khandani. Communication over X channel: Signalling and multiplexing gain. Technical Report UW-ECE-2006-12, University of Waterloo, July 2006.

[39] M. A. Maddah-Ali, S. A. Motahari, and Amir K. Khandani. Signaling over mimo multi-base systems: Combination of multi-access and broadcast schemes. In *IEEE International Symposium on Information Theory*, Seattle, WA, USA, 2006.

[40] M.A. Maddah-Ali, A. Mobasher, and Amir K. Khandani. Fairness in multiuser systems with Polymatroid capacity region. *IEEE Trans. Inform. Theory*, June 2006. Submitted.

[41] H. Mahdavi-Doost, M. Ebrahimi, and A.K. Khandani. Characterization of rate region in interference channels with constrained power. Technical report, University of Waterloo, 2007. available at www.cst.uwaterloo.ca.

[42] K. Marton. A coding theorem for the discrete memoryless broadcast channel. *IEEE Trans. Inform. Theory*, IT-25:306–311, May 1979.

[43] C.B. Peel, B.M. Hochwald, and A.L. Swindlehurst. A vector-perturbation technique for near-capacity multiantenna multiuser communication-part I: channel inversion and regularization. *IEEE Trans. on Commun.*, 53:195 – 202, Jan. 2005.

[44] G. Polya and G. Szego. *Problems and Theorems in Analysis*, volume 2. Springer-Verlag, Heidelberg, 1976.

[45] B. Rimoldi and R. Urbanke. A rate-splitting approach to the Gaussian multiple-access channel. *IEEE Trans. Inform. Theory*, IT-42:364–375, March 1996.

[46] H. Sato. On degraded gaussian two-user channels. *IEEE Trans. Inform. Theory*, IT-24:637–640, Sept. 1978.

[47] H. Sato. The capacity of the gaussian interference channel under strong interference. *IEEE Trans. Inform. Theory*, IT-27:786–788, Nov. 1981.

[48] A. Schrijver. A combinatorial algorithm for minimizing submodular functions in strongly polynomial time. *Journal of Combinatorial Theory, B80*, pages 346–355, 2000.

[49] S. Shamai and S. Verdu. The impact of frequency-flat fading on the spectral efficiency of CDMA. *IEEE Trans. Inform. Theory*, IT-47:1302–1327, 2001.

[50] X. Shang, B. Chen, and M.J. Gans. On the achievable sum rate for MIMO interference channels. *IEEE Trans. Inform. Theory*, IT-52:4313 – 4320, 2006.

[51] C. E. Shannon. Two-way communication channels. In *4th Berkeley Symp. Math. Stat. Prob.*, pages 611–644, Adelaide, Australia, Sept. 1961. University of California Press.

[52] M. Sharif and B. Hassibi. A comparison of time-sharing, DPC, and bemforming for MIMO broadcast channels with many users. *IEEE Trans. on Comm.*, 2004. Submitted for Publication.

[53] Y. Shi and E. J. Friedman. Algorithms for implementing fair wireless power allocations. In *the 9th Canadian Workshop on Information Theory*, pages 171–174, Montreal, Quebec, Canada, June 2005.

[54] S. Shamai (Shitz) and B.M. Zaidel. Enhancing the cellular downlink capacity via co-processing at the transmitting end. In *IEEE Vehicular Technology Conference*, volume 3, pages 1745 – 1749, May 2001.

[55] N. V. Smirnov. Limit distributions for the terms of a variational series. In *Trudy Mat. Inst.*, volume 25, 1949.

[56] Q.H. Spencer, A.L. Swindlehurst, and M. Haardt. Zero-forcing methods for downlink spatial multiplexing in multiuser MIMO channels. *IEEE Transactions on Acoustics, Speech, and Signal Processing*, 52:461–471, Feb. 2004.

[57] V. Tarokh, N. Seshadri, and A. R. Calderbank. Space-time code for high data rate wireless communication: Performance criterion and code construction. *IEEE Trans. Inform. Theory*, IT-44:744–765, Mar. 1988.

[58] I. E. Telatar. Capacity of multi-antenna Gaussian channels. *Europ. Trans. Telecommun.*, pages 585–595, Nov. 1999.

[59] D.N.C. Tse and S.V. Hanly. Multiaccess fading channels. I. Polymatroid structure, optimal resource allocation and throughput capacities. *IEEE Trans. Inform. Theory*, IT-44:2796–2815, Nov. 1998.

[60] D.N.C. Tse and P. Viswanath. *Fundamentals of Wireless Communication.* Cambridge University Press, first edition, 2005.

[61] Z. Tu and R.S. Blum. Multiuser diversity for a dirty paper approach. *IEEE Communications Letters*, 7:370–372, Aug. 2003.

[62] S. Vishwanath and S.A. Jafar. On the capacity of vector Gaussian interference channels. In *IEEE Information Theory Workshop*, pages 365– 369, Austin, TX, USA, 2004.

[63] S. Vishwanath, N. Jindal, and A. Goldsmith. Duality, achievable rates, and sum-rate capacity of Gaussian MIMO broadcast channels. *IEEE Trans. Inform. Theory*, IT-49:2658–2668, Oct. 2003.

[64] P. Viswanath and D.N.C. Tse. Sum capacity of the vector Gaussian broadcast channel and uplink-downlink duality. *IEEE Trans. Inform. Theory*, IT-49:1912 – 1921, Aug. 2003.

[65] P. Viswanath, D.N.C Tse, and R. Laroia. Opportunistic beamforming using dumb antennas. *IEEE Trans. Inform. Theory*, 48:1277–1294, June 2002.

[66] H. Weingarten, Y. Steinberg, and S. Shamai (Shitz). The capacity region of the Gaussian MIMO broadcast channel. In *38th Annual Conference on Information Sciences and Systems (CISS 2004)*, Princeton, NJ, March 2004.

[67] H. Weingarten, Y. Steinberg, and S. Shamai (Shitz). The capacity region of the Gaussian MIMO broadcast channel. *IEEE Trans. Information Theory*, 2004. Submitted for Publication.

[68] D. J. A. Welsh. *Matroid Theory*. Academic Press, London, 1976.

[69] S. Ye and R.S. Blum. Optimized signaling for MIMO interference systems with feedback. *IEEE Transactions on Signal Processing*, 51:2839– 2848, 2003.

[70] W. Yu. A dual decomposition approach to the sum power Gaussian vector multiple access channel sum capacity problem. In *37th Annual Conference on Information Sciences and Systems (CISS)*, March 2003.

[71] W. Yu and J. Cioffi. Sum capacity of vector Gaussian broadcast channels. *IEEE Trans. Inform. Theory*, IT-50:1875 – 1892, Sept. 2004. submitted for Publication.

[72] W. Yu and W. Rhee. Degrees of freedom in multi-user spatial multiplex systems with multiple antennas. *IEEE Transactions on Communications*, 54:1747– 1753, Oct. 2006.

[73] X. Zhang, J. Chen, S. B. Wicker, and T. Berger. Successive coding in multiuser information theory. *IEEE Trans. Inform. Theory*, 2006. submitted for publication.